

8-2016

Improving the Laboratory Design of Asphalt Mixtures to Enhance Asphalt Pavement Durability

Ali Hekmatfar

Purdue University

Follow this and additional works at: https://docs.lib.purdue.edu/open_access_dissertations



Part of the [Civil Engineering Commons](#), and the [Transportation Engineering Commons](#)

Recommended Citation

Hekmatfar, Ali, "Improving the Laboratory Design of Asphalt Mixtures to Enhance Asphalt Pavement Durability" (2016). *Open Access Dissertations*. 771.

https://docs.lib.purdue.edu/open_access_dissertations/771

This document has been made available through Purdue e-Pubs, a service of the Purdue University Libraries. Please contact epubs@purdue.edu for additional information.

**PURDUE UNIVERSITY
GRADUATE SCHOOL
Thesis/Dissertation Acceptance**

This is to certify that the thesis/dissertation prepared

By Ali Hekmatfar

Entitled

IMPROVING THE LABORATORY DESIGN OF ASPHALT MIXTURES TO ENHANCE ASPHALT PAVEMENT
DURABILITY

For the degree of Doctor of Philosophy

Is approved by the final examining committee:

John E. Haddock

Chair

Rebecca McDaniel

John Olek

Na Lu

To the best of my knowledge and as understood by the student in the Thesis/Dissertation Agreement, Publication Delay, and Certification Disclaimer (Graduate School Form 32), this thesis/dissertation adheres to the provisions of Purdue University's "Policy of Integrity in Research" and the use of copyright material.

Approved by Major Professor(s): John E. Haddock

Approved by: Dulcy M. Abraham

Head of the Departmental Graduate Program

5/4/2016

Date

IMPROVING THE LABORATORY DESIGN OF ASPHALT MIXTURES TO
ENHANCE ASPHALT PAVEMENT DURABILITY

A Dissertation

Submitted to the Faculty

of

Purdue University

by

Ali Hekmatfar

In Partial Fulfillment of the

Requirements for the Degree

of

Doctor of Philosophy

August 2016

Purdue University

West Lafayette, Indiana

To my parents

Reza and Sheila

For all love and support they have given me throughout all these years.

ACKNOWLEDGEMENTS

First and foremost, I would like to express my sincere gratitude to my advisor Professor John E. Haddock for his invaluable support, advice, guidance, and friendship throughout my doctorate program at Purdue University. I have learned so much under his supervision. Professor Haddock has provided me with valuable guidance and it was a great pleasure to work with him.

I would like to thank my examination committee members, Dr. Rebecca McDaniel, Professor Jan Olek, and Professor Na Lu for serving on my defense committee and for their support and advice throughout my time at Purdue. I would like to especially thank Mr. Gerald Huber for his valuable advice and constant support throughout the course of my PhD study. Special thanks to Dr. Ayesha Shah and Mr. Bill Pine who have taught me so much and supported and helped me throughout my research.

The laboratory experiments reported in this thesis were conducted at the Indiana Department of Transportation Research Division-North Central Superpave Center Laboratory in West Lafayette, Indiana and I would like to thank both for the support that has made the research possible. I also gratefully acknowledge the support of the Joint Transportation Research Program jointly administered by the Indiana Department of

Transportation and Purdue University. I would especially like to thank Heritage Research Group for all their support throughout my PhD study. I also acknowledge the assistance of Mr. Masoud Ghavani and Mr. Robert Spragg.

I would like to thank my sisters, Sara and Sogol for their patience and help throughout my studies. Finally, I offer my deepest gratitude and appreciation to my parents, Reza and Sheila, for all the love and support they have given throughout the years. This thesis would not have been written without them and I cannot thank them enough for their understanding and unconditional support throughout my life. They have been always been my motivation in life.

TABLE OF CONTENTS

	Page
LIST OF TABLES	vii
LIST OF FIGURES	x
ABSTRACT	xii
CHAPTER 1. INTRODUCTION	1
1.1 Introduction.....	1
1.2 Objectives	4
1.3 Scope.....	4
1.4 Organization of Dissertation.....	5
CHAPTER 2. LITERATURE REVIEW	6
2.1 Background.....	6
2.1.1 Materials.....	8
2.1.2 Asphalt Binder.....	8
2.1.3 Aggregate	9
2.1.4 Additives and Modifiers.....	10
2.1.5 Flexible Pavement Distresses.....	10
2.2 History of Volumetric Mixture Design.....	14
2.3 “State of the Art” in Asphalt Mixture Design	17
2.3.1 Marshall Mixture Design Method	17
2.3.2 LCPC Mixture Design Method	18
2.3.3 Superpave Mixture Design Method	21
CHAPTER 3. LABORATORY RESEARCH APPROACH	23
3.1 Laboratory Mixture Design	27
3.2 Field Trials Mixture Design.....	30

	Page
3.2.1 SR-13 Project	31
3.2.2 Georgetown Road Project	33
CHAPTER 4. LABORATORY MIXTURE PERFORMANCE	37
4.1 Dynamic Modulus Testing	37
4.2 Flow Number Testing	40
4.3 Preparing Specimens	42
4.4 Category 4, 19.0-mm Mixture	43
4.5 Category 3, 9.5-mm Mixture	47
4.6 Category 4, 9.5-mm Mixture	51
4.7 Statistical Analysis.....	54
4.7.1 Category 4, 19.0-mm Mixture.....	54
4.7.2 Category 3, 9.5-mm Mixture.....	56
4.7.3 Category 4, 9.5-mm Mixture.....	58
CHAPTER 5. FIELD MIXTURE PERFORMANCE	60
5.1 SR-13 Project.....	61
5.1.1 Pre-Field Trial Laboratory Testing	61
5.1.2 Field Trial Production Testing	64
5.1.3 Post-Field Trial Testing.....	69
5.2 Georgetown Road	97
5.2.1 Plant Mixed-Laboratory Compacted Testing	98
5.2.2 Plant-Mixed-Field-Compacted Testing	108
CHAPTER 6. SUMMARY AND CONCLUSIONS	119
6.1 Conclusions.....	121
CHAPTER 7. RECOMMENDATIONS FOR SUPERPAVE MIXTURE DESIGN TO OBTAIN BETTER IN-FIELD COMPACTION AND DURABILITY	123
LIST OF REFERENCES	125
BIBLIOGRAPHY	130
PUBLICATIONS.....	132
VITA.....	133

LIST OF TABLES

Table	Page
Table 3.1 Asphalt pavement categories.	25
Table 3.2 Experimental design.	25
Table 3.3 Aggregate gradations (percent passing) and specific gravities.....	26
Table 3.4 Asphalt mixture gradations and combined aggregate specific gravities.....	27
Table 3.5 Mixture design volumetrics.	28
Table 3.6 SR-13, Aggregate gradations and specific gravities.	31
Table 3.7 SR-13, Field core densities.	33
Table 3.8 Georgetown Road, Aggregate gradations and specific gravities.....	34
Table 3.9 Georgetown Road, Field core densities.	35
Table 4.1 Dynamic modulus specimen air voids data.	42
Table 4.2 Category 4, 19.0-mm mixture flow number data.....	46
Table 4.3 Category 3, 9.5-mm mixture flow number results.....	50
Table 4.4 Category 4, 9.5-mm mixture flow number results.....	53
Table 4.5 Category 4, 19.0-mm statistical summary.	55
Table 4.6 Category 4, 19.0-mm Bonferroni groupings.....	56
Table 4.7 Category 3, 9.5-mm statistical summary.	57
Table 4.8 Category 3, 9.5-mm Bonferroni groupings.....	58
Table 4.9 Category 4, 9.5-mm statistical summary.	59
Table 4.10 Category 4, 9.5-mm Bonferroni groupings.....	59
Table 5.1 Test specimen air voids.....	62
Table 5.2 Dynamic modulus data.	62
Table 5.3 Re-designed mixture data (truck samples).....	64
Table 5.4 Re-designed mixture data (plate samples).	66

Table	Page
Table 5.5 Estimated volumetric properties at 30 gyrations.	67
Table 5.6 SR-13, Field core densities.	68
Table 5.7 Post field trial testing plan.	69
Table 5.8 Post construction mixture statistical summary.	73
Table 5.9 Post construction mixture flow number results.	73
Table 5.10 Aged (8-year) dynamic modulus data.	74
Table 5.11 Aged (8-year) mixture Bonferroni groupings.	76
Table 5.12 Aged (8 years) flow number data.	77
Table 5.13 Aged (8 year) flow number Bonferroni groupings.	77
Table 5.14 Beam specimen air void contents.	78
Table 5.15 Beam fatigue, initial stiffness.	79
Table 5.16 Beam fatigue, number of cycles to failure.	79
Table 5.17 Beam fatigue Bonferroni groupings.	80
Table 5.18 Recovered asphalt binder continuous grades.	81
Table 5.19 Porosity and Air Voids Results.	85
Table 5.20 SR-13 Bailey Method Aggregate Ratios	90
Table 5.21 Hydraulic Conductivity Results.	94
Table 5.22 SR-13 Tortuosity Results.	96
Table 5.23 Georgetown Road Testing Plan.	98
Table 5.24 Laboratory specimen dynamic modulus statistical summary.	101
Table 5.25 Laboratory specimen dynamic modulus Bonferroni groupings.	101
Table 5.26 Laboratory compacted FN summary (51°C).	102
Table 5.27 Laboratory compacted FN Bonferroni groupings.	103
Table 5.28 Laboratory specimen SCB critical strain energy release rate.	105
Table 5.29 Georgetown Rd, porosity test results	106
Table 5.30 Hydraulic conductivity results vs. air void	107
Table 5.31 Georgetown Road Tortuosity Results.	108
Table 5.32 Dynamic modulus summary, field cores.	114
Table 5.33 Dynamic modulus, field cores Bonferroni groupings.	114

Table	Page
Table 5.34 Georgetown Road field semi-circular AV% data.	116
Table 5.35 Georgetown Road field cores, critical strain energy release rate.	116
Table 5.36 Georgetown Road field cores, recovered asphalt binder grades.	117

LIST OF FIGURES

Figure	Page
Figure 1.1 Failure in Asphalt Pavement.	2
Figure 1.2 Permeability vs. In-place Air Voids.	3
Figure 2.1 Conventional flexible pavement cross-section.	7
Figure 2.2 Full-depth asphalt pavement cross-section.	7
Figure 2.3 Composite pavement cross-section.	8
Figure 2.4 Permanent Deformation (rutting) distress.	11
Figure 2.5 Fatigue cracking in asphalt pavements.	12
Figure 2.6 Low temperature thermal cracking.	13
Figure 3.1 Category 4, 19.0-mm mixture gradations.	28
Figure 3.2 Category 3, 9.5-mm mixture gradations.	29
Figure 3.3 Category 4, 9.5-mm mixture gradations.	30
Figure 3.4 SR-13, Field trial mixture gradations.	32
Figure 3.5 Georgetown Road, Field trial mixture gradations.	35
Figure 4.1 Phase angle in dynamic modulus test.	38
Figure 4.2 Dynamic modulus master curve for two mixtures (log-log plot).	39
Figure 4.3 Dynamic modulus master curve for two mixtures (semi-log plot).	40
Figure 4.4 Typical data from flow number test.	41
Figure 4.5 Category 4, 19.0-mm master curves (log-log).	44
Figure 4.6 Category 4, 19.0-mm master curves (semi-log).	44
Figure 4.7 Dynamic modulus as a function of gyrations.	47
Figure 4.8 Category 3, 9.5-mm master curves (log-log).	48
Figure 4.9 Category 3, 9.5-mm master curves (semi-log).	49
Figure 4.10 Category 4, 9.5-mm master curves (log-log).	52

Figure	Page
Figure 4.11 Category 4, 9.5-mm master curves (semi-log).	52
Figure 5.1 Dynamic modulus data for the mixture designs.	63
Figure 5.2 Post construction mixture master curves (log-log).	71
Figure 5.3 Post construction mixture master curves (semi-log).	72
Figure 5.4 Aged (8-year) mixture master curves (log-log).	75
Figure 5.5 Aged (8-year) mixture master curves (semi-log).	75
Figure 5.6 Example of break between coarse and fine aggregate for 19.0 NMPS mixture.	87
Figure 5.7 Coarse-graded mixture fractions.	88
Figure 5.8 Bailey Method Coarse Aggregate Ratio.	89
Figure 5.9 FDOT Hydraulic Conductivity (Falling Head Permeability) Permeameter.	93
Figure 5.10 Laboratory compacted specimen master curves (log-log plot).	100
Figure 5.11 Laboratory compacted specimen master curves (semi-log plot).	100
Figure 5.12 Laboratory specimen SCB test results.	105
Figure 5.13 Hamburg test results, standard mixture cores.	109
Figure 5.14 Hamburg test results, re-designed mixture cores.	110
Figure 5.15 Coring horizontally from road cores.	111
Figure 5.16 Two small specimens (38-mm x 110-mm) taken from road cores.	112
Figure 5.17 Master curves, field cores (log-log plot).	113
Figure 5.18 Master curves, field cores (semi-log plot).	113
Figure 5.19 Georgetown Road field cores, SCB test results.	115

ABSTRACT

Hekmatfar, Ali. Ph.D., Purdue University, August 2016. Improving the Laboratory Design of Asphalt Mixtures to Enhance Asphalt Pavement Durability. Major Professor: John E. Haddock.

Most departments of transportation, including Indiana's, currently use the Superpave mixture design method to design asphalt mixtures. This method specifies that the optimum asphalt content for a given gradation be selected at 4 percent air voids. During construction, these mixtures are typically compacted to 7-8 percent air voids. If mixtures were designed to be more compactable in the field they could be compacted to the same density as the laboratory mixture design, which would increase pavement durability by decreasing the in-place air voids. The objective of this research was to enhance the asphalt mixture design method in order to increase in-place asphalt pavement durability without sacrificing the permanent deformation characteristics of the mixture.

Three asphalt mixtures were designed using the standard Superpave design method at 100 gyrations of the Superpave Gyratory Compactor, suitable for traffic levels of 3 to 30 million Equivalent Single Axle Loads. Each mixture was then used as a starting point to design three additional mixtures using 70, 50, and 30 gyrations, with optimum binder content chosen at 5 percent air voids, rather than the currently specified 4 percent. The effective asphalt content was held constant for the original and redesigned mixtures.

Permanent deformation characteristics of each three sets of four mixtures were determined by measuring the dynamic modulus and flow number. The results suggest that the mixture designs produced using 70, 50, and 30 gyrations had permanent deformation characteristics equal to or better than the original 100-gyrations mixtures.

After promising laboratory results, two field trials were placed on SR-13 near Fort Wayne, Indiana, and on Georgetown Road in Indianapolis, Indiana. Samples from the standard and re-designed mixtures collected during construction were compacted and tested to determine permanent deformation characteristics. The results suggest that the re-designed mixtures should have similar permanent deformation performance to their standard mixture counterparts. Field density test results indicate the re-designed mixtures can be field compacted to 5 percent air voids using the same compactive effort as was used for the standard mixtures.

CHAPTER 1. INTRODUCTION

1.1 Introduction

In United States (US) there are more than 2 million miles of paved roads, which about 93 percent of those are surfaced with asphalt mixtures. Most of them are conventional flexible pavements; while others are just asphalt overlays on top of concrete pavements. Asphalt pavements provide the highest level of drivability at the best economical price (National Asphalt Pavement Association, 2014; Asphalt Pavement Alliance, 2014).

The asphalt mixtures that comprise the bulk of these pavements are engineered products composed of approximately 95 percent aggregate and 5 percent asphalt binder, by mass. When properly combined and constructed, the aggregate acts to carry the applied loads while the asphalt binder, acts like a “glue” to bond the aggregates together. Asphalt pavements are permanent structures means they never need to be replaced; but needs maintenance every 20-25 years. (National Asphalt Pavement Association, 2014).

Asphalt pavements in Indiana currently have nominal service lives of 15-20 years. Generally, these pavements reach the end of their service lives based on durability issues associated with asphalt binder aging. As the asphalt binder ages, stiffness and embrittlement increase. In terms of surface condition, the results are typically displayed as cracking, which is usually non-load associated (thermal or reflective) but may also include load associated (fatigue) cracking as seen in Figure 1.1. Asphalt binder aging is predominantly related to oxidation, which is controlled by access of air into the asphalt pavement. Reducing the air permeability of compacted asphalt mixtures decreases the rate of asphalt binder aging, and thus allows for a longer pavement life.



Figure 1.1 Failure in Asphalt Pavement (Concrete Parking, 2011).

The current Indiana Department of Transportation (INDOT) method of design and construction (quality assurance) of asphalt pavements targets a 4 percent air voids (V_a)

content in the laboratory compacted specimens. On the road, the density acceptance criterion for INDOT Section 401, *Quality Control. Quality Assurance, QC/QA, Hot Mix Asphalt, HMA, Pavement*, mixtures is based on 90 percent of field core densities being within statistical limits with a lower threshold limit of 91 percent of the mixture maximum theoretical specific gravity (G_{mm}). The average density needed to comply with this specification is approximately 93 percent (7 percent V_a). The result is that when the in-place density specification is met, 10 percent of the pavement area may have a density of less than 91 percent, meaning a V_a content of more than 9 percent. Test data has shown (Figure 1.2) that when in-place densities begin to rise above 8 percent, air permeability begins to increase dramatically (Cooley et al, 2002).

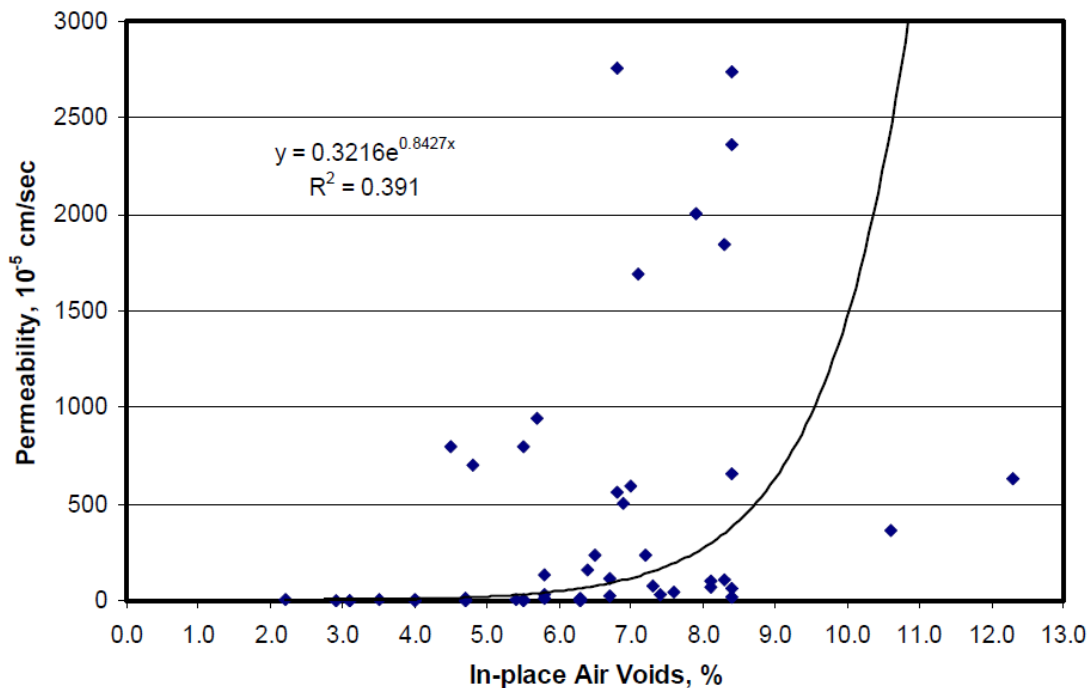


Figure 1.2 Permeability vs. In-place Air Voids (Cooley et al, 2002).

Increasing average in-place asphalt mixture densities to 95 percent (V_a of 5 percent) would significantly decrease asphalt binder aging. Conservatively, the estimated pavement life increase would be two to three years, representing a 12 to 20 percent increase in pavement life. The key to achieving this in-place density is to optimize the relationship between laboratory and field compaction.

1.2 Objectives

Since increasing asphalt mixture field densities can lead to increased pavement life, the objective of the research is to enhance the asphalt mixture laboratory design procedure as it relates to field compaction in order to increase asphalt pavement durability without sacrificing permanent deformation characteristics of the mixtures. The mixtures designed with the enhanced method are expected to be compacted in the field to the laboratory design level (5% air voids) and to withstand additional densification under traffic (remain at 5% air voids).

1.3 Scope

The original scope of this research encompassed a laboratory effort aimed at developing an enhanced asphalt mixture design method that would allow for a mixture in the laboratory to be designed at the same density (air voids) to which it will be compacted when placed in the field. However, after the laboratory study began, it was decided that a field trial should be completed to see if the laboratory findings were applicable to the field. Two trial

sections were built, one on SR-13 near Fort Wayne, Indiana, and the second on Georgetown Road in Indianapolis, Indiana. During construction, asphalt mixture samples from both the original and re-designed mixtures were obtained and tested.

1.4 Organization of Dissertation

This dissertation contains 7 chapters, the layout of which is:

- Chapter 1: Introduction
- Chapter 2: Literature Review
- Chapter 3: Material Selection and Mixture Design
- Chapter 4: Laboratory Mixture Performance
- Chapter 5: Field Trials Mixture Performance
- Chapter 6: Summary of Findings and Conclusions
- Chapter 7: Recommendations for Superpave Mixture Design to Obtain Better In-Field Compaction and Durability

CHAPTER 2. LITERATURE REVIEW

2.1 Background

The word “pavement” comes from the original Latin, “pavire,” meaning to beat or tread down, and later, “Pavimentum,” meaning trodden-down floor (Whitaker, 2010). Today there are two types of pavements, flexible and composite, that make use of asphalt mixtures. Flexible pavements can be further divided into conventional flexible pavements (Figure 2.1) and full-depth pavements (Figure 2.2). The former is constructed of granular materials overlain with asphalt mixtures, while the latter eliminates the granular materials and the asphalt mixture is placed directly on the subgrade. Composite pavements are composed of both portland cement concrete (PCC) and asphalt mixtures. Traditionally, the term composite pavement has referred to older PCC pavements that were rehabilitated by adding some thickness of an asphalt overlay (Figure 2.3). However, today the term composite pavement could just as easily refer to PCC placed over an old flexible pavement, a process known as “whitetopping,” or even an asphalt underlayment for a new continuously reinforced concrete pavement (CRCP) (Huang, 2004). The focus of the research described in this document is on conventional flexible pavements, although the outcomes may be just as applicable to full-depth asphalt and the asphalt portions of composite pavements.

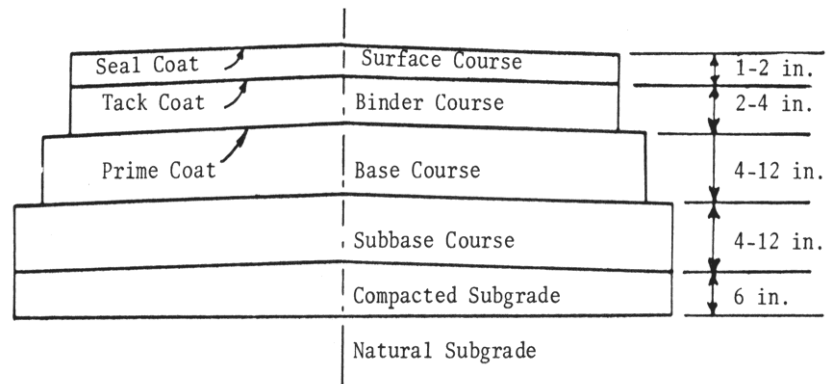


Figure 2.1 Conventional flexible pavement cross-section (Huang, 2004).

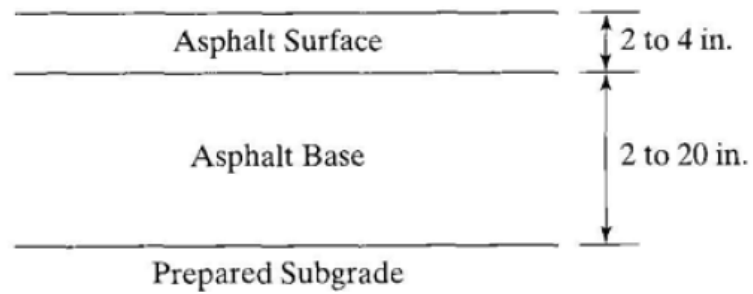


Figure 2.2 Full-depth asphalt pavement cross-section (Huang, 2004).

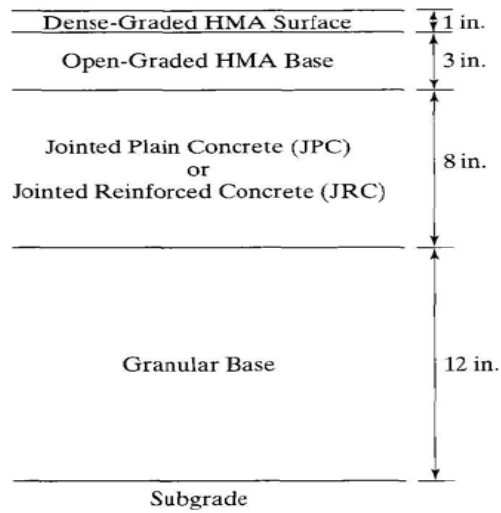


Figure 2.3 Composite pavement cross-section (Huang, 2004).

2.1.1 Materials

In addition to aggregates and asphalt binder, asphalt mixtures may contain one, or any combination of asphalt binder modifiers, such as crumb rubber or polymers, reclaimed asphalt pavement (RAP), reclaimed asphalt shingles (RAS), and several other types of additives or modifiers.

2.1.2 Asphalt Binder

The vast majority of asphalt binders used throughout the world today are obtained through distillation of crude oil (petroleum) using various refining techniques. At room temperature (25°C) asphalt binder is a highly viscous, black material whose primary purpose is in the production of asphalt mixtures for pavements. Worldwide, asphalt binders are most

typically classified by one of three grading systems, penetration grading, viscosity grading, or performance grading. The performance grading system, developed during the Strategic Highway Research Program (SHRP), selects an appropriate binder grade based on the climate in which it will be put into service, and is the most widely used asphalt grading system in the US. For example a performance graded PG 64-22 grade is intended for use in a climate which has an average seven-day maximum temperature of 64°C and a minimum pavement design temperature of -22°C. Typical performance graded binders are PG 64-22, PG 64-28, and PG 70-22 (Brown et al, 2009).

2.1.3 Aggregate

Aggregates used in asphalt mixtures are largely from locally sourced, natural rock supplies. Rock formations, and the aggregates produced from them can be divided into three types, igneous, sedimentary, and metamorphic. Natural and manufactured sands can also be used in asphalt mixtures. The natural sands consist primarily of the most resistant final residue of natural rock deterioration, while crushing natural rock produces the latter. Non-naturally occurring aggregates, such as blast furnace and steel slags can also be used. Slags are a byproduct of iron and steel production.

The physical properties of aggregates, and to a lesser extent, the chemical properties, determine their suitability for use in asphalt mixtures. Aggregates are usually classified into one of three size groups: coarse aggregates, fine aggregates, and mineral fillers. Coarse aggregates are those larger than the No. 4 (4.75-mm) sieve and sands are smaller than the

No. 4 (4.75-mm) sieve, but larger than the No. 200 (0.075-mm) sieve. Mineral fillers are materials with particles all smaller than the No. 200 (0.075-mm) sieve. Aggregates suitable for use in asphalt mixtures will be hard, tough, strong, durable, properly graded, with low porosity and clean, rough surfaces (Brown et al, 2009).

2.1.4 Additives and Modifiers

The use of modifiers in asphalt mixtures has increased significantly in the past 15-20 years with the goal of enhancing asphalt mixture performance. Some additives are blended into the asphalt binder and others are added directly to the asphalt mixture. A few of the most common binder additives are styrene butadiene styrene (SBS), styrene butadiene rubber (SBR), and ground tire rubber (GTR). While modifiers improve one or more asphalt mixture properties, they can sometimes also worsen one or more properties. For example, a given additive might improve the stiffness of an asphalt mixture at high temperatures, but also make that mixture more brittle at low temperatures (Brown et al, 2009).

2.1.5 Flexible Pavement Distresses

The resistance, or lack thereof, to pavement distresses is a measure of asphalt mixture performance in flexible pavements. The three main flexible pavement distresses are permanent deformation, usually manifested as rutting, fatigue cracking, and thermal cracking. How well an asphalt mixture resists these distresses defines the mixture's durability (Brown et al, 2009).

Permanent deformation, or rutting, is permanent or unrecoverable deformation in one or more of the pavement layers due to inadequate layer thickness for the applied traffic, or due to inadequate strength of one or more of the layer materials. Classical rutting occurs in the subgrade and the resulting deformation at the surface is simply due to the pavement layers conforming to the subgrade shape. Due to increased traffic and tire pressures over the last 30 years, rutting of the asphalt surface mixture has become more common. This type of rutting is due to shear failure in the asphalt surface mixture and can be addressed by materials and asphalt mixture design. To resist asphalt mixture shear failure, the asphalt surface mixture should contain high quality aggregates having a proper gradation, adequate asphalt binder content, and the correct asphalt binder grade. Figure 2.4 shows rutting distress for asphalt pavements (Anderson et al, 2002; Brown et al, 2009).



Figure 2.4 Permanent Deformation (rutting) distress (National Highway Institute, 1998).

Fatigue cracking occurs in pavements under repeated traffic loads. Fatigue resistance is a function of pavement design, materials, and asphalt mixture design. If a pavement has inadequate thickness, poor materials, or improperly designed asphalt mixtures, or any

combination of the three, the likelihood of fatigue cracking is increased. From a mixture design standpoint, data have shown that asphalt mixtures with higher asphalt binder contents, higher densities (lower air voids), or both tend to have better fatigue resistance than the mixtures with lower asphalt binder contents and densities (higher air voids). Figure 2.5 shows fatigue cracking for asphalt pavements (Asphalt Research Program, 1994; Brown et al, 2009).

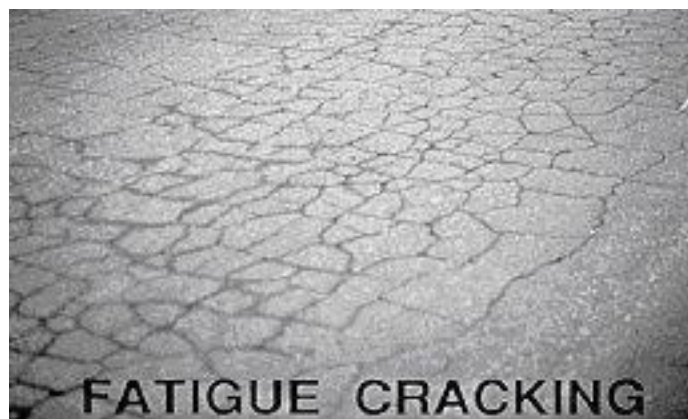


Figure 2.5 Fatigue cracking in asphalt pavements (National Highway Institute, 1998).

At low temperatures the asphalt surface mixture of a flexible pavement will attempt to contract. As it does so, since it is effectively “pinned” at either end due to its length, stress will begin to build in the mixture. If this stress exceeds the tensile strength of the mixture, the mixture will begin to crack at repeated intervals in order to relieve the stress. This “low temperature” cracking is primarily a function of the low temperature properties of the asphalt binder in the mixture. However, low temperature cracking can be somewhat controlled by mixture design; a mixture with higher density (lower air voids) and thicker asphalt binder films surrounding the aggregate particles will be more resistant to low

temperature cracking. Figure 2.6 shows low temperature thermal cracking for asphalt pavements (Marasteanu et al, 2012; Brown et al, 2009).



Figure 2.6 Low temperature thermal cracking (Marasteanu et al, 2009).

Durability- how long an asphalt mixture performs without severe rutting, cracking, or other type of distress - determines pavement performance. An asphalt mixture must contain adequate amounts of aggregates and asphalt binder, and be compacted to the proper density, in order for it to successfully complete its service life. The primary reason for conducting a laboratory mixture design for asphalt mixtures is to determine the best combination of available materials in order to achieve proper compaction on the road and in turn to optimize the asphalt mixture performance (Oliver, 2007; Vivar and Haddock, 2006).

2.2 History of Volumetric Mixture Design

The design of asphalt mixtures has been studied since the early 1900's. From the beginning there was a desire to understand the interaction of aggregates, asphalt binder, and the voids created during compaction. In the days before a formal mixture design method was developed, asphalt binder content was determined by evaluating gradation. In order to provide satisfactory durability, minimum asphalt binder thickness should be provided (Goetz, 1989).

By the 1920's, during development of the Hubbard-Field method of mixture design, the air void content was found to be an important parameter related to a mixtures' field performance. "The Hubbard-Field mixture design method is based on air voids percent and a minimum amount of asphalt binder thickness." (Hubbard et al., 1935). Voids in total mixture and voids in aggregate mass were two volumetric properties that were specified (Hubbard et al., 1935; Hubbard et al., 1932).

Separate from the work of Hubbard and Field, the Michigan State Highway Department developed a mixture design method in the early 1930's in which the shape of the gradation curve was evaluated and expressed as a "Gradation Modulus" from which the "Bituminous Capacity of Aggregate" was determined (Vokac, 1932).

The mixture designs that were discussed above were all according to a “gradation law” which controlled the properties of an asphalt mixture and that the asphalt binder demand was tied to gradation.

The Marshall method of mixture design was developed as an advancement of the Hubbard-Field method. In the Hubbard-Field method a Proctor hammer (the same as used in soils) was used to compact asphalt mixture samples. In the Marshall method, the diameter of the hammer face was increased to match the diameter of the specimen. The Hubbard-Field stability test, an extrusion type test, was replaced with the Marshall stability test.

Superpave grew as an extension of Marshall mixture design. Important components of the Marshall method were carried over to Superpave (Cominsky et al., 1994). Mixture volumetric properties - that is, air voids, voids in the mineral aggregate (VMA) and voids filled with asphalt (VFA) - are empirical properties that control mixture behavior. These were carried forward from the Marshall method and incorporated into the Superpave asphalt mixture design method. However, a gyratory compactor replaced the Marshall hammer for mixture specimen compaction. The Marshall stability test was to be replaced by a test or tests that would measure more fundamental engineering properties, but to-date work continues on mixture property tests and none have been widely adopted. In the meantime, Superpave designed mixtures are controlled through the volumetric properties.

In concept, asphalt mixture is a simple material, merely a combination of aggregate and asphalt binder. The objective when designing an asphalt mixture is to optimize its properties with respect to the stability, durability, flexibility, fatigue resistance, skid resistance, permeability, and workability. This is often accomplished with the evaluation of the volumetric properties (V_a , VMA, and VFA), which are important to the engineering properties of the mixture. Air voids are the small air spaces between the binder-coated aggregate particles in an asphalt mixture, while VMA is defined as the inter-granular void space between the aggregate particles in a compacted asphalt mixture,

including the air voids and the volume of effective asphalt binder (V_{be}). VFA is the percentage of the VMA that is filled with asphalt binder.

Historically, asphalt mixture design methods used empirical design properties established on the basis of observed field performance. That is how the volumetric properties were first identified as being performance related. Generally, when the volumetric properties are correct, asphalt mixture performance will be adequate. However, the specification of volumetric properties does not guarantee the performance of the mixture and that is why a simple performance test is being sought.

Today in the U.S., asphalt mixture design is currently in a state of change with the advent of the Superpave mixture design method and the phasing out of older methods. Since early implementation started in 1994, Superpave mixtures have become common in nearly all parts of the country. In the next few years it is expected that even more asphalt mixtures will be designed using Superpave concepts as additional states, as well as other countries begin to adopt the method.

2.3 “State of the Art” in Asphalt Mixture Design

The Superpave asphalt mixture design method contains elements of both the Marshall mixture design method and the mixture design method developed by the Laboratoire Central des Ponts et Chaussées (LCPC), the French equivalent of the Federal Highway Administration (FHWA). To truly understand the various asphalt mixture design methods it is important to consider the relationship and differences in philosophy among the three methods, Marshall, LCPC, and Superpave.

2.3.1 Marshall Mixture Design Method

The Marshall mixture design philosophy involves selecting an aggregate gradation and a compaction level. Aggregate is mixed with varying percentages of asphalt binder and then compacted using a drop hammer. The air voids in the compacted samples are then determined and compared to the specification values. Normally, 3-5% air voids is desired with a VMA requirement that is based on the nominal maximum size of the aggregate blend. If the specified air voids cannot be achieved by merely varying the asphalt content, a new aggregate gradation, or even the use of new aggregate materials, must be examined. A design is selected when the gradation is within a specified range and the volumetrics meet specified criteria (Asphalt Institute, 1989).

The philosophy of Marshall design compaction is that the density of specimens in the mold should match the ultimate density that will be obtained after the mixture has been in service for some period of time. Typically air voids in the Marshall mold were designed to be from

3 to 5% (McFadden, 1948; Griffith, 1949) while the mixture was expected to be compacted to 8 to 10% air voids on the road. After being trafficked – some believe for two to four years, others believe at the end of in-service life (15-20 years) – the density would increase, leaving only 3 to 5% air voids in the pavement.

Early developmental research for the Marshall design method sought to correlate the density of field test sections to the number of blows of a Marshall hammer. As a result, the design compaction level is related to the expected amount of traffic. Three levels of compaction were recommended, 35, 50 and 75 blows on each side of a specimen to be used for light, medium and heavy traffic, respectively (McFadden, 1948).

2.3.2 LCPC Mixture Design Method

In the 1960's and 70's, LCPC developed a new method of mixture design. The design method is based on the principle that an asphalt mixture should be designed and, during construction, compacted to its ultimate density. Therefore, no post construction densification is anticipated. The density at the end of the mixture's in-service life is the same as the density immediately after construction.

Developmental research for the LCPC method sought to establish a laboratory design compactive effort to match the compaction that occurs during construction. LCPC defined

a standard rolling train as 16 passes of a 3 tonnes (6,600 lbs) pneumatic-tired roller and having a tire pressure of 600 kPa (87 psi).

A full-scale laboratory compaction bench was built and a range of different mixtures was compacted. The compaction bench was 2.1 m (7 feet) wide and 4.2 m (14 feet) long with one pneumatic tire. It was discovered that for a specific mixture the density achieved under a standard rolling train was related to the lift thickness. When lift thickness was too thin, density was lower (Moutier, 1977).

As a result, a standard lift thickness was established based on maximum aggregate size. The required lift thickness is five times the maximum aggregate size. This is equivalent to six times the nominal maximum aggregate size as defined by the Superpave mixture design method. So for a 0/14 mixture, the maximum aggregate size is 14 mm (0.55 in.) and the lift thickness is 80 mm (3 in.), about six times the nominal maximum aggregate size of 12.5 mm (0.5 inch). The method results in the use of thick lifts in France. In the U.S. lifts tend to be thinner; about four times the nominal maximum aggregate size.

For laboratory compaction, LCPC chose a gyratory compactor. They had prior experience with the Marshall hammer and with static compaction (the Duriez method of mixture design, used before the LCPC method, used static compaction). In 1959, a French delegation visited Texas and witnessed the Texas gyratory compactor. Studies were done, and by 1968 a gyratory compaction protocol was developed in France.

The Texas compactor uses an angle of nearly six degrees and applies gyrations at the rate of one per second in bursts of three gyrations. After each set of gyrations the specimen is checked for resistance to further compaction. If the specimen is not yet resistant enough, an additional set of gyrations is applied. Compaction is complete when the specimen is sufficiently resistant to compaction (Ortolani et al., 1951).

LCPC designed and constructed a gyratory compactor that applied gyrations continuously instead of in bursts. Studies were done to investigate the effect of gyratory angle and vertical pressure for different types of mixtures. Studies were also done to select specimen size. As a result of these studies LCPC standardized the gyratory angle at one degree with a vertical pressure of 600 kPa (87 psi). LCPC also monitored the rate of increase in density and discovered a nearly linear relationship between density and the log of the number of gyrations (Moutier, 1974).

After correlating compaction curves in the gyratory to densification curves from the laboratory compaction bench, LCPC set the design number of gyrations to equal the lift thickness in millimeters. Therefore, a 14-mm maximum size mixture (12.5-mm nominal maximum size) would be constructed 80 mm (3 in.) thick (six times maximum size) and the design compaction would be 80 gyrations.

In the LCPC method, the design asphalt binder content is fixed for each mixture type; there are adjustment factors for asphalt absorption, aggregate specific gravity, and gradation or surface area. Since the effective asphalt binder volume is fixed, the design method becomes

one of selecting an aggregate structure to provide the correct range of air voids at the design compaction. The range of allowable air voids is 4 to 8 percent. Most designers target 5% air voids. In the field, the required density is 95% of maximum theoretical gravity. LCPC has documented that there is little or no increase in density under traffic during the pavement in-service life.

2.3.3 Superpave Mixture Design Method

The Superpave mixture design method and procedures were developed as part of the Strategic Highway Research Program (SHRP) to be a comprehensive system for the design and modeling of asphalt materials. Asphalt binder testing was implemented to relate the performance of the binder to the climate and traffic level. Aggregate quality specifications were established in an effort to improve the performance of the resulting mixtures. The gyratory compactor was developed as a laboratory tool that more closely simulates field compaction of asphalt mixtures.

During SHRP, developmental studies focused on relating gyratory compactive effort to the density of pavements at the end of their in-service lives. The underlying principle in SHRP was carried over from the Marshall method. The design air voids were to be selected at a low level (air voids were 4% instead of the range of 3 to 5%) and construction air voids were expected to be 8%. The N-design experiment during SHRP determined the number of gyrations required to match in-place density for pavements that were at least 12 years

old and had been subjected to various levels of traffic as measured by Equivalent Single Axle Loads (ESAL) (Huber et al., 1994). The decision to fix design air voids at 4%, instead of using the range of 3 to 5% came about because of an issue dealing with VMA.

In the late 1980's the Asphalt Institute was evaluating issues dealing with VMA. The reason for VMA, since its inclusion in Marshall design in 1962, was to ensure that a mixture had a minimum volume of effective asphalt binder and a minimum volume of air voids. Minimum VMA was fixed according to aggregate nominal maximum aggregate size and was constant regardless of the design air voids. As a result the minimum effective volume of asphalt binder could vary. For example, a 12.5-mm nominal maximum size mixture required 14% VMA. The volume of effective asphalt binder could range from 11 to 9% depending on whether the design air voids were chosen at 3 or 5 percent. As a result, in 1989 the Asphalt Institute changed the design criteria in MS-2, the *Manual of Mix Design Methods*, from a range of 3 to 5% to a single value of 4 percent.

During SHRP, consideration was given to discontinuing the use of VMA and instead specifying a minimum effective asphalt volume, for example, specifying a minimum effective asphalt volume of 10% for a 12.5-mm nominal maximum mixture, and allowing the air void content to range between 3 to 5%. Instead, the decision was made to keep VMA as a design criterion. To prevent the problem of effective asphalt volume varying depending on design air voids, the decision was made to adopt the Asphalt Institute recommendation of a constant 4% design air void criteria.

CHAPTER 3. LABORATORY RESEARCH APPROACH

In order to complete the study objective to enhance asphalt mixture laboratory design as it relates to field compaction without sacrificing mixture permanent deformation characteristics, three appropriate asphalt mixtures that had been used on INDOT projects were chosen for testing. This involved considering various combinations of factors such as traffic categories, aggregate types, mixture types (gradations), and asphalt binder types. These three existing mixture designs were used as the basis for the mixtures evaluated in this study.

Each of the three existing mixtures used RAP, RAS, or both. These recycled materials served to further confound the laboratory experiment. Therefore, a standard mixture design meeting all applicable INDOT specifications was completed using the current INDOT mixture design method with the same materials and design gyrations as the existing mixtures but excluding RAP and RAS. The three resulting asphalt mixture designs are referred to in this report as the “standard” mixture designs.

For each standard mixture design, three additional mixture designs were completed using lower N_{design} levels. The optimum binder content for each of these “re-designed” mixtures was selected at 5 percent air voids; the V_{be} and VMA were the same as in the

corresponding standard design. It was important to keep the V_{be} as constant as possible for each set of mixtures (standard and re-designed) because it is the effective binder that promotes asphalt mixture durability. In order to increase the design air voids by one percent, but keep the V_{be} constant, the VMA must increase by one percent, which can be achieved by varying the aggregate proportions to meet the design criteria.

With the job-mix formula (JMF) for standard and re-designed mixtures established, test specimens were prepared for dynamic modulus and flow number testing according to AASHTO T 342-11, "Determining Dynamic Modulus of Hot Mix Asphalt (HMA)," and AASHTO TP 79-10, "Determining the Dynamic Modulus and Flow Number for Hot Mix Asphalt (HMA) Using the Asphalt Mixture Performance Tester (AMPT)," respectively. Specimens for the standard designs were produced at their anticipated density in the field which is 7 percent air voids according to current test method standards. Specimens for the re-designed mixtures were produced at 5 percent air voids; this is the anticipated in-service air voids level for the re-designed mixtures.

The dynamic modulus ($|E^*|$) and the flow number (FN) were determined for the standard and re-designed mixtures. The $|E^*|$ is commonly referred to as the asphalt mixture stiffness, and FN is believed to denote the onset of tertiary (plastic) flow in an asphalt mixture. A higher value of $|E^*|$ indicates a stiffer mixture. The FN is believed to be a reliable indicator of in-service rutting; the higher the FN, the more loading an asphalt mixture can tolerate without rutting. The resulting data were analyzed to determine how the dynamic moduli and flow number values for the re-designed mixtures compared to those of the standard mixtures.

In order to keep the experiment to a manageable level, the three asphalt mixtures were chosen to represent two traffic categories (Categories 3 and 4, as shown in Table 3.1), both requiring an N_{design} of 100 gyrations. These two traffic levels account for approximately 50 percent of the asphalt mixture designs used in Indiana. The mixtures are of two sizes, 9.5- and 19.0-mm. Following conventional practice, 100 gyrations of the Superpave Gyratory Compactor (SGC) were used when designing the standard mixtures. The re-designed mixtures were designed using 70, 50 and 30 gyrations of the SGC. Again, optimum binder content for re-designed mixtures was selected at 5 percent air voids, not 4 percent as the standard mixtures. The experimental design is shown in Table 3.2.

Table 3.1 Asphalt pavement categories.

Category	Equivalent Single Axle Loads	N_{design}
1	< 300,000	50
2	300,000 to < 3,000,000	75
3	3,000,000 to < 10,000,000	100
4	10,000,000 to < 30,000,000	100
5	$\geq 30,000,000$	125

Table 3.2 Experimental design.

				Mixture Type		
				9.5-mm	19.0-mm	
Pavement Category	3	Number of Gyrations	30	X		
			50	X		
			70	X		
	4		30	X	X	
			50	X	X	
			70	X	X	

In consultation with the Study Advisory Committee (SAC) the following additional experimental factors and factor levels were chosen:

- One asphalt binder grade, PG 64-22.
- One aggregate gradation type, coarse-graded, defined as a mixture with a gradation that passes below the primary control sieve (PCS) control point.
- Three coarse aggregate types, limestone, dolomite, and air-cooled blast furnace (ACBF) slag.

Fine aggregates used in the mixtures include limestone, dolomite, and natural sands. Baghouse fines from an asphalt plant were also incorporated to ensure adequate levels of fines (minus 0.075 mm material) and proper dust ratios. The gradations and bulk specific gravities (G_{sb}) of the aggregates are shown in Table 3.3.

Table 3.3 Aggregate gradations (percent passing) and specific gravities.

Materials	Limestone				Blast Furnace Slag	Dolomite			Natural Sand	Bag House Fines
Sieve Size, mm	#8	#11	#12	#24 Sand	#11	#11	#12	#24 Sand		
25.0	100.0									
19.0	90.3									
12.5	49.7	100.0	100.0		100.0	100.0	100.0			
9.5	25.8	83.3	99.6	100.0	84.4	89.1	99.9	100.0	100.0	
6.3	13.0	44.2	63.8	99.6	41.5	43.3	79.9	99.7	98.6	
4.75	6.8	25.2	46.4	99.4	21.7	22.1	70.7	99.6	97.9	
2.36	2.6	4.7	11.1	90.6	6.0	6.8	20.8	94.9	90.8	
1.18	2.0	2.2	4.1	56.0	4.4	2.9	6.3	63.4	75.3	
0.600	1.7	1.9	2.5	33.4	3.7	1.8	2.6	36.7	57.3	100.0
0.300	1.4	1.7	2.1	16.1	3.2	1.4	1.6	20.1	23.4	99.4
0.150	1.2	1.5	1.9	7.8	2.6	1.2	1.2	8.9	2.4	97.8
0.075	1.0	1.4	1.7	5.0	2.0	0.9	1.0	4.4	1.1	94.6
G_{sb}	2.664	2.664	2.655	2.671	2.442	2.681	2.688	2.748	2.612	2.700

3.1 Laboratory Mixture Design

The Category 4, 19.0-mm asphalt mixtures consisted of limestone coarse aggregate, limestone and natural sand, and baghouse fines as filler. Several trial gradations were tested before the final mixture gradations were determined. The gradations for the standard and re-designed mixtures are given in Table 3.4 and plotted in Figure 3.1. The volumetric properties of the mixtures at optimum binder contents are shown in Table 3.5.

Table 3.4 Asphalt mixture gradations and combined aggregate specific gravities.

Mixture Sieve Size, mm	Category 4, 19.0-mm				Category 3, 9.5-mm				Category 4, 9.5-mm		
	N100	N70	N50	N30	N10 0	N70	N50	N30	N10 0	N50	N30
25.0	100.0	100.0	100.0	100.0							
19.0	97.4	97.4	96.1	95.3							
12.5	86.4	86.4	79.9	75.5	100.0	100.0	100.0	100.0	100.0	100.0	100.0
9.5	77.0	77.4	68.4	62.1	97.4	97.3	95.6	95.4	95.3	94.7	94.1
6.3	59.6	60.7	55.1	51.8	75.8	76.0	71.6	72.6	72.8	72.2	71.4
4.75	51.2	52.7	48.6	46.8	65.4	65.7	60.0	61.6	61.9	61.3	60.5
2.36	36.5	38.2	37.8	39.3	33.0	34.7	38.1	43.7	34.0	38.2	42.4
1.18	22.8	23.9	23.9	25.5	19.1	20.4	24.6	29.5	20.4	24.9	29.2
0.600	14.6	15.3	15.3	16.6	12.4	12.9	16.1	19.4	12.8	16.4	19.7
0.300	8.5	8.8	8.8	9.7	7.8	7.7	9.5	11.3	7.6	9.9	11.5
0.150	5.6	5.7	5.6	6.4	4.9	4.4	5.3	6.0	4.2	5.7	6.1
0.075	4.4	4.5	4.4	5.1	4.0	3.4	4.0	4.5	3.0	4.3	4.6
G _{sb}	2.665	2.665	2.650	2.651	2.692	2.692	2.692	2.694	2.631	2.630	2.626

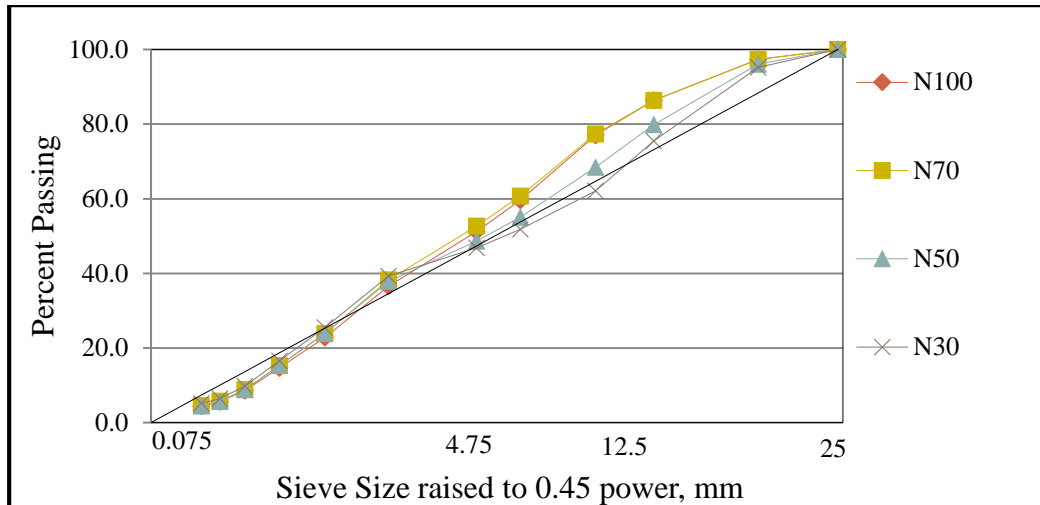


Figure 3.1 Category 4, 19.0-mm mixture gradations.

Table 3.5 Mixture design volumetrics.

Category 4, 19.0-mm Mixture						
N_{design}	Avg. V_a , %	Avg. G_{sb}	Avg. VMA, %	Avg. VFA, %	P_{be} , %	Avg. Dust Ratio
100	4.0	2.665	13.6	70.6	4.1	1.1
70	4.9	2.665	14.5	66.3	4.1	1.1
50	4.9	2.650	14.4	66.0	4.1	1.1
30	4.9	2.651	14.9	67.2	4.3	1.2
Category 3, 9.5-mm Mixture						
N_{design}	Avg. V_a , %	Avg. G_{sb}	Avg. VMA, %	Avg. VFA, %	P_{be} , %	Avg. Dust Ratio
100	4.1	2.692	15.0	72.9	4.6	0.9
70	5.1	2.692	16.0	67.9	4.6	0.7
50	4.9	2.692	15.8	68.9	4.6	0.9
30	5.3	2.694	16.3	67.6	4.7	0.9
Category 4, 9.5-mm Mixture						
N_{design}	Avg. V_a , %	Avg. G_{sb}	Avg. VMA, %	Avg. VFA, %	P_{be} , %	Avg. Dust Ratio
100	3.8	2.631	15.0	74.9	4.8	0.6
50	4.9	2.630	16.4	70.0	5.0	0.9
30	5.0	2.626	16.4	69.6	5.0	0.9

The Category 3, 9.5-mm asphalt mixtures were produced from limestone coarse aggregate, limestone sand, and baghouse fines as filler. The gradations of the four mixtures are shown in Table 3.4 and plotted in Figure 3.2; the volumetric properties are shown in Table 3.5.

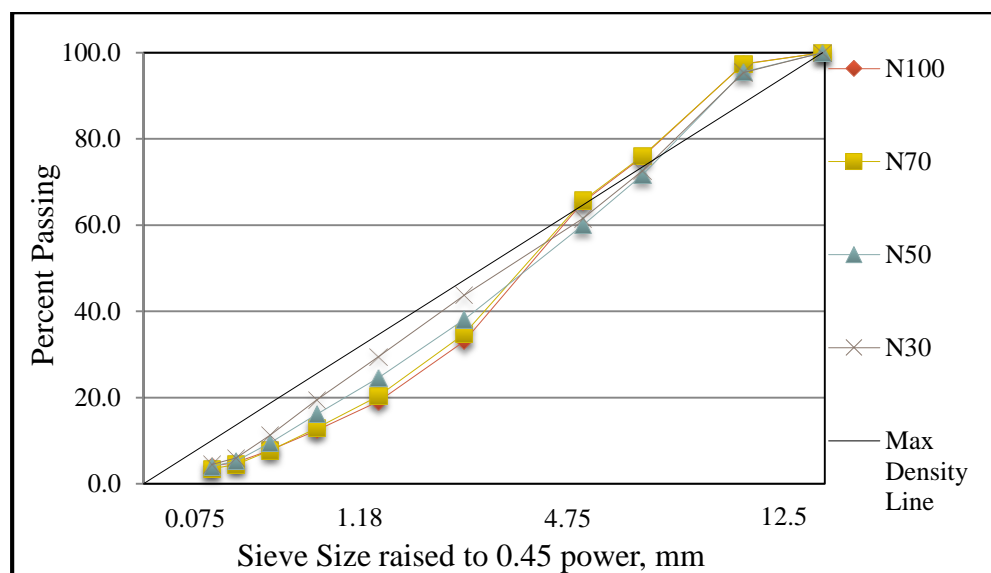


Figure 3.2 Category 3, 9.5-mm mixture gradations.

Finally, the Category 4, 9.5-mm mixtures were made with dolomite and slag coarse aggregates, dolomite and natural sands, and baghouse fines. The gradations of the mixtures are shown in Table 3.4 and plotted in Figure 3.3. The volumetric properties are given in Table 3.5. Only three mixture designs were completed for this mixture, the standard design with an N_{design} of 100, and re-designed mixtures compacted with N_{design} values of 50 and 30. Mixture design data from both the Category 4, 19.0-mm and Category 3, 9.5-mm mixtures indicated little difference between the 100-gradation and 70-gradation mixtures when the optimum binder content was chosen at 4 and 5 percent air voids respectively. Lowering the number of design gyrations by 30 effectively raised the mixture air voids by

one percent. Thus the gradation was either not changed or changed only slightly from the original; therefore the 70-gradation mix was eliminated for the third mixture.

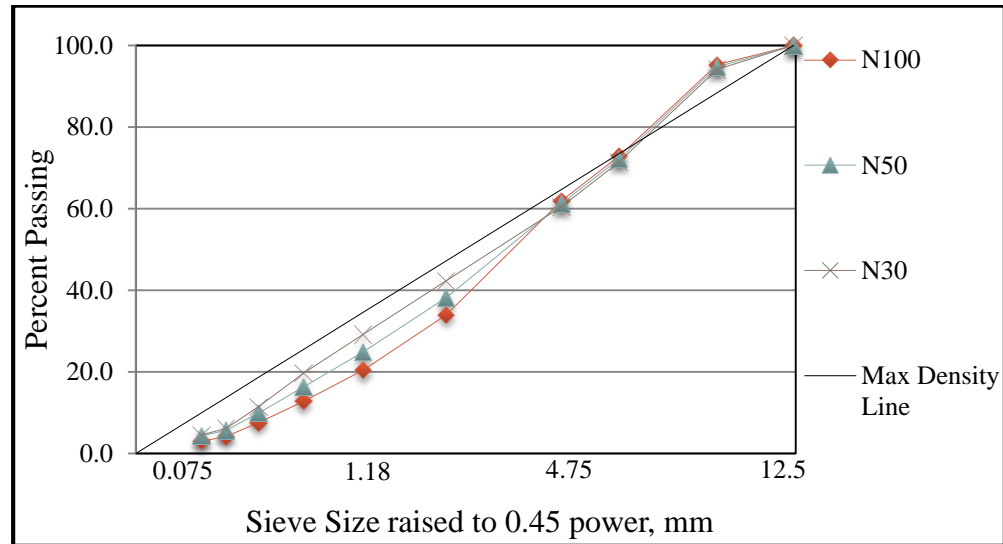


Figure 3.3 Category 4, 9.5-mm mixture gradations.

3.2 Field Trials Mixture Design

The SAC suggested two trial sections be placed using the enhanced asphalt mixture design method developed in the study. The INDOT complied with this request, and the first trial section was built on SR-13 near Fort Wayne, Indiana, and the second on Georgetown Road in Indianapolis, Indiana. During construction, mixture samples from both the conventional and trial pavement sections were obtained. Additionally, in November 2013, approximately four months after construction, INDOT took several cores from the SR-13 trial section, and 20 cores per each design were obtained from Georgetown Road.

3.2.1 SR-13 Project

The SR-13 project required the existing road surface to be milled and an overlay placed. The new asphalt overlay mixture was designed as a Category 4, 9.5-mm surface. This means the design was done using 100 gyrations of the SGC and optimum asphalt binder content was chosen at 4% air voids. It was initially decided by the SAC, in consultation with the research team, that the re-designed mixture for use on the project should be designed using 30 gyrations of the SGC and selecting the optimum asphalt binder content at 5% air voids. Later, the decision was made to change the 30-gyrations design to a 50-gyrations design instead. Both the original and re-designed mixtures consisted of steel slag and limestone coarse aggregates, limestone and natural sands, recycled asphalt shingles (RAS), and a PG 70-22 asphalt binder. The aggregate gradations of both mixtures are given in Table 3.6 and shown graphically in Figure 3.4. Relatively small changes in the aggregate proportions were needed to allow the re-designed mixture to achieve the design air voids at reduced gyrations.

Table 3.6 SR-13, Aggregate gradations and specific gravities.

Sieve Size, mm	Original (N100)	Re-designed (N50)
	Percent Passing	
12.5	100.0	100.0
9.5	92.0	89.6
6.3	71.8	70.4
4.75	62.0	61.1
2.36	46.4	40.1
1.18	32.0	27.7
0.6	22.7	19.5
0.3	13.4	11.0
0.15	7.5	6.0
0.075	4.8	4.4
G _{sb}	2.953	2.972

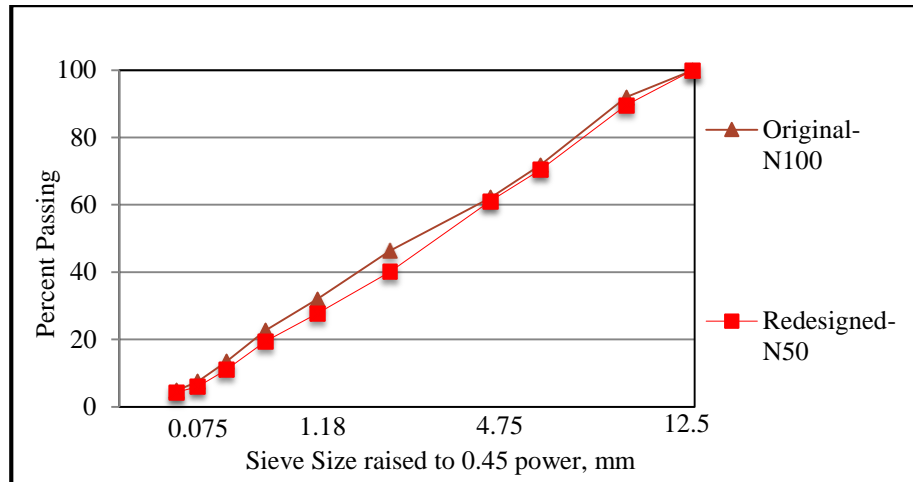


Figure 3.4 SR-13, Field trial mixture gradations.

A total of nine sublots of the original mixture and three sublots of the re-designed mixture were placed. For a surface mixture, INDOT specifications define a subplot as 544 tonnes (600 tons) of mixture. As a standard quality assurance measure INDOT extracted two cores from each subplot to establish the in-place mixture densities. The data is summarized in Table 3.7. The overall average in-place density of the original mixture was 91.8%; for the re-designed mixture the average was 94.7%, close to the goal of 95%. The contractor reported that the re-designed mixture field density was achieved without making any changes in the rollers or rolling patterns.

Table 3.7 SR-13, Field core densities.

Mixture	Sublot Number	Density, Percent of G_{mm}		
		Core 1	Core 2	Average
Original (N100)	1	92.3	89.7	91.0
	2	90.3	94.6	92.5
	3	92.6	92.7	92.6
	4	92.4	93.9	93.1
	5	90.5	90.0	90.3
	6	90.2	90.0	90.1
	7	92.4	91.4	91.9
	8	92.6	92.4	92.5
	9	92.3	92.4	92.3
Re-designed (N50)	1	92.3	94.5	93.4
	2	93.6	94.7	94.1
	3	96.3	96.7	96.5

3.2.2 Georgetown Road Project

The City of Indianapolis, in cooperation with the INDOT and the asphalt paving contractor, agreed to a second trial project on Georgetown Road. As part of a widening and re-paving project, the city agreed to allow placement of an experimental section of intermediate asphalt mixture that was designed using the modified mixture design method. The standard and trial mixtures were placed as a 3-inch thick intermediate layer. The standard mixture was designed as a Category 3, 19.0-mm mixture using 100 gyrations of the SGC and choosing the optimum binder content at 4 percent air voids. Both mixtures made use of limestone coarse aggregate, dolomite sand, RAP, RAS, and a PG 64-22 binder. The aggregate gradations of both mixtures are given in Table 3.8 and shown graphically in

Figure 3.5. Similar to SR-13 project, small changes in the aggregate proportions were needed to allow the re-designed mixture to achieve the design air voids at reduced gyrations.

As requested by the research committee the contractor extracted 20 cores per each mixture for density and additional testing. The data is summarized in Table 3.9. The overall average in-place density of the original mixture was 94.0%; for the re-designed mixture the average was 94.8%, close to the goal of 95%. The contractor reported that the re-designed mixture field density was achieved without making any changes in the rollers or rolling patterns.

Table 3.8 Georgetown Road, Aggregate gradations and specific gravities.

Sieve Size, mm	Original (N100)	Re-designed (N30)
	Percent Passing	
25.0	100.0	100.0
19.0	96.2	95.3
12.5	84.1	82.1
9.5	73.2	73.0
6.3	53.6	56.6
4.75	44.1	47.0
2.36	31.0	32.6
1.18	20.0	20.8
0.6	13.1	13.9
0.3	7.9	9.4
0.15	5.1	6.9
0.075	4.1	5.7
G _{sb}	100.0	100.0

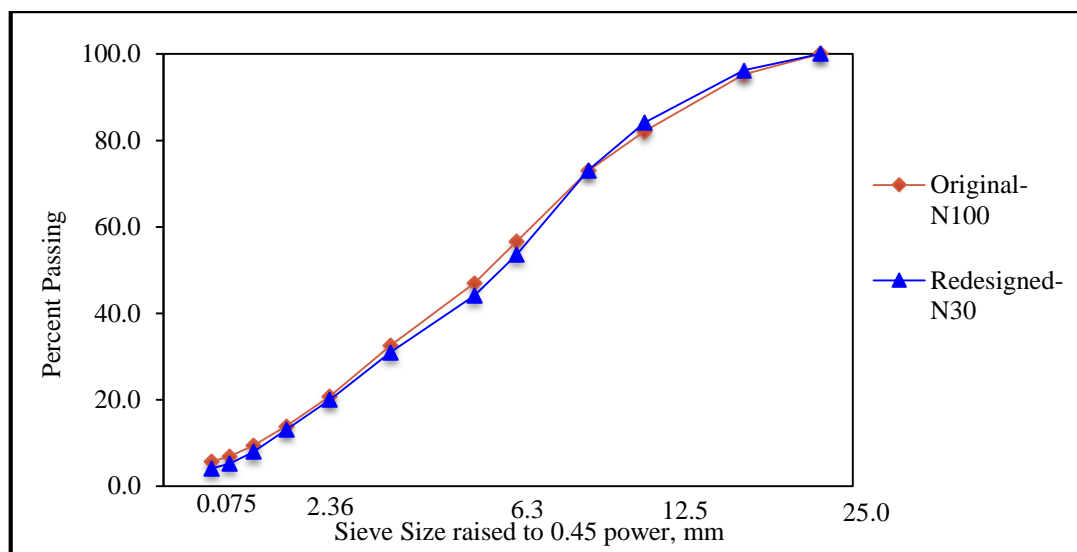


Figure 3.5 Georgetown Road, Field trial mixture gradations.

Table 3.9 Georgetown Road, Field core densities.

N100				N30			
Cores No.	G _{mb}	G _{mm}	AV%	Cores No.	G _{mb}	G _{mm}	AV%
N100-1	2.378	2.509	5.2	N30-41	2.393	2.502	4.4
N100-2	2.352		6.3	N30-42	2.401		4.0
N100-3	2.347		6.5	N30-43	2.401		4.0
N100-4	2.363		5.8	N30-44	2.396		4.2
N100-5	2.369		5.6	N30-45	2.371		5.2
N100-6	2.359		6.0	N30-46	2.382		4.8
N100-7	2.352		6.3	N30-47	2.368		5.4
N100-8	2.360		5.9	N30-48	2.365		5.5
N100-9	2.362		5.8	N30-49	2.380		4.9
N100-10	2.317		7.7	N30-50	2.369		5.3
N100-11	2.316		7.7	N30-51	2.369		5.3
N100-12	2.343		6.6	N30-52	2.378		4.9
N100-13	2.368		5.6	N30-53	2.388		4.5
N100-14	2.408		4.0	N30-54	2.382		4.8
N100-15	2.379		5.2	N30-55	2.376		5.0
N100-16	2.417		3.7	N30-56	2.382		4.8
N100-17	2.345		6.5	N30-57	2.383		4.8
N100-18	2.329		7.2	N30-58	2.377		5.0

Table 3.9 continued

N100-19	2.325		7.3	N30-59	2.368		5.4
N100-20	2.358		6.0	N30-60	2.387		4.6
Average AV%	6.0			Average AV%	4.8		
SD AV%	1.05			SD AV%	0.44		

CHAPTER 4. LABORATORY MIXTURE PERFORMANCE

As mentioned in the previous chapter, in order to evaluate and compare the rutting performance of the two mixture designs (standard and re-designed), dynamic modulus and flow number tests have been performed. The results are presented here.

4.1 Dynamic Modulus Testing

Asphalt mixture is a viscoelastic material, meaning that the stiffness of this material changes from winter to summer and at different vehicle speeds. In order to identify the stiffness of asphalt mixtures over a range of temperatures and loading rates, dynamic modulus tests were performed. In the dynamic modulus test, a haversine fixed load is applied and the resulting strain is calculated. As shown in Figure 4.1, there is a lag between stress and strain which is called the phase angle, ϕ , and which identifies how viscous the material is. “A phase angle of 90° represents an entirely viscous material, whereas, 0° represents an entirely elastic material.” (Asphalt Technology News, 2014).

The $|E^*|$ test (AASHTO T 342) was performed and master curves developed according to the second-order polynomial fit found in AASHTO PP 62, “Developing Dynamic

Modulus Curves for Hot Mix Asphalt (HMA).” The test was performed at six frequencies (25, 10, 5, 1, 0.5, and 0.1 Hz) and four temperatures (4, 21, 37, and 50°C). Dynamic modulus master curves would be different at different temperatures. So, a reference temperature needs to be defined, and the results measured at different temperatures are shifted to the reference temperature using time-temperature superposition. For this study the reference temperature was 30°C.

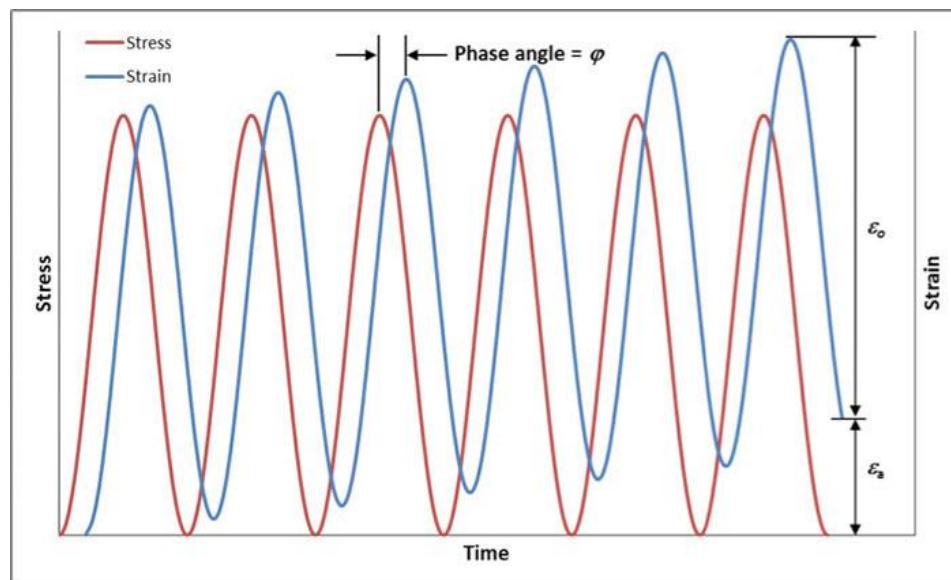


Figure 4.1 Phase angle in dynamic modulus test (Asphalt Technology News, 2014).

There are two primary reasons for using dynamic modulus testing data. “First, it is used in pavement design to predict pavement responses for a given vehicle’s speed and a pavement temperature. This is important for mechanistic-empirical (M-E) pavement design, which relies on engineering properties of the pavement layers to predict pavement performance. Second, it is used to compare the relative stiffness of different asphalt mixtures.” (Asphalt Technology News, 2014). Results of a study by NCAT, shown in

Figure 4.2 indicates that increasing RAP content of an asphalt mixture will increase the stiffness of the asphalt material over different temperatures and frequencies. Usually asphalt materials master curves are illustrated as log-log plot to demonstrate asphalt mixture stiffness' differences at lower frequencies. However, master curves can also be plotted with y-axis on the arithmetic scale to illustrate the difference in mixture stiffness at the higher frequencies as shown in Figure 4.3. With a semi-log plot the difference between the moduli of the two mixtures at higher loading rates or lower temperatures is more evident (Asphalt Technology News, 2014).

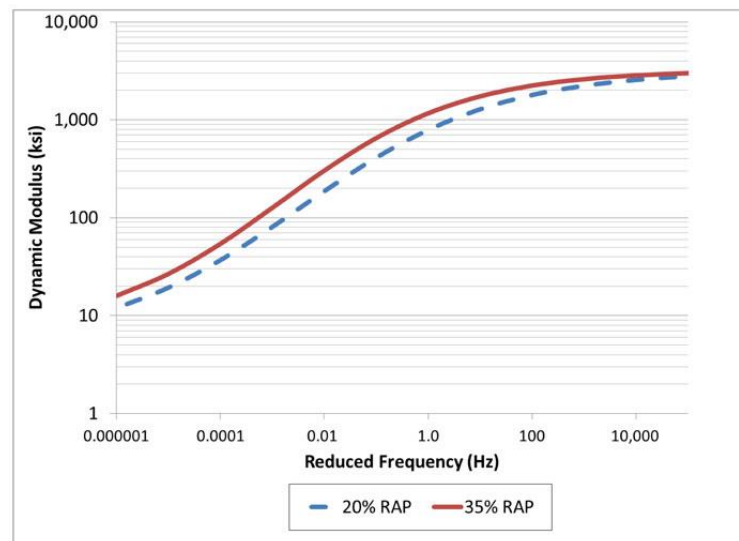


Figure 4.2 Dynamic modulus master curve for two mixtures (log-log plot) (Asphalt Technology News, 2014).

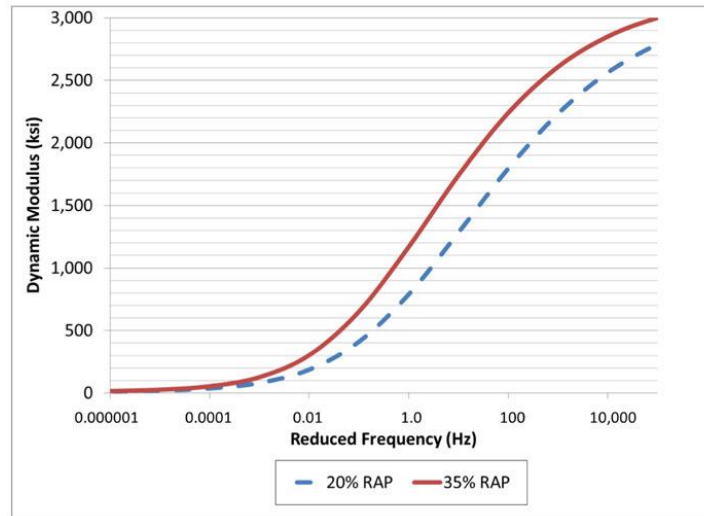


Figure 4.3 Dynamic modulus master curve for two mixtures (semi-log plot) (Asphalt Technology News, 2014)

4.2 Flow Number Testing

“The flow number (FN) test is a dynamic creep test where a haversine type of loading (0.9 sec) is applied with rest periods (0.1 sec) between loadings, which simulates driving a heavy vehicle repeatedly over an asphalt pavement.” (Advanced Asphalt Technologies, 2011).

The FN test was completed using the AMPT (unconfined), according to AASHTO TP 79 with a deviator stress (σ_d) of 600 kPa and contact stress of 30 kPa (5 percent of σ_d) at a temperature of 50.5°C. This temperature was selected based on the LTTPBind database (Advanced Asphalt Technologies, 2011).

Figure 4.4, shows how permanent deformation occurs under repeated loading and rest period for asphalt mixtures. As seen in Figure 4.4 the permanent strain versus load cycle curves divided into three zones. In the primary zone, the strain rate (slope of the curve) decreases; in the secondary zone, the permanent strain rate is constant; and in the tertiary zone the permanent strain rate dramatically increases. The initiation of tertiary zone where the rate of permanent strain will change from zero to positive number has been defined as the flow number. It is believed that the flow number value is related to the rutting performance of asphalt materials. As the flow number value increases, rutting resistance also increases (Advanced Asphalt Technologies, 2011). The Francken Model was used for curve fitting.

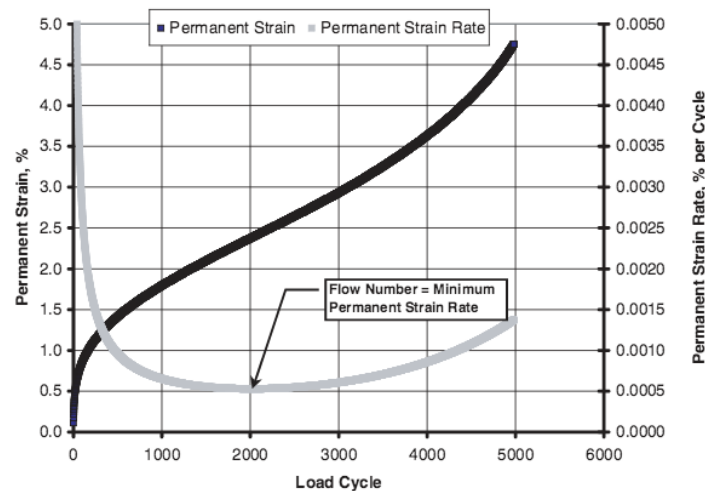


Figure 4.4 Typical data from flow number test (Advanced Asphalt Technologies, 2011).

4.3 Preparing Specimens

Once the mixture designs were complete, four test specimens of each mixture were produced to a specific air void content corresponding to the expected field compaction level. Samples of the standard mixtures (N100) were compacted to 7 percent air voids (after coring and sawing) to simulate field compaction at the start of the pavement life. Test specimens for the re-designed mixtures were compacted, cored and sawed to produce 5 percent air voids in the test specimens, again to simulate anticipated field compaction at the start of the pavement life. Once the test specimens were fabricated and air void contents checked, AASHTO T 342 and TP 79 tests were performed. Table 4.1 shows the air void contents for the $|E^*|$ specimens prior to testing. The cells in Table 4.1 with no data are where no samples could be tested due to lack of material.

Table 4.1 Dynamic modulus specimen air voids data.

Category 4, 19.0-mm Mixture						
N _{design}	Sample 1	Sample 2	Sample 3	Sample 4	Average	SD
100	7.1	7.5	7.1	— ¹	7.2	0.23
70	5.5	5.3	4.7	— ¹	5.2	0.42
50	4.7	4.9	5.2	4.7	4.9	0.24
30	4.6	4.7	5.2	5.4	5.0	0.39
Category 3, 9.5-mm Mixture						
N _{design}	Sample 1	Sample 2	Sample 3	Sample 4	Average	SD
100	7.7	7.2	6.5	6.7	7.0	0.54
70	4.8	4.7	5.0	5.4	5.0	0.31
50	4.7	4.6	4.8	4.9	4.8	0.13
30	5.1	4.9	5.1	4.9	5.0	0.12
Category 4, 9.5-mm Mixture						
N _{design}	Sample 1	Sample 2	Sample 3	Sample 4	Average	SD
100	6.9	6.9	7.1	7.0	7.0	0.10
50	4.8	5.1	4.8	4.8	4.9	0.15
30	5.1	5.1	4.9	4.9	5.0	0.12

¹ No specimens were available for testing.

4.4 Category 4, 19.0-mm Mixture

The Category 4, 19.0-mm mixture $|E^*|$ master curves for all four gyration levels are plotted on a log-log graph in Figure 4.5. For better clarity at the high temperature frequencies, the data is shown on a semi-log plot in Figure 4.6. The results show that the 70-gyration (N70) mixture is the stiffest of the four mixtures, the N100 mixture the least stiff. The 30- and 50-gyration (N30, N50) mixtures are between the two and appear to be about the same. The fact that the N30, N50, and N70 mixtures all have a higher $|E^*|$ values than the N100 mixture is not surprising considering the N100 specimens were compacted to 7 percent air voids and the N30, N50, and N70 specimens to 5 percent air voids. In general, the denser a mixture, the stiffer it will be, as long as it is not so dense that it becomes susceptible to plastic flow. Regardless of the specimen air voids, it is important to note that all three of the re-designed mixtures have $|E^*|$ values higher than the standard design. In theory this implies the re-designed mixtures should have better rutting performance than the standard mixture when compacted to the anticipated field density.

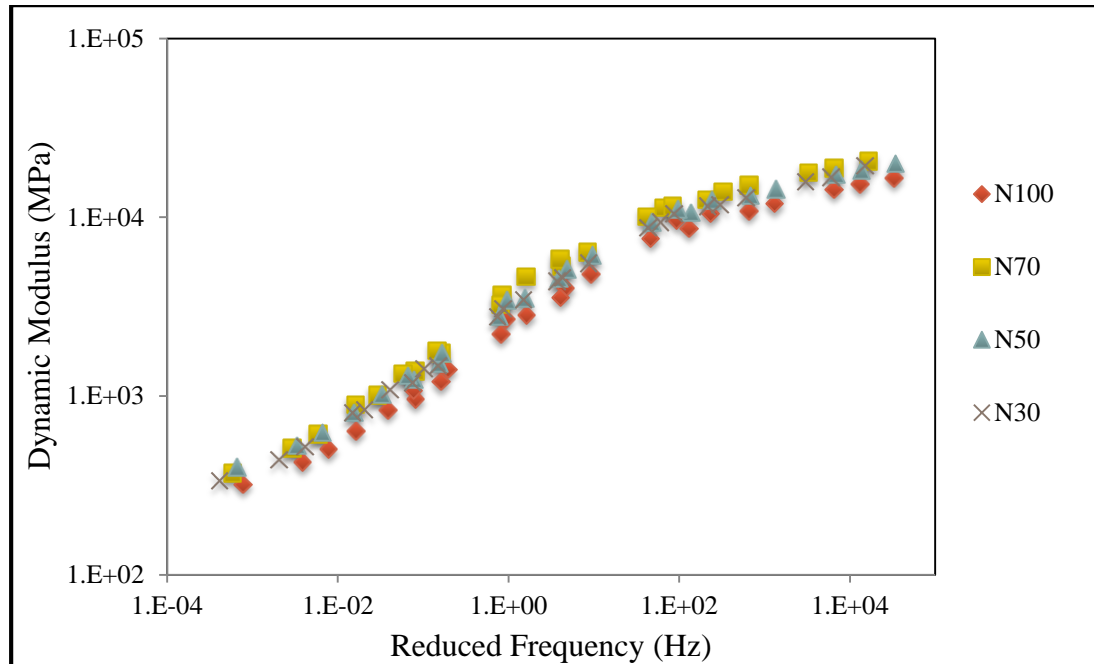


Figure 4.5 Category 4, 19.0-mm master curves (log-log).

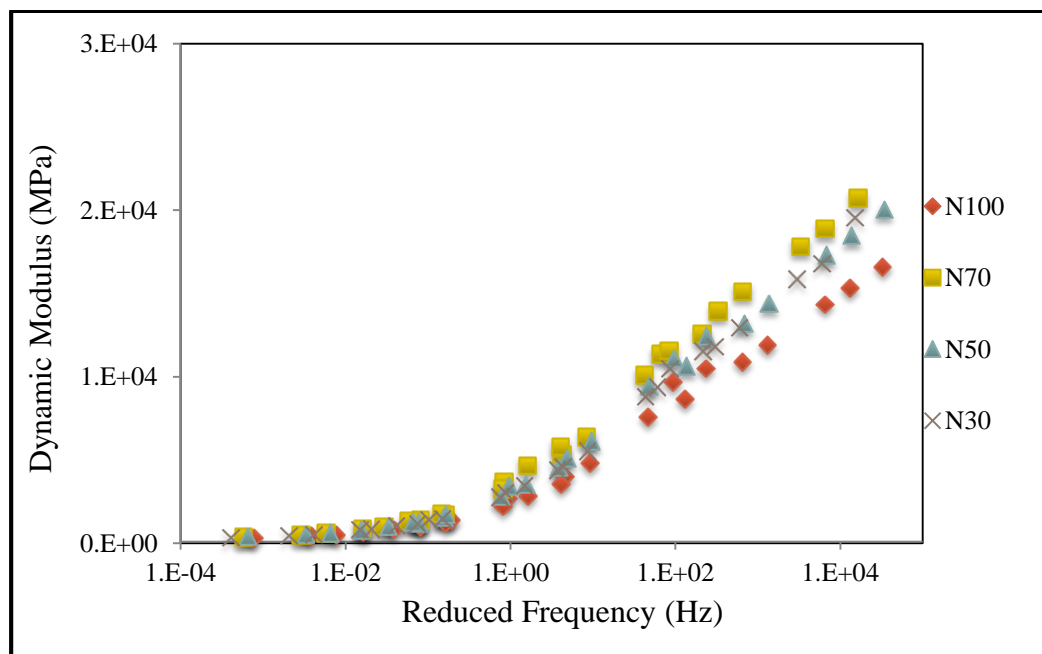


Figure 4.6 Category 4, 19.0-mm master curves (semi-log).

Table 4.2 shows the FN results for Category 4, 19.0-mm mixture designs. Due to a lack of materials, it was not possible to make a separate set of specimens for FN testing. Instead, the $|E^*|$ specimens were used for FN testing. This resulted in the low air voids as shown in Table 4.2; the specimens were consolidated in the $|E^*|$ tests. While reusing the $|E^*|$ specimens for FN testing is not strictly correct according to standard test methods, it does allow for a relative comparison. Some of the $|E^*|$ specimens were not reusable and thus the lack of data in some data cells.

The FN results indicate that all three of the re-designed mixtures have higher FN values than does the standard mixture. The N50 and N70 mixtures have FN values over twice as large as the standard design. Also, the strain at FN is lower for the re-designed mixtures than for the standard mixture. Both these results suggest the re-designed mixtures should be able to withstand higher levels of traffic than the standard design before the onset of rutting when compacted to the anticipated field density.

Table 4.2 Category 4, 19.0-mm mixture flow number data.

	N100						
	Sample 1	Sample 2	Sample 3	Sample 4	Sample 5	Average	SD
Air Voids, %	6.7	7.0	6.7	— ¹	— ¹	6.8	0.17
Flow Number	191	132	164	— ¹	— ¹	162	30
Strain @ FN, $\mu\epsilon$	21,881	27,129	22,938	— ¹	— ¹	23,983	2,776
	N70						
	Sample 1	Sample 2	Sample 3	Sample 4	Sample 5	Average	SD
Air Voids, %	5.1	4.9	4.1	— ¹	— ¹	4.7	0.53
Flow Number	371	360	427	— ¹	— ¹	386	36
Strain @ FN, $\mu\epsilon$	20,230	18,245	16,331	— ¹	— ¹	18,269	1,950
	N50						
	Sample 1	Sample 2	Sample 3	Sample 4	Sample 5	Average	SD
Air Voids, %	4.3	4.2	4.0	4.0	— ¹	4.1	0.15
Flow Number	220	337	424	410	— ¹	348	93
Strain @ FN, $\mu\epsilon$	20,179	20,722	18,973	19,654	— ¹	19,882	747
	N30						
	Sample 1	Sample 2	Sample 3	Sample 4	Sample 5	Average	SD
Air Voids, %	4.0	4.1	4.8	5.3	5.0	4.6	0.60
Flow Number	210	221	162	140	194	185	34
Strain @ FN, $\mu\epsilon$	23,862	23,171	20,811	21,542	21,066	22,090	1350

¹ No specimens were available for testing.

The $|E^*|$ and FN data can be plotted as a function of the number of gyrations used to compact the mixture design specimens. An example of this is shown in Figure 4.7. The figure shows the $|E^*|$ at 50°C for 10 and 25 Hz. A polynomial trend line has been used to fit both the 10 and 25 Hz data. The equations can each be solved to determine the number of gyrations that results in the peak $|E^*|$ values. The peak $|E^*|$ value for the 10 Hz data occurs at 65 gyrations; the peak $|E^*|$ for the 25 Hz data at 63 gyrations. When this technique is used for the $|E^*|$ data at the 6 and 50°C data, and the FN, the overall average optimum number of gyrations is 53.

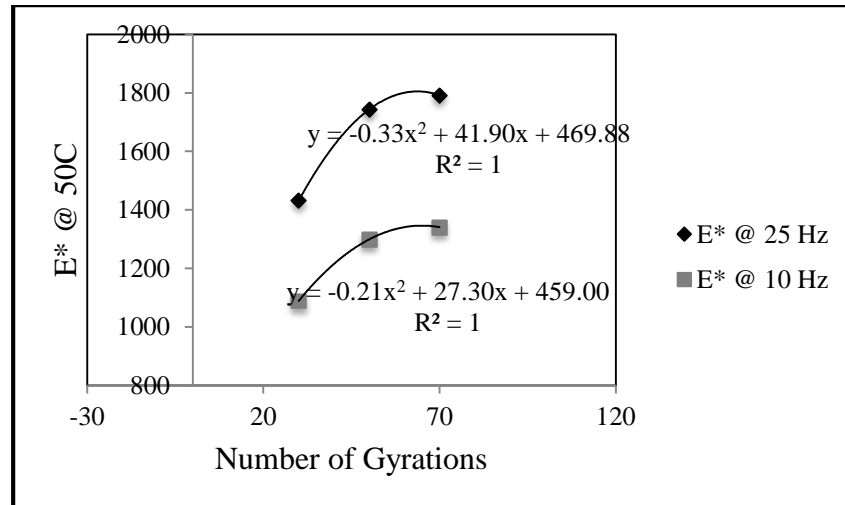


Figure 4.7 Dynamic modulus as a function of gyrations.

4.5 Category 3, 9.5-mm Mixture

For the Category 3, 9.5-mm mixture, specimens were prepared and tested in a similar fashion to the 19.0-mm mixture. In addition to the specimens for the standard and three re-designed mixtures, an additional set of N100 test specimens was produced. This second set of N100 mixture test specimens was compacted to 5 percent air voids, as were the re-designed mixture specimens. This was done in order to compare the $|E^*|$ and FN data for standard mixture to the re-designed mixtures when all of the test specimens have similar air voids content. The $|E^*|$ master curves for the five groups of specimens are shown in Figure 4.8. For better clarity of the high frequency data, the semi-log plot is shown in Figure 4.9.

The $|E^*|$ results indicate that all the mixtures have approximately same stiffness, although at higher frequency, the N30 mixture shows a slightly higher stiffness compared to the other mixtures. In general, the standard N100 mixture specimens compacted to 5 percent air voids have $|E^*|$ values approximately equivalent to the re-designed mixtures and $|E^*|$ values higher than the standard N100 mixture specimens compacted to 7 percent air voids. This would seem to validate the theory that, for a given mixture, the more densely compacted the mixture, the higher the stiffness. Thus, producing asphalt mixtures with in-place air voids of 5 percent should yield better rutting performance than compacting mixtures to in-place air voids of 7-8 percent as is done currently. However, over-compacting mixtures will cause the air voids to become low enough to make them susceptible to plastic flow, thus causing them to rut under traffic loads.

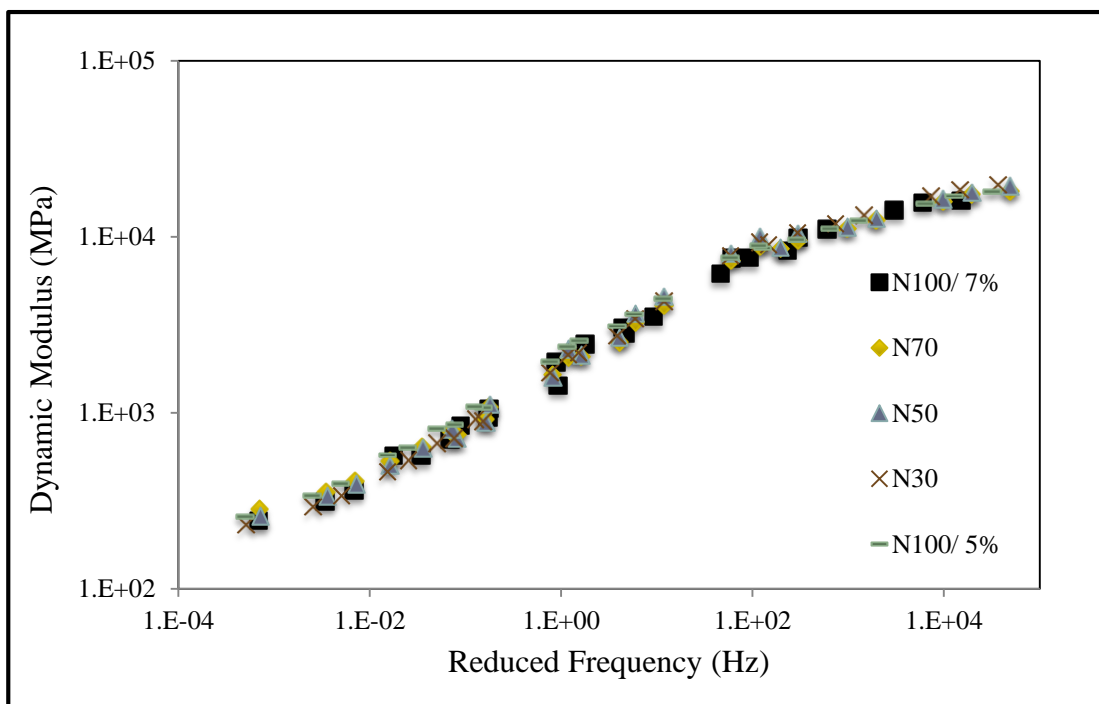


Figure 4.8 Category 3, 9.5-mm master curves (log-log).

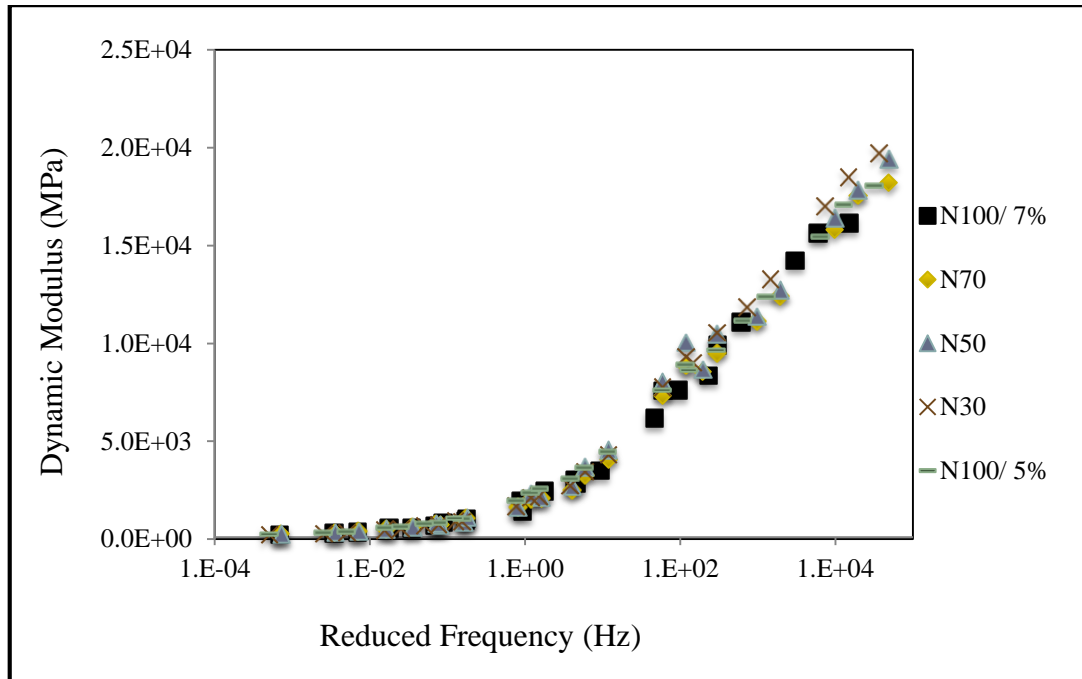


Figure 4.9 Category 3, 9.5-mm master curves (semi-log).

Table 4.3 shows the FN results for the Category 3, 9.5-mm mixture. Rather than re-using the $|E^*|$ specimens for FN testing of these mixtures, new specimens were made for FN testing. However, due to limitations of materials quantities, it was not possible to produce and test four specimens for each mixture. Also, the N100 standard design specimens compacted to 5 percent air voids were not tested for FN, again due to materials limitations. The data in the table indicate that all three re-designed mixtures have higher FN values than does the standard mixture. The strain at FN data is somewhat conflicting with the N30 and N50 re-designed mixtures having higher strains at FN than the standard mixture; the N70 re-designed mixture has a strain at FN lower than does the standard mixture.

Table 4.3 Category 3, 9.5-mm mixture flow number results.

	N100					
	Sample 1	Sample 2	Sample 3	Sample 4	Average	SD
Air Voids, %	8.0	7.0	7.3	7.0	7.3	0.5
Flow Number	92	101	61	109	91	21
Strain @ FN, $\mu\epsilon$	18,366	18,436	16,886	18,769	18,114	837
	N70					
	Sample 1	Sample 2	Sample 3	Sample 4	Average	SD
Air Voids, %	5.5	4.8	4.8	— ¹	5.0	0.40
Flow Number	161	176	165	— ¹	167	8
Strain @ FN, $\mu\epsilon$	17,650	18,296	17,166	— ¹	17,704	567
	N50					
	Sample 1	Sample 2	Sample 3	Sample 4	Average	SD
Air Voids, %	4.5	4.5	4.6	— ¹	4.5	0.15
Flow Number	183	156	151	— ¹	163	17
Strain @ FN, $\mu\epsilon$	18,008	18,861	24,030	— ¹	20,300	3,259
	N30					
	Sample 1	Sample 2	Sample 3	Sample 4	Average	SD
Air Voids, %	5.3	5.0	4.9	— ¹	5.1	0.21
Flow Number	141	162	164	— ¹	156	13
Strain @ FN, $\mu\epsilon$	19,000	19,419	19,193	— ¹	19,204	210

¹ No specimens were available for testing.

Overall, the $|E^*|$ and FN data for the Category 3, 9.5-mm mixture appear to indicate that, were these mixtures placed in the field, the re-designed mixtures would be expected to perform as well as the standard mixture in terms of rutting resistance.

The $|E^*|$ and FN data for the Category 3, 9.5-mm mixture was plotted as a function of the number of gyrations used to compact the mixture specimens, as was done for the Category 4, 19.0-mm mixture. However, for the Category 3, 9.5-mm mixture, the low temperature (4°C) $|E^*|$ and FN data produced no peak values. Instead, for these two sets of data, the number of gyrations producing the highest values was chosen as the optimum number of

gyrations and included in the overall average. The overall average optimum number of gyrations for this mixture appears to be 53.

4.6 Category 4, 9.5-mm Mixture

For the Category 4, 9.5-mm mixture, specimens were prepared and tested in a similar fashion to the previous mixtures. However, since the results from the two previously tested mixtures indicated little difference between the standard N100 mixtures and the N70 re-designed mixtures, no N70 mixture was designed and tested for the Category 4, 9.5-mm mixture. Only three sets of mixture specimens were tested for this mixture; the standard N100 mixture and the N30 and N50 re-designed mixtures.

Figures 4.10 and 4.11 show the $|E^*|$ results for Category 4, 9.5mm mixtures. The $|E^*|$ data indicate that all the mixtures have approximately the same stiffness, although at higher frequency, the N50 mixture shows a slightly higher stiffness than does the N30 mixture. The N100 standard mixture has the lowest stiffness of the three mixtures.

The FN results for the Category 4, 9.5-mm mixture are shown in Table 4.4. The data show that the N30 and N50 re-designed mixtures have FN values over twice as high as the standard N100 design. Additionally, both the re-designed mixtures have lower strain at FN values than does the standard design. As noted earlier, both these results suggest the re-designed mixtures should be able to withstand higher levels of traffic than the standard design before the onset of rutting when compacted to the anticipated field density.

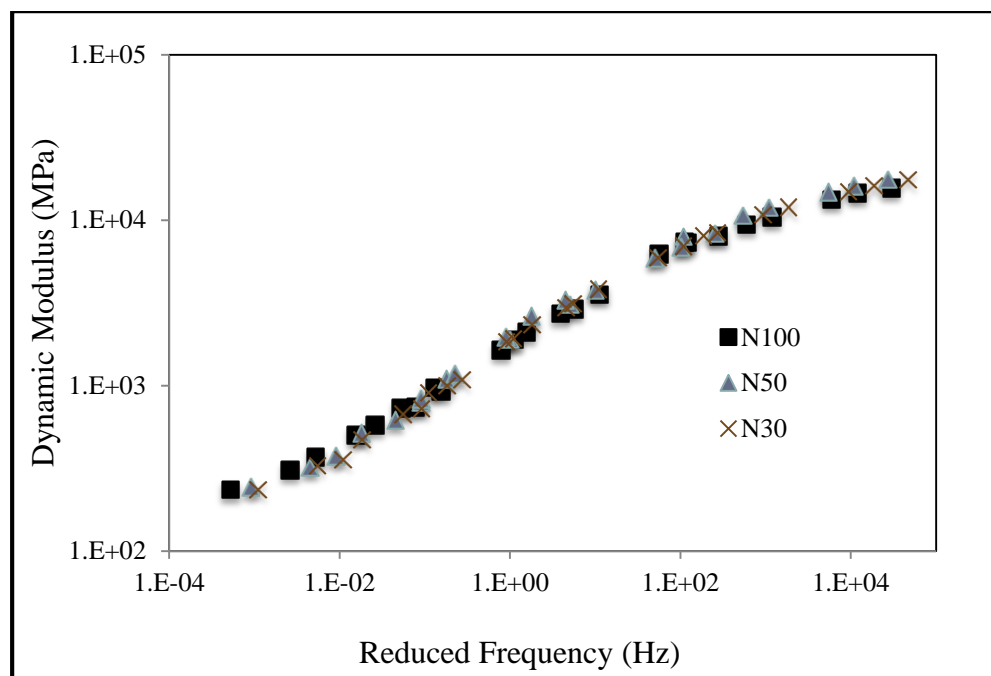


Figure 4.10 Category 4, 9.5-mm master curves (log-log).

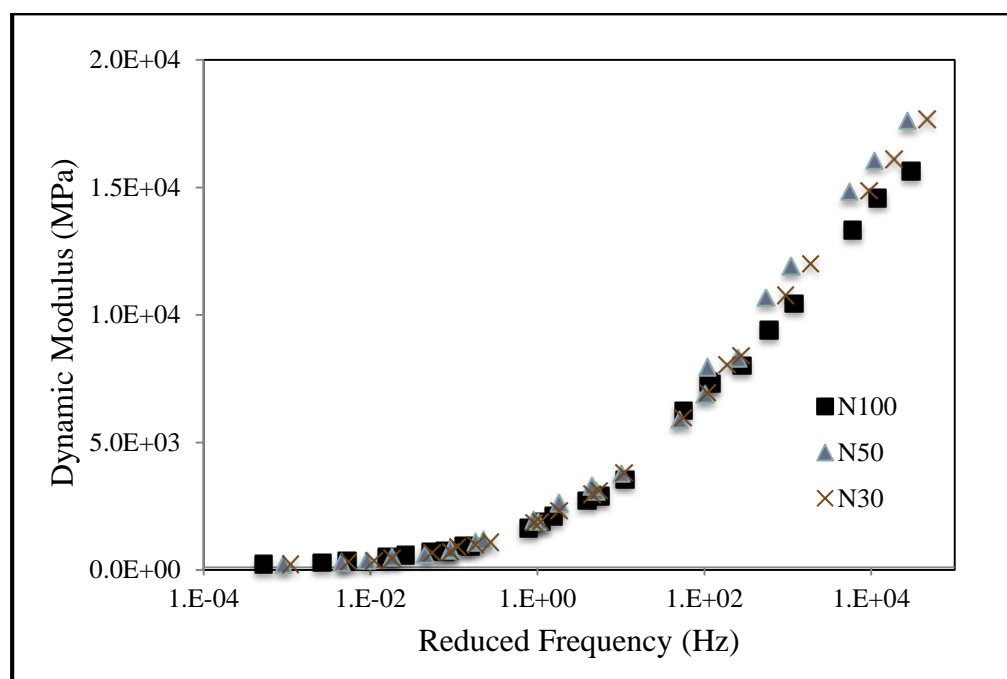


Figure 4.11 Category 4, 9.5-mm master curves (semi-log).

Table 4.4 Category 4, 9.5-mm mixture flow number results.

	N100						
	Sample 1	Sample 2	Sample 3	Sample 4	Sample 5	Average	SD
Air Voids, %	6.5	6.5	6.7	6.7	— ¹	6.6	0.12
Flow Number	157	173	162	147	— ¹	160	11
Strain @ FN, $\mu\epsilon$	17,269	18,657	23,497	21,448	— ¹	23,983	2,793
	N50						
	Sample 1	Sample 2	Sample 3	Sample 4	Sample 5	Average	SD
Air Voids, %	5.2	5.5	5.3	5.4	5.4	5.3	0.11
Flow Number	226	207	303	318	212	253	53
Strain @ FN, $\mu\epsilon$	20,600	19,756	22,556	21,751	20,013	20,935	1,188
	N30						
	Sample 1	Sample 2	Sample 3	Sample 4	Sample 5	Average	SD
Air Voids, %	5.3	5.3	5.1	5.3	— ¹	5.3	0.10
Flow Number	209	218	231	184	— ¹	211	20
Strain @ FN, $\mu\epsilon$	19,654	22,812	19,702	21,973	— ¹	21,033	1,607

¹ No specimens were available for testing.

Determining an optimum number of gyrations for the Category 4, 9.5-mm mixture is somewhat more problematic than for the prior two cases. For this mixture there are only two data points (N30, N50) for the $|E^*|$ and FN data. No curve fit can be established for only two points. Therefore, the gyration level that produced the highest $|E^*|$ or FN was chosen for use in calculating the optimum number of gyrations. Using this approach, the overall average optimum number of gyrations for this mixture appears to be 42. However, since no curve fit could be established, one might consider assigning lesser importance to the 42 gyrations than to the 53 and 52 gyrations determined for the mixtures with more data.

4.7 Statistical Analysis

Statistical summaries and analyses of the $|E^*|$ data were completed for each of the three mixtures. Within each mixture type, the Bonferroni method was used to compare the re-designed and standard mixtures to determine if the mixtures were statistically significantly different. The Bonferroni method has chosen over the Tukey method due to the fact that Bonferroni method is more powerful when the number of comparisons is small where Tukey method is more powerful for large numbers of comparisons. The Bonferroni method allows for a direct statistical comparison of the mean values of a variable. In this case, the Bonferroni method null hypothesis is that there are no differences between the average $|E^*|$ values of the mixtures ($\mu_{N30} = \mu_{N50} = \mu_{N70} = \mu_{N100}$).

4.7.1 Category 4, 19.0-mm Mixture

The statistical summary of the $|E^*|$ data is shown in Table 4.5; the summary includes the average $|E^*|$ values at each temperature and frequency, along with the coefficient of variation (CV) for the averages. The summary statistics seem reasonable, except perhaps for the CV for the N30 value at 6°C and 25 Hz. The CV tends to increase as the test temperature increases. This is to be expected; as the specimens become less stiff, the measurement of $|E^*|$ becomes less precise. In the case of the N30 CV previously mentioned, the value appears to be higher than it should be. In reviewing the individual $|E^*|$ data values, one of the specimens has an $|E^*|$ that is much different than the others. This is the likely reason for the high CV. If this one data point were removed, the average $|E^*|$ of the N30,

6°C, 25 Hz data would be slightly over 17,000 MPa with a CV of 1.6%, a value much more consistent with the other data.

Table 4.6 contains the statistical groupings of the data using the Bonferroni method. There is some variation in the data, but overall the results indicate that statistically there are only minor differences in the $|E^*|$ values of the standard and re-designed mixtures. This suggests that the re-designed mixtures should perform at least as well in the field as the standard mixture.

Table 4.5 Category 4, 19.0-mm statistical summary.

25 Hz	N30		N50		N70		N100	
	Average $ E^* $, MPa	C.V., %	Average $ E^* $, MPa	C.V., %	Average $ E^* $, MPa	C.V., %	Average $ E^* $, MPa	C.V., %
6°C	19,554	15.2	20,041	6.4	20,145	9.6	16,166	9.0
22°C	11,276	3.7	12,465	7.4	12,132	9.3	10,088	11.0
37°C	4,157	6.4	4,552	9.4	5,299	15.0	3,561	7.7
50°C	1,431	7.9	1,743	6.3	1,792	13.1	1,366	0.6
10 Hz	N30		N50		N70		N100	
	Average $ E^* $, MPa	C.V., %	Average $ E^* $, MPa	C.V., %	Average $ E^* $, MPa	C.V., %	Average $ E^* $, MPa	C.V., %
6°C	16,770	1.8	18,477	5.2	18,277	7.2	14,898	5.2
22°C	10,328	3.3	11,097	4.0	11,219	5.4	9,207	11.3
37°C	3,236	7.6	3,547	6.4	4,251	10.7	2,841	6.7
50°C	1,089	7.9	1,299	9.1	1,341	10.8	1,052	2.1

Table 4.6 Category 4, 19.0-mm Bonferroni groupings.

Test Frequency	25 Hz		10 Hz	
Test Temperature	p-value ($\alpha = 0.05$)	Grouping	p-value ($\alpha = 0.05$)	Grouping
6°C	0.0933	(N70=N50=N30=N100)	0.0028	(N50=N70=N30); (N30=N100)
22°C	0.0295	(N50=N70=N30); (N70=N30=N100)	0.0080	(N70=N50=N30); (N30=N100)
37°C	0.0065	(N70=N50=N30); (N50=N30=N100)	0.0008	(N70=N50=N30); (N50=N30=N100)
50°C	0.0042	(N70=N50); (N50=N30); (N30=N100)	0.0096	(N70=N50=N30); (N50=N30=N100)

4.7.2 Category 3, 9.5-mm Mixture

The statistical summary of the $|E^*|$ data for the Category 3, 9.5-mm mixture is shown in Table 4.7. The summary includes the average $|E^*|$ values at each temperature and frequency, along with the CV for the averages. The averages and CV are consistent for the data, although it should be noted that the CV for the 50°C data is lower than for the 37°C data. The CV values for the 50°C data appear to be in fairly good agreement with the 4 and 21°C data; this might suggest some error in the 37°C testing though none was detected during testing or subsequent data analyses.

Table 4.7 Category 3, 9.5-mm statistical summary.

25 Hz	N30		N50		N70		N100/7%		N100/5%	
	Average E* , MPa	C.V., %	Average E* , MPa	C.V., %	Average E* , MPa	C.V., %	Average E* , MPa	C.V., %	Average E* , MPa	C.V., %
4°C	19,715	4.4	19,413	4.0	18,226	8.2	16,144	13.1	18,055	6.2
21°C	10,529	6.3	10,480	3.7	9,504	8.8	8,351	10.7	9,660	10.7
37°C	2,756	8.1	2,678	13.4	2,529	11.2	3,046	20.2	3,109	5.7
50°C	919	7.5	1,114	5.3	1,081	8.1	944	6.2	1,085	5.8
10 Hz	N30		N50		N70		N100/ 7%		N100/5%	
	Average E* , MPa	C.V., %	Average E* , MPa	C.V., %	Average E* , MPa	C.V., %	Average E* , MPa	C.V., %	Average E* , MPa	C.V., %
4°C	18,492	6.1	17,843	3.3	17,543	6.7	15,639	6.4	17,089	5.5
21°C	9,331	7.1	10,042	5.6	8,864	9.2	7,628	11.5	8,921	9.2
37°C	2,191	10.7	2,136	15.4	2,092	14.0	2,461	20.4	2,588	6.3
50°C	671	7.9	811	4.4	789	7.0	707	6.1	810	4.2

In general, the standard N100 mixture design with test specimens compacted to 7 percent air voids has the lowest $|E^*|$ value. The only exception is at 37°C when the N100 standard mixture (7 percent air voids) has the second highest $|E^*|$ value at both 10 and 25 Hz; the N100 mixture with specimens compacted to 5 percent air voids has the highest $|E^*|$ value at both frequencies.

Results of the Bonferroni method are shown in Table 4.8. This data indicates that at a test temperature of 37°C, there are no differences in the $|E^*|$ values of the five mixtures for both test frequencies (10 and 25 Hz). At 50°C, for both frequencies, the N30 and N100/5% mixtures are not equivalent to any other mixtures. At the two higher temperatures, the

results are somewhat contradictory. This suggests that the re-designed mixtures may or may not perform as well as the standard mixture.

Table 4.8 Category 3, 9.5-mm Bonferroni groupings.

Test Frequency	25 Hz		10 Hz	
Test Temperature	p-value ($\alpha = 0.05$)	Grouping	p-value ($\alpha = 0.05$)	Grouping
4°C	0.03729	(N50=N70=N100/7%); (N30=N50=N100/5%)	0.01992	(N70=N100/7%); (N30=N50=N70=N100/5%)
21°C	0.02429	(N70=N100/7%); (N30=N50=N100/5%=N70)	0.01885	(N70=N100/7%); (N30=N50=N100/5%=N70)
37°C	0.32682	(N100/5%=N100/7%=N30=N50=N70)	0.35636	(N100/5%=N100/7%=N30=N50=N70)
50°C	0.00439	(N50=N100/5%=N70=N100/7%=N30)	0.0021	(N50=N100/5%=N70=N100/7%=N30)

4.7.3 Category 4, 9.5-mm Mixture

The statistical summary of the $|E^*|$ data for the Category 4, 9.5-mm mixture is shown in Table 4.9. The summary includes the average $|E^*|$ values at each temperature and frequency, along with the CV for the averages. The averages and CV are consistent. The N30 and N50 re-designed mixtures tend to have higher $|E^*|$ values than the standard N100 mixture.

Table 4.9 Category 4, 9.5-mm statistical summary.

25 Hz	N30		N50		N100	
	Average E* , MPa	C.V., %	Average E* , MPa	C.V., %	Average E* , MPa	C.V., %
4°C	17,682	2.8	17,610	0.9	15,632	1.9
21°C	8,392	3.7	8,308	2.5	8,025	3.7
37°C	2,970	4.8	3,297	2.8	2,721	4.4
50°C	1,093	8.8	1,171	4.1	971	11.7
10 Hz	N30		N50		N100	
	Average E* , MPa	C.V., %	Average E* , MPa	C.V., %	Average E* , MPa	C.V., %
4°C	16,107	3.0	16,055	1.4	14,591	2.3
21°C	6,957	4.0	6,897	2.6	7,364	1.1
37°C	2,334	7.4	2,632	2.7	2,105	6.8
50°C	910	8.9	829	3.1	731	12.1

The Bonferroni method results are shown in Table 4.10. This data indicates that at a test temperature of 21°C and a frequency of 25 Hz, there is no statistically significant difference between the N30, N50, and N100 mixtures. Also, at 37°C, the N100 mixture is not equivalent to the other mixtures at 25 Hz; however, at 10 Hz, it is the N50 mixture that appears to be unequal to the others. Overall it would appear that the re-designed mixtures are at least as stiff as the standard mixture and thus equivalent rutting performance would be expected.

Table 4.10 Category 4, 9.5-mm Bonferroni groupings.

Test Frequency	25 Hz		10 Hz	
Test Temperature	p-value ($\alpha = 0.05$)	Grouping	p-value ($\alpha = 0.05$)	Grouping
4°C	0.00002	(N100); (N30=N50)	0.00031	(N50=N100); (N30=N50)
21°C	0.20278	(N30=N50=N100)	0.04165	(N100=N30); (N30=N50)
37°C	0.00039	(N100); (N50=N30)	0.00136	(N50); (N30=N100)
50°C	0.03879	(N30=N100); (N50=N30)	0.03752	(N30=N50); (N50=N100)

CHAPTER 5. FIELD MIXTURE PERFORMANCE

The objective of the subject study was to enhance asphalt laboratory mixture design as it relates to field compaction in order to increase in-place asphalt pavement durability without sacrificing permanent deformation characteristics of the mixtures. The original scope of the study encompassed a laboratory effort aimed at developing a modified asphalt mixture design method that would allow for mixture in the laboratory to be compacted to the same density, as it would be when incorporated into the pavement. The effort was successfully completed as shown in the previous chapter.

During the execution of the project the Study Advisory Committee (SAC) suggested a trial section be placed using the modified asphalt mixture design method developed in the study. The Indiana Department of Transportation (INDOT) complied with this request, and two trial sections were built on SR-13 near Fort Wayne and Georgetown Road in Indianapolis, Indiana. During construction, mixture samples and cores from both the conventional and trial pavement sections were obtained.

5.1 SR-13 Project

As mentioned in Chapter 3, two mixtures were designed as a Category 4, 9.5-mm surface for the SR-13 project. The first one was the original or standard mixture based on Superpave design to be designed at 4% air voids using the 100 gyration level and the second one was the re-designed mixture using 50 gyrations and designed at 5% air voids. It was initially decided by the SAC, in consultation with the research team, that the re-designed mixture for use on the project should be designed using 30 gyrations of the SGC and selecting the optimum asphalt binder content at 5% air voids. Later, the decision was made to change the 30-gyration design to a 50-gyration design instead.

5.1.1 Pre-Field Trial Laboratory Testing

Once the mixture re-design was complete, the contractor produced 150 mm diameter SGC specimens for both the standard (N100) and re-designed (N30) mixtures. These specimens were then cored to produce 100-mm diameter specimens for $|E^*|$ and FN testing. The test specimens' air voids are shown in Table 5.1. As seen in the table, the air voids for both specimen groups are low. The N100 specimens should have average air voids of approximately 7 percent; the N30 specimens should have average air voids of approximately 5 percent. The results are 1.2% and 1.3% lower than target values for the N100 and N30 designs respectively. However, since project construction had already started and time was short, it was decided to test the specimens.

The specimens were tested to determine $|E^*|$ at 37°C over a range of frequencies. The $|E^*|$ data for the two mixtures are in Table 5.2 and are shown plotted in Figure 5.1. As the data clearly show, the re-designed (N30) mixture has a higher $|E^*|$ value at every frequency. However, statistically, there are no differences between the $|E^*|$ values for the mixtures ($\alpha=0.05$). Therefore, it was concluded that the N30 mixture is at least as stiff as the N100 mixture and should therefore perform as well in the field, if it is compacted to 5 percent air voids.

Table 5.1 Test specimen air voids.

N _{design}	Sample 1	Sample 2	Sample 3	Average	SD
100	5.6	6.3	5.6	5.8	0.38
30	4.0	3.9	3.1	3.7	0.53

Table 5.2 Dynamic modulus data.

Test Frequency, Hz	N30		N100	
	Average $ E^* $, MPa	CV, %	Average $ E^* $, MPa	CV, %
0.1	584	11.4	421	12.3
0.2	737	9.7	540	12.1
0.5	1,002	8.7	751	12.0
1.0	1,258	8.0	954	11.7
2.0	1,578	7.7	1,206	11.5
5.0	2,131	7.7	1,659	10.6
10.0	2,645	7.6	2,072	10.0
20.0	3,257	7.2	2,575	9.6
25.0	3,427	6.2	2,708	9.5

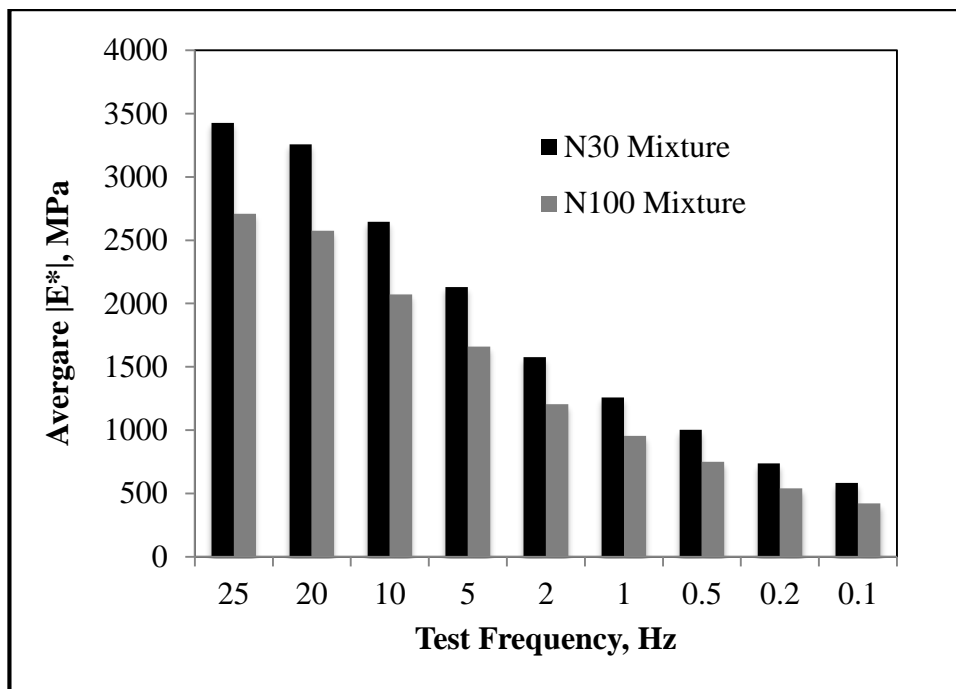


Figure 5.1 Dynamic modulus data for the mixture designs.

When the $|E^*|$ testing was complete, due to time and material availability challenges, the same specimens were reused for FN testing. Again, this is not in compliance with the standard test methods, but it does allow for a relative comparison of the mixtures. The N30 mixture yielded a FN of 1181 (C.V.=33.2%) and the N100 mixture a FN of 841 (C.V.=12.9%). A statistical comparison indicates that there is no significant difference between these values. This suggests that the re-designed N30 mixture will have at least the same rutting performance in the field as the N100 standard mixture. However, it is again important to remember that to do so, the re-designed mixture must be compacted to 5 percent air voids in the field. The net effect of laboratory comparison of the two mixture designs is that they have about the same mechanical properties as regards stiffness and rutting resistance.

5.1.2 Field Trial Production Testing

Based on the pre-trial laboratory testing of standard (N100) and re-designed (N30) mixtures, two different sections were constructed on SR-13, one with the 100-gyraton mixture and the other with the 30-gyraton mixture. During the production and placement of the re-designed mixture two companion samples were taken from the truck at 145 tonnes (160 tons) of production. One sample was extracted using the solvent method; the binder from the second sample was removed using the ignition oven method. No compacted specimens were produced or maximum specific gravities determined for these samples. The aggregate gradations and binder contents for these two samples are shown in Table 5.3.

Table 5.3 Re-designed mixture data (truck samples).

Sample Point, tonnes		145		345		526
Sieve Size, mm	Design	Solvent	Ignition	N30	N50	N50
12.5	100.0	100.0	100.0	100.0	Same gradation and binder content as N30.	100.0
9.5	92.0	89.4	92.5	93.1		89.6
4.75	63.0	56.7	60.2	65.4		61.1
2.36	41.0	35.9	37.5	42.8		40.1
1.18	27.5	24.5	25.3	29.1		27.7
0.600	19.0	17.3	17.7	20.2		19.5
0.300	12.0	10.5	10.5	11.2		11.0
0.150	7.5	6.3	6.2	6.2		6.0
0.075	5.5	4.9	4.7	4.6		4.4
Binder Content, %	5.10	5.38	5.38	5.65		5.32
Air Voids, %	5.0	— ¹	— ¹	6.7	5.5	— ¹
VMA, %	15.3	— ¹	— ¹	19.0	18.0	— ¹

—¹ Not determined.

Given the data results obtained from the 145 tonnes (160 tons) samples, a decision was made to change the aggregate blend in order to adjust the gradation. This resulting aggregate blend was used for all subsequent mixture production. A sample of the mixture was again taken from a truck at 345 tonnes (380 tons) and the material used to determine the aggregate gradation, binder content, and volumetric properties. As seen from Table 5.3, the binder content, air voids, and VMA were all higher than the target values.

Since the volumetrics were high when 30 gyrations were used to compact the specimens, additional specimens were produced from the 345 tonnes (380 tons) sample; these latter specimens were compacted with 50 gyrations of the SGC. As seen in Table 5.3, using 50 gyrations resulted in volumetrics closer to the target values. Given the results from this testing, the decision was made to change the re-designed mixture from a 30-gyrations to 50-gyrations mixture design. The VMA at 50 gyrations was still high, but the steel slag was known to have a variable specific gravity, so less confidence was placed on the calculated number.

The final truck sample was taken at 526 tonnes (580 tons). The ignition oven was used to determine aggregate gradation and asphalt binder content. No compacted specimens were produced or maximum specific gravities determined for this sample. As can be seen from Table 5.4, the gradation was reasonable and the binder content was slightly high but closer to target value.

Plate sampling from behind the paver was also completed during the production and placement of the re-designed mixture according to the INDOT standard method. The test results obtained from plate samples are shown in Table 5.4. The ignition oven was used to determine binder content and provide aggregate gradations for all plate samples.

Table 5.4 Re-designed mixture data (plate samples).

Sample Point, tonnes		345	437	740	1188
Sieve Size, mm	Design	Ignition	Sublot 1	Sublot 2	Sublot 3
12.5	100.0	100.0	100.0	100.0	100.0
9.5	92.0	91.3	91.9	90.3	92.7
4.75	63.0	63.1	65.8	61.3	63.6
2.36	41.0	41.8	42.3	40.7	41.0
1.18	27.5	28.7	28.4	28.0	28.3
0.600	19.0	20.2	19.8	19.9	20.1
0.300	12.0	11.5	11.4	11.5	11.5
0.150	7.5	6.5	6.3	6.4	6.5
0.075	5.5	4.9	4.6	4.8	4.9
Binder Content, %	5.10	5.48	5.61	5.47	5.45
Air Voids, %	5.0	3.4	3.9	3.6	3.5
VMA, %	15.3	15.5	16.0	15.4	16.0
Road Core A Density, % G_{mm}	Not Applicable	— ¹	92.30	93.59	96.29
Road Core B Density, % G_{mm}	Not Applicable	— ¹	94.53	94.68	96.69
Average Road Core Density, % G_{mm}	Not Applicable	— ¹	93.42	94.14	96.49

—¹ Not determined.

The first plate sample was obtained at 345 tonnes (380 tons) and is from the same tonnage as the N30 and N50 truck samples discussed previously (Table 5.3). Subsequent plate samples were taken at 437, 740, 1188 tons. All of the plate sample test data was obtained after the decision was made to change the re-designed mixture to a 50-gradation mixture.

The plate sample data indicate that aggregate gradation control was good. However, the binder content was high and the laboratory air voids low in all of the samples. The mixture VMA was close to the target, but variable, most likely due to issues with the steel slag G_{sb} . For this reason, little emphasis should be placed on VMA values. Finally, the overall average road core density for the three sublots was 94.7%, close to the 95.0% target in-place density. This density was achieved without any changes to the rollers or rolling patterns that were used for the standard (N100) mixture.

Overall the data from the field trial appears to indicate that changing the re-designed mixture's design gyrations from 30 to 50 probably should not have been done. The change was made based on one sample that was taken early in the production process. Using the field data and volumetric relationships established by the Bailey Method, it is estimated that had the re-designed mixture remained a 30-gyraton design, the air voids and VMA would have increased by about 1.18%, on average. The estimated air voids and VMA values are shown in Table 5.5. The average laboratory air voids is estimated at 4.9%, almost exactly the target value of 5.0 percent. The estimated VMA is high, but again, this is likely due to issues with the steel slag G_{sb} , and perhaps the VMA should therefore be de-emphasized for this project.

Table 5.5 Estimated volumetric properties at 30 gyrations.

Property	Sublot 1	Sublot 2	Sublot 3	Average
Air Voids, %	5.1	4.8	4.7	4.9
VMA, %	17.2	16.6	17.2	17.0

A total of nine sublots of the original mixture and three sublots of the re-designed mixture were placed. For a surface mixture, INDOT specifications define a subplot as 544 tonnes (600 tons) of mixture. As a standard quality assurance measure INDOT extracted two cores from each subplot to establish the in-place mixture densities. The data is summarized in Table 5.6. The overall average in-place density of the original mixture was 91.8%; for the re-designed mixture the average was 94.7%, close to the goal of 95%. The contractor reported that the re-designed mixture field density was achieved without making any changes in the rollers or rolling patterns.

Table 5.6 SR-13, Field core densities.

Mixture	Sublot Number	Density, Percent of G_{mm}		
		Core 1	Core 2	Average
Original (N100)	1	92.3	89.7	91.0
	2	90.3	94.6	92.5
	3	92.6	92.7	92.6
	4	92.4	93.9	93.1
	5	90.5	90.0	90.3
	6	90.2	90.0	90.1
	7	92.4	91.4	91.9
	8	92.6	92.4	92.5
	9	92.3	92.4	92.3
Re-designed (N50)	1	92.3	94.5	93.4
	2	93.6	94.7	94.1
	3	96.3	96.7	96.5

5.1.3 Post-Field Trial Testing

The primary reason for modifying the mixture design method is to produce asphalt mixtures that can be compacted to higher densities in the field. Typically, an asphalt mixture is compacted to approximately 93 percent density in the field. With the modified mixture design method, the contractor was able to achieve approximately 95 percent density during construction. It is hypothesized that the additional densification will extend the life of an asphalt mixture by slowing the embrittlement of the asphalt binder and increasing the fatigue life of the asphalt mixture. This hypothesis can be tested through binder and mixture testing as outlined in Table 5.7.

Table 5.7 Post field trial testing plan.

Test	Approximate Mixture Aged Condition	
	Post Construction	8 Years
Binder Grading	X	X
Dynamic Modulus	X	X
Flow Number	X	X
Fatigue Test	X	X
Porosity	X	X
Hydraulic Conductivity	X	X
Electrical Resistivity	X	X

The aged conditions must be approximated. The post-construction condition (immediately after construction) was simulated using loose mixture samples taken during the time of construction. To approximate eight years of in-service aging, the mixtures were tested after

being conditioned according to AASHTO R30, “Mixture Conditioning of Hot Mix Asphalt (HMA).”

All of the field material used for the post field trial testing was collected after producing 345 tonnes (380 tons) of mixture on the project, when the change was made to the 50-gradation mixture. Again, specimens for the standard design were produced at 7 percent air voids according to current test method standards. Specimens for the re-designed mixture were produced at 5 percent air voids. In order to produce the test specimens the field-sampled mixtures had to be re-heated, split into appropriate sizes, and the specimens compacted. All re-heating was performed carefully and consistently at the lowest possible temperature. Once the samples were produced they were tested as previously described.

5.1.3.1 Dynamic Modulus and Flow Number Testing

The dynamic modulus and flow number were determined for the post-construction and long-term aged mixtures according to AASHTO TP 79 as previously described. Figures 5.2 and 5.3 show plots of the $|E^*|$ data from the two mixtures; Figure 5.2 is the more common log-log plot of the data, while Figure 5.3 shows the data in semi-log form. This latter plot normally allows a better view of the high frequency data. The results of both plots clearly show that the re-designed mixture (N50) has a lower $|E^*|$ value over the frequency range than does the standard (N100) mixture. This result is different than the findings from the earlier laboratory study, which indicated that the re-designed mixtures

typically had $|E^*|$ values at least as high as, and often higher than, the standard design. Testing and analyses of the field mixtures during the mixture design phase of the SR-13 project indicated no differences in $|E^*|$ values between the re-designed and standard mixtures.

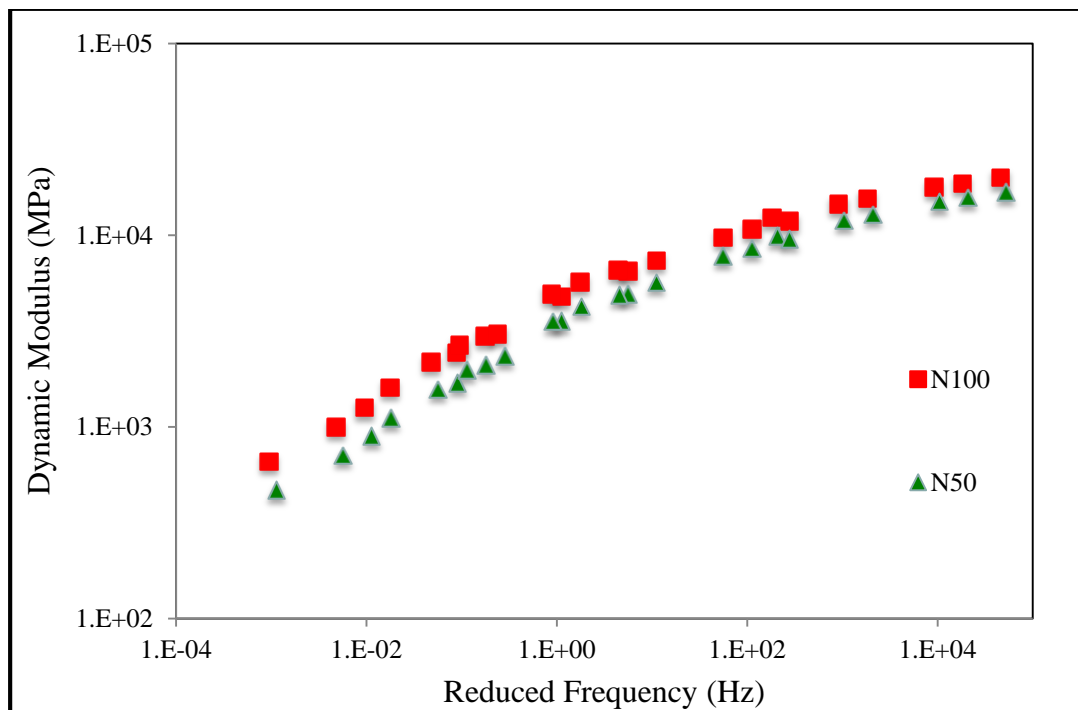


Figure 5.2 Post construction mixture master curves (log-log).

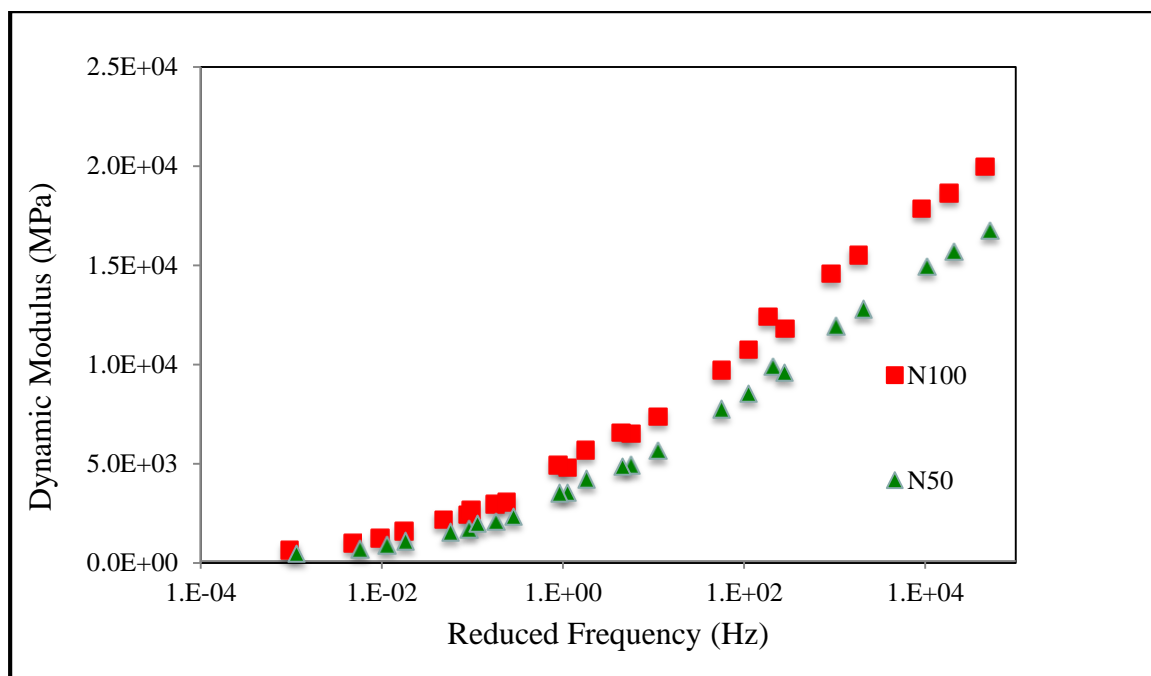


Figure 5.3 Post construction mixture master curves (semi-log).

To decide if there is an actual difference between the $|E^*|$ values of the two plant-produced mixtures, a t-Test was used to compare the means. Table 5.8 is a summary of the $|E^*|$ data of the field mixtures. The statistical analysis indicates that with 95 percent confidence ($\alpha=0.05$) it can be concluded that the standard and re-designed mixture designs have different $|E^*|$ values; the $|E^*|$ values are higher for the standard mixture.

Table 5.9 shows the FN results for the re-designed and standard mixtures. The data indicate the standard mixture has a higher flow number and less cumulative strain at FN than the re-designed mixture. This suggests the standard mixture may have better rutting performance than the re-designed mixture and is again opposite the FN results obtained during the mixture design phase of the field trial.

Table 5.8 Post construction mixture statistical summary.

25 Hz	N100		N50	
	Average [E*], MPa	C.V., %	Average [E*], MPa	C.V., %
4°C	19,980	4.0	16,754	2.2
21°C	11,819	2.3	9,595	4.9
37°C	6,572	4.0	4,867	8.1
50°C	3,059	8.3	2,343	8.1
10 Hz	N100		N50	
	Average [E*], MPa	C.V., %	Average [E*], MPa	C.V., %
4°C	18,648	3.4	15,713	1.6
21°C	10,764	3.8	8,544	6.5
37°C	5,683	6.1	4,243	6.1
50°C	2,673	8.0	1,977	7.8

Table 5.9 Post construction mixture flow number results.

Design	Air Voids, %	Flow Number	Strain @ Flow Number ($\mu\epsilon$)
N100-1	7.4	8,224	18,402
N100-2	6.8	5,716	18,793
N100-3	6.6	6,473	18,412
N100-4	6.7	7,447	18,869
N100-5	7.3	6,412	22,594
Average	7.0	6,854	19,414
C.V., %	5.2	14.3	9.2
N50-1	4.5	1,476	23,886
N50-2	5.4	2,066	25,344
N50-3	5.4	1,638	23,188
N50-4	5.2	2,484	21,984
N50-5	5.0	1,831	25,005
Average	5.1	1,899	23,881
C.V., %	7.3	20.8	5.7

For eight years of in-service life, the flow number testing was completed using specimens that had been first been used in the dynamic modulus tests due to lack of materials. The

$|E^*|$ data from the two mixtures is summarized in Table 5.10 and plotted in Figures 5.4 and 5.5. While the log-log plot (Figure 5.4) shows the two mixtures have similar modulus curves, the semi-log plot indicates otherwise, with the re-designed mixture (N50) having a lower $|E^*|$ value over the frequency range.

Table 5.10 Aged (8-year) dynamic modulus data.

@ 25 Hz	N100		N50	
	Avg. $ E^* $, MPa	C.V., %	Avg. $ E^* $, MPa	C.V., %
4°C	21482	8.8	20261	5.8
21°C	14089	9.5	13060	10.0
37°C	8648	9.0	8007	11.5
50°C	5130	19.3	4561	18.9
@ 10 Hz	N100		N50	
	Avg. $ E^* $, MPa	C.V., %	Avg. $ E^* $, MPa	C.V., %
4°C	20258	5.4	19102	6.2
21°C	12802	10.1	11920	10.7
37°C	7723	10.2	7018	13.4
50°C	4253	21.5	3681	25.6

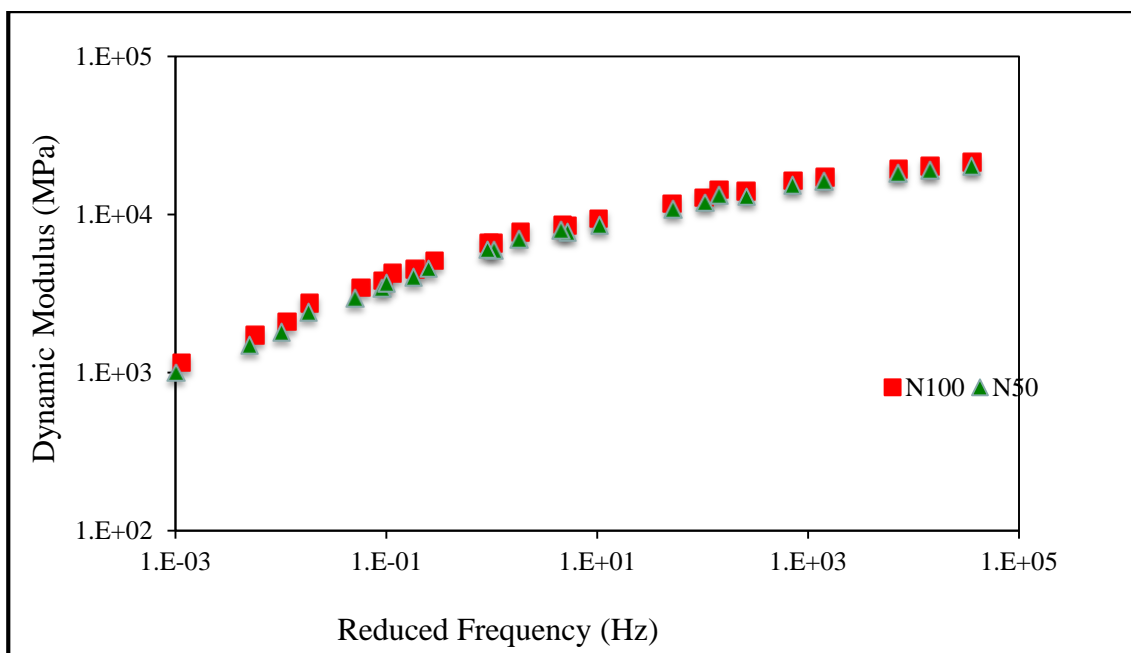


Figure 5.4 Aged (8-year) mixture master curves (log-log).

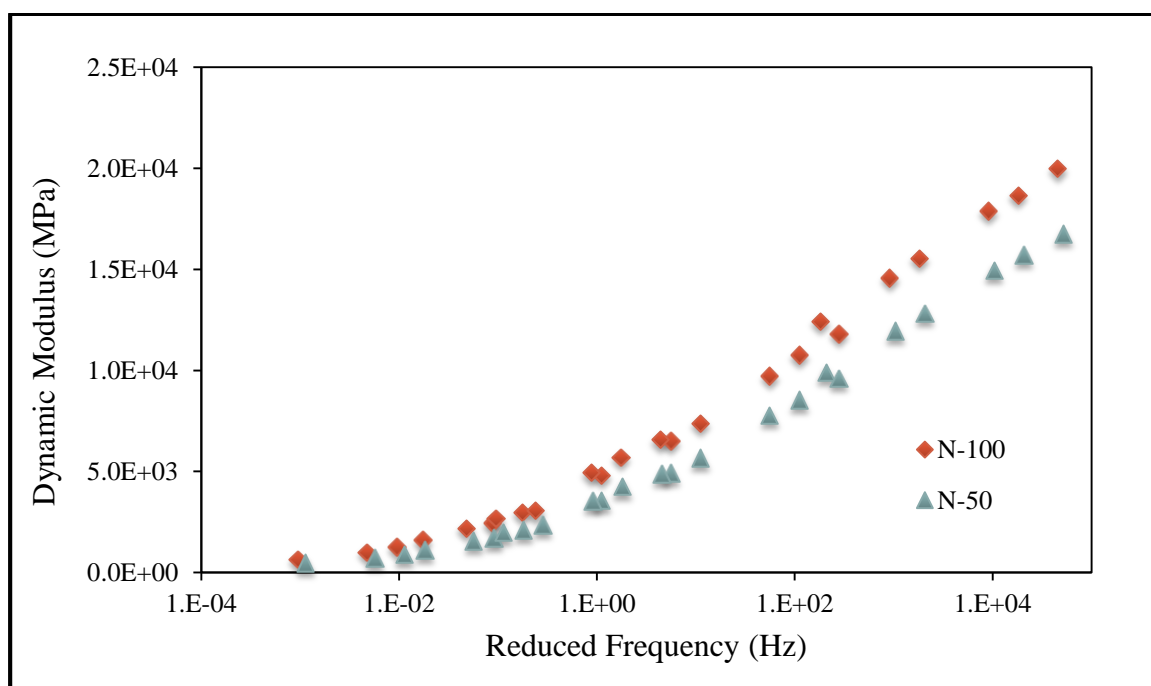


Figure 5.5 Aged (8-year) mixture master curves (semi-log).

A standard t-Test was used to determine if the apparent differences in the mean $|E^*|$ values of the two mixtures were statistically significant. The Bonferroni method results are shown in Table 5.11. The analysis indicates that with 95 percent confidence ($\alpha=0.05$) it can be concluded that there is no statistical difference between the mean $|E^*|$ values of the standard and re-designed mixtures.

Table 5.11 Aged (8-year) mixture Bonferroni groupings.

Test Frequency	25 Hz		10 Hz	
Test Temperature	p-value ($\alpha = 0.05$)	Grouping	p-value ($\alpha = 0.05$)	Grouping
4°C	0.33	(N100=N50)	0.24	(N100=N50)
21°C	0.35	(N100=N50)	0.41	(N100=N50)
37°C	0.38	(N100=N50)	0.34	(N100=N50)
50°C	0.45	(N100=N50)	0.46	(N100=N50)

Table 5.12 shows the FN results for the re-designed and standard field mixtures. The data indicates both designs have almost the same flow number and cumulative strain at FN. This suggests both designs may have similar rutting performance in the field. The Bonferroni method results are shown in Table 5.13. The analysis indicates that with 95 percent confidence ($\alpha=0.05$) it can be concluded that there are no significant differences between the mean flow number and mean strain at flow number for the standard and re-designed mixtures.

Table 5.12 Aged (8 years) flow number data.

	N100					
	Sample 1	Sample 2	Sample 3	Sample 4	Avg.	SD
Air voids, %	8.1	7.8	6.0	— ¹	7.3	1.1
Flow Number (FN)	8976	9380	8194	— ¹	8850	603
Strain @ FN, $\mu\epsilon$	12,066	9,751	15,966	— ¹	12594	3141
	N50					
	Sample 1	Sample 2	Sample 3	Sample 4	Avg.	SD
Air voids, %	6.3	6.9	6.0	5.2	6.1	0.7
Flow Number (FN)	8759	7345	10000	10000	9026	1264
Strain @ FN, $\mu\epsilon$	13,477	15,878	9,952	17,058	14091	3136

¹ No specimens were available for testing.

Table 5.13 Aged (8 year) flow number Bonferroni groupings.

Flow Number (FN)		Strain @ FN, $\mu\epsilon$	
p-value ($\alpha = 0.05$)	Grouping	p-value ($\alpha = 0.05$)	Grouping
0.84	(N100=N50)	0.56	(N100=N50)

5.1.3.2 Beam Fatigue Test

Samples of both the standard and re-designed mixtures were tested according to AASHTO T 321, “Determining the Fatigue Life of Compacted Hot Mix Asphalt (HMA) Subjected to Repeated Flexural Bending.” For each mixture (standard and re-designed) two sets of beams (three beams per set) were prepared. One set per mixture was tested in the post-construction condition; the second set was tested after oven conditioning, to approximate

the mixtures' fatigue properties after eight years of in-service life. Table 5.14 shows the air void contents of the beam specimens.

Table 5.14 Beam specimen air void contents.

Specimen	Age, years	Air Voids, %
N100 ¹ -2	0 ³	11.2
N100-4	0	7.9
N100-5	0	9.4
Average		9.5
Standard Deviation		1.65
N100-1	8	9.8
N100-3	8	10.6
N100-6	8	8.4
Average		9.6
Standard Deviation		1.11
Specimen	Age, years	Air Voids, %
N50 ² -1	0	4.6
N50-2	0	4.4
N50-5	0	8.7
Average		5.9
Standard Deviation		2.43
N50-3	8	4.0
N50-4	8	6.8
N50-6	8	8.0
Average		6.3
Standard Deviation		2.05

³ Denotes the post-construction condition

The average target air void contents for the beam specimens were 7 percent and 5 percent for the standard and re-designed mixtures respectively. As indicated in the table, these targets were not met, but due to lack of material it was not possible to make additional

beam specimens. Also as shown in the table, the beam specimens were placed into groups such that the average air voids of the two groups (for each mixture) were approximately equal. All the testing was completed at 20°C. Table 5.15 and 5.16 show the initial stiffness and number of cycles to failure results.

Table 5.15 Beam fatigue, initial stiffness.

Mixture	Age, years	Initial Stiffness (MPa)				
		Specimen 1	Specimen 2	Specimen 3	Average	SD
N100 ¹	0 ³	6266	— ⁴	6878	6572	433
N100	8	7056	7965	— ⁵	7511	643
N50 ²	0	8415	8569	6927	7970	907
N50	8	10186	7476	6446	8036	1932

⁴ Temperature was not constant during testing

⁵ Did not follow the expected trend of dissipated energy versus load cycles

Table 5.16 Beam fatigue, number of cycles to failure.

Mixture	Age, years	Cycles to failure (multiples by 1000 sec)				
		Specimen 1	Specimen 2	Specimen 3	Average	SD
N100 ¹	0 ³	177	— ⁴	1030	604	603
N100	8	1050	507	— ⁵	779	384
N50 ²	0	354	599	200	384	201
N50	8	755	318	249	441	274

During testing of N100 post-construction Specimen 2, the temperature chamber failed so the temperature was not held constant. The result was an abnormal decline in beam flexural stiffness. Additionally, data from one of the standard design (Specimen 3) eight-year specimen does not follow the expected trend of dissipated energy, which has to decrease

with load cycle increment. The reason for this has not been identified, but the inaccurate results have not been included in the analyses.

The fatigue test results indicate that although the standard mixture has slightly lower initial stiffness, it may endure more cycles to failure when compared to the re-designed mixture, for both the post-construction and after eight years of service conditions. Also, while the increase in initial stiffness after temperature conditioning is to be expected, the increase in fatigue life after temperature conditioning is counter-intuitive. As an asphalt mixture ages, it would be expected to become more brittle, thereby causing the fatigue life of the mixture to decrease, not increase. The Bonferroni method results are shown in Table 5.17. The analysis indicates that with 95 percent confidence ($\alpha=0.05$) it can be concluded that there is no significant difference between the initial stiffness and cycles to failure for the standard and re-designed mixtures, which might be a result of high standard deviation within the replicates. Overall, the beam fatigue results of the experiment are questionable, at best.

Table 5.17 Beam fatigue Bonferroni groupings.

Age, years	Initial Stiffness (MPa)		Cycles to Failure (multiples by 1000 sec)	
	p-value ($\alpha = 0.05$)	Grouping	p-value ($\alpha = 0.05$)	Grouping
0 ³	0.14	(N100 ¹ =N50 ²)	0.76	(N100=N50)
8	0.75	(N100=N50)	0.88	(N100=N50)

5.1.3.3 Asphalt Binder Extraction, Recovery, and Grading

The asphalt binders in the mixture samples at the two aged conditions (post construction and eight-year in-service life) were recovered and tested to determine the binder grades according to AASHTO M 320, “Performance Graded Asphalt Binder.” A PG 70-22 was the original binder used for both designs. Due to lack of materials, it was necessary to recover the binder from the beam fatigue specimens, after the fatigue testing had been completed. In order to do so without further aging the binder, once the beams had been fatigue tested they were heated only enough to allow them to be broken apart into loose mixture. Binder recovery was then completed according to AASHTO T 319, “Quantitative Extraction and Recovery of Asphalt Binder from Asphalt Mixtures.” Following recovery the performance grade of the binders was determined according to AASHTO T 315, “Determining the Rheological Properties of Asphalt Binder Using a Dynamic Shear Rheometer (DSR),” and AASHTO T 313, “Determining the Flexural Creep Stiffness of Asphalt Binder Using the Bending Beam Rheometer (BBR).” The continuous performance grades of the recovered binders are shown in Table 5.18.

Table 5.18 Recovered asphalt binder continuous grades.

Mixture	Age, years	Original Binder Grade	Recovered Continuous Grade
Original	0 ¹	PG 70-22	PG 97-20
Original	8		PG 104-16
Re-designed	0 ¹		PG 88-22
Re-designed	8		PG 99-18

¹ Denotes the post-construction condition

Asphalt binder aging, through the oxidation process, stiffens binder thereby potentially increasing both the high and low temperatures at which an asphalt binder will meet the applicable specifications. As the data in Table 5.18 show, the high temperature grade for the post-construction binder was three standard grades higher than the original PG 70 grade for the re-designed mixture and over four standard grades higher than the original binder grade (using extrapolated 6-degree increment). There was no low temperature grade change for the post-construction re-designed mixture and only a slight temperature grade change for the post-construction original mixture.

The results for the specimens conditioned in the laboratory to mimic eight years of aging had more aging than did the post-construction mixtures. The high temperature grade increased nearly five standard grades beyond the original PG 70 for the re-designed mixture and nearly six standard grades for the original mixture. The low temperature grade for the post-construction re-designed mixture was four degrees warmer, while the low temperature grade for the original mixture was six degrees warmer.

The trend in the binder changes are as expected (i.e., aging stiffens the binder), although in some cases the results show more aging than might be expected. This could possibly be due to the addition of shingles in the mixtures. However, the results do seem to indicate the re-designed mixtures tend to age less, when compared to the standard mixture. Therefore, the re-designed mixture may offer better durability than the original mixtures.

5.1.3.4 Porosity

Durability of asphalt mixtures can be determined by the air voids contents of mixtures. As air voids content increases, water permeability also increases, resulting in lower mixture durability that can often cause early failure. “Percent porosity” defines the percent of air voids that are accessible to water and thus control durability. Two specimens with same air voids content can have different porosity and durability; however, asphalt mixtures with same percent porosity will have the same durability. So, for evaluating durability of asphalt mixtures, the percent of air voids accessible to water is of concern (CoreLok Manual, 2011).

Percent porosity is defined as the percentage of air voids in an asphalt mixture that water can penetrate. This parameter can be calculated using two specific gravities values, bulk specific gravity and apparent maximum gravity of the asphalt mixture specimens. Porosity is a good indicator of asphalt mixture durability and has a good correlation with asphalt mixtures permeability (CoreLok Manual, 2011).

To calculate the percent porosity of an asphalt mixture, a specimen is vacuum-sealed in a bag using the CoreLok equipment. It is then submerged in water for 4 minutes until the water level stabilizes. After 4 minutes the bag is opened, under water and water is allowed to penetrate into the specimen for another 4 minutes. The mass of the bag, mass of the vacuum-sealed specimen with the bag, and the combined mass of the specimen and the bag in water after bag opening are recorded and used to calculate the two densities. The percent porosity is calculated using Equation 5.1.

$$\% \text{ Porosity or } \%P = \left(\frac{\rho_1 - \rho_2}{\rho_2} \right) \times 100 \quad \text{Equation 5.1}$$

where:

ρ_1 = density of the vacuum-sealed compacted specimen, and

ρ_2 = density of the vacuum-sealed compacted specimen after opening under water.

The porosity of both the original and redesigned mixtures was determined in two different aging conditions and the results are shown in Table 5.19.

As seen in Table 5.19, aged mixtures have higher porosity compared to unaged mixtures although their air void contents do not change, or even reduce. Aging increases the porosity because the binder film thickness is reduced, leading to a larger volume of water permeable channels in the mixture into which water can more easily penetrate. As seen in Table 5.19, although the re-designed mixtures have lower air voids (4.4 and 3.4 percent) compared to the standard mixtures (7.2 and 7.4), the re-designed mixtures have higher porosity for both aging conditions (5.74 and 6.85 for re-designed mixtures compared to 5.52 and 6.51 for original mixtures). These mixtures have same V_{be} and the only valid reason for this unexpected phenomena (higher porosity for re-designed mixture with lower air void when comparing to standard mixture) is the difference between aggregate structures as would be discussed further in the Bailey Method section.

Table 5.19 Porosity and Air Voids Results.

Mixture	Sample 1	Sample 2	Sample 3	Sample 4	Avg. Porosity %	C.V. %	Avg. AV%
N100- Unaged	5.65	5.42	5.48	— ¹	5.52	2.2	7.2
N100-Aged	6.76	6.24	6.52	— ¹	6.51	4.0	7.4
N50- Unaged	5.71	5.68	5.46	6.11	5.74	4.8	4.4
N50-Aged	7.03	7.33	6.18	— ¹	6.85	8.7	3.4

¹ No specimens were available for testing.

5.1.3.4.1 Bailey Method

The aggregate skeleton of an asphalt mixture is what carries the traffic loads placed on the compacted asphalt pavement. The asphalt mixtures' aggregate skeleton properties are highly related to aggregate gradation, shape, texture, and strength. Before Bailey method, the only available tool for asphalt mixture gradation evaluation was 0.45-power grading chart. The Bailey method is based on the aggregate packing characteristics and uses VMA, V_a , and compaction properties to evaluate the asphalt mixture design. The Bailey method is to help to evaluate and increase aggregate interlock and thus improved rutting performance (Vavrik et al., 2002).

Based on Superpave mixture design, definition of coarse aggregate is any particle that is retained on the 4.75- mm sieve while fine aggregate is any aggregate that passes the 4.75- mm sieve and is retained on the 0.075-mm sieve. The same sieve (4.75-mm sieve) is used for all different asphalt mixtures. However, the definition of coarse and fine aggregate is

more specific for Bailey method and is related on the nominal maximum aggregate size (Vavrik et al., 2002). The Bailey method definitions are:

- Coarse Aggregate: Large particles that create voids in asphalt mixture.
- Fine Aggregate: Small particles that fill the voids created by the coarse aggregate in the mixture.

The primary control sieve (PCS) defines the threshold of coarse and fine aggregate, and the PCS is based on the nominal maximum particle size (NMPS) of the asphalt mixture's skeleton. Figure 5.6 shows how coarse and fine aggregate would be evaluated. The PCS is defined as the closest sieve to the result of the PCS formula in Equation 5.2 (Vavrik et al., 2002):

$$PCS = NMPS \times 0.22 \quad \text{Equation 5.2}$$

where:

PCS = primary control sieve for the overall blend, and

NMPS = Nominal maximum particle size for the overall blend, which is one sieve larger than the first sieve to retain more than 10% (as defined by Superpave terminology).

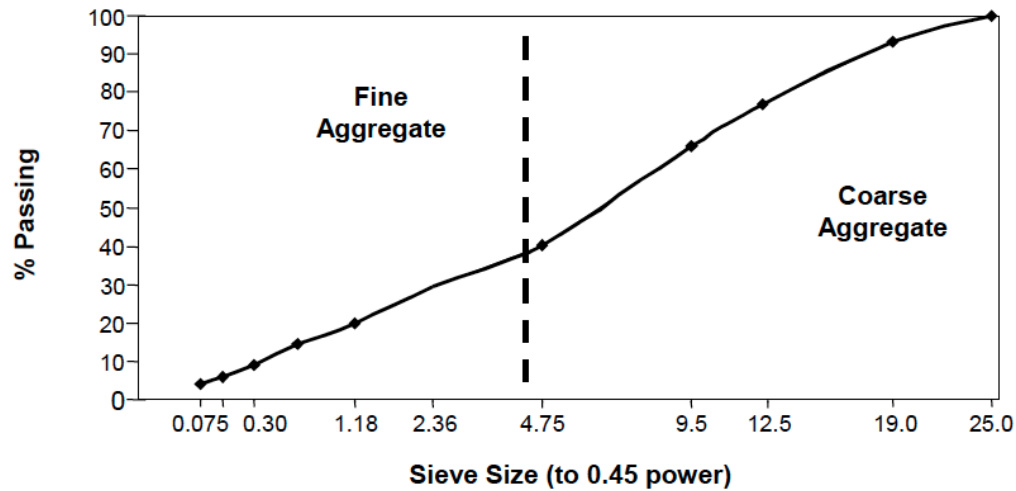


Figure 5.6 Example of break between coarse and fine aggregate for 19.0 NMPS mixture (Vavrik et al., 2002).

Moreover, the Bailey aggregate gradation is divided into three specific portions. The coarse fraction of the gradation includes the particles larger than the PCS sieve. The fine aggregate fraction includes all the particle sizes smaller than the PCS and is separated and evaluated as two fractions. The secondary control sieve (SCS) is defined same as PCS but for fine fraction instead of whole gradation which becomes the threshold between the larger and smaller fine aggregate particles. Figure 5.7 shows how the gradation is divided into the three aggregate portions (Vavrik et al., 2002).

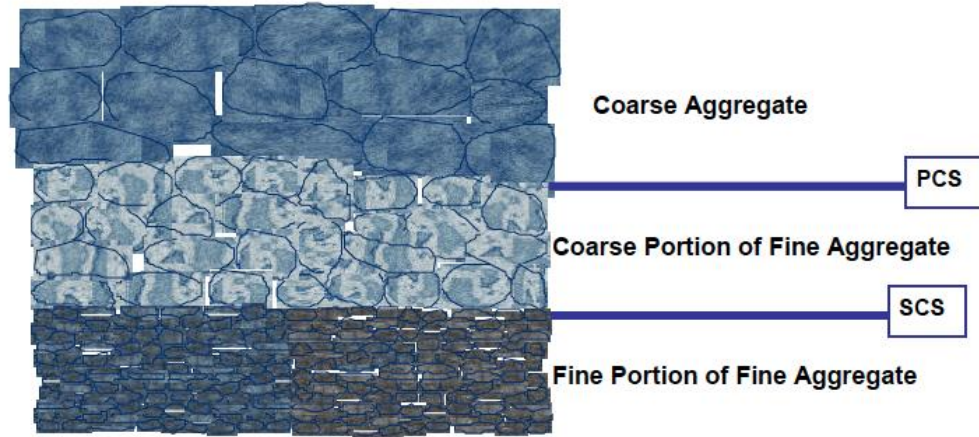


Figure 5.7 Coarse-graded mixture fractions (Vavrik et al., 2002).

The three aggregate fractions are used to define three aggregate ratios, Coarse Aggregate (CA), Fine Aggregate Coarse (FA_c), and Fine Aggregate Fine (FA_f Ratio), as shown in Equations 5.3 to 5.5. These ratios characterize aggregate packing. Changes in each portion will change asphalt mixture characteristics (Vavrik et al., 2002).

$$CA\ Ratio = \frac{(\% \text{ Passing Half Sieve} - \% \text{ Passing PCS})}{(100\% - \% \text{ Passing Half Sieve})} \quad \text{Equation 5.3}$$

$$FA_c = \frac{\% \text{ Passing SCS}}{\% \text{ Passing PCS}} \quad \text{Equation 5.4}$$

$$FA_f = \frac{\% \text{ Passing TCS}}{\% \text{ Passing SCS}} \quad \text{Equation 5.5}$$

- CA Ratio: Describes how the coarse aggregate particles pack.

- FA_c Ratio: Describes how the coarse portion of the fine aggregate packs.
- FA_f Ratio: Describes how the fine portion of the fine aggregate packs.

The “half sieve” is the closest sieve to one half the size of the NMSA as shown in Figure 5.8. CA ratio is the amount of material between the half sieve and the PCS, divided by the amount of material retained above the half sieve. Although some fine particles may contribute material to the coarse fraction, the CA ratio is controlled by the coarse aggregate blend by volume and the gradation of the individual coarse aggregate used (Vavrik et al., 2002).

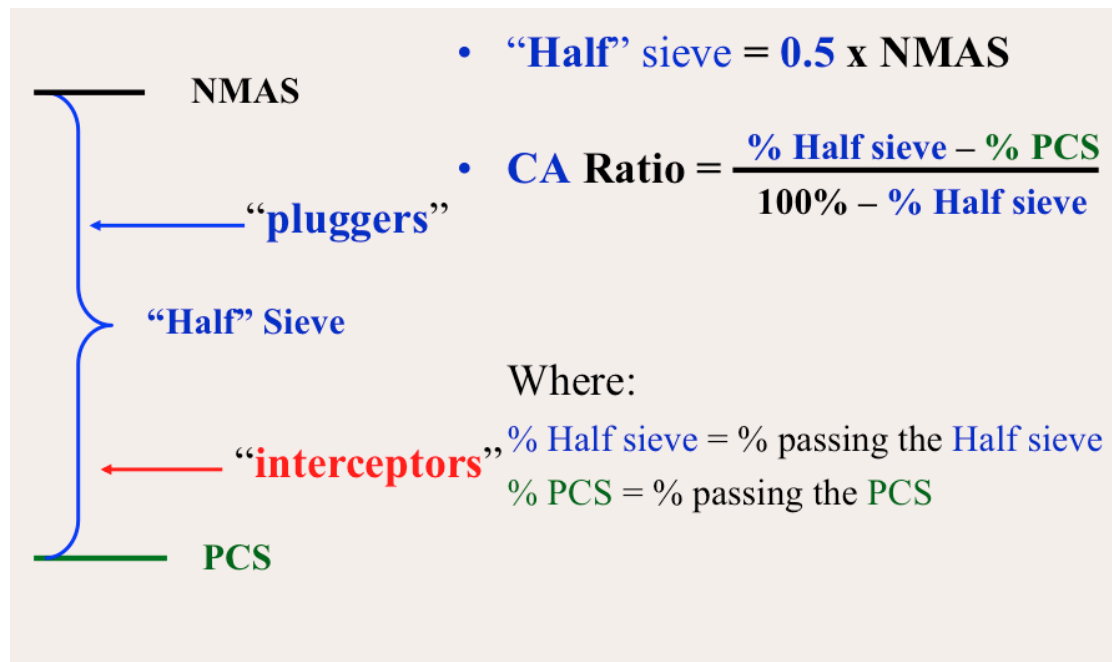


Figure 5.8 Bailey Method Coarse Aggregate Ratio.

As shown in Figure 5.8, the “pluggers” are the large coarse particles (larger than the half sieve) in the coarse fraction that form the primary aggregate skeleton. The “interceptors” are the smaller coarse particles (smaller than the half sieve) in the coarse fraction, which serve to hold the larger coarse particles apart and support them. The amount of each fraction (pluggers and interceptors) can have a significant effect of asphalt mixture performance. Theoretically, the higher the interceptors percentage, the more the water-permeable channels in an asphalt mixture, and thus the higher the porosity and hydraulic conductivity.

For the SR-13 project, all three ratios were calculated for the standard and re-designed mixtures as shown in Table 5.20.

Table 5.20 SR-13 Bailey Method Aggregate Ratios

Mixture	Half Sieve (mm)	PCS (mm)	CA Ratio	SCS (mm)	FA _c	FA _f
Original - N100	4.75	2.36	0.411	0.600	0.489	0.330
Redesigned - N50	4.75	2.36	0.540	0.600	0.487	0.307

As seen in Table 6.20, the FA_c ratios of the two mixtures are essentially the same, while the FA_f ratios are only slightly different. However, the CA ratio for re-designed mixture is significantly higher than that of the standard mixture. This suggests the re-designed mixture has more interceptor particles, which may cause more water permeable channels and higher porosity in the mixture.

5.1.3.5 Hydraulic Conductivity

“Another indicator of permeability and durability of asphalt mixtures is the hydraulic conductivity or falling head permeability. Darcy showed that water flow is related to the hydraulic gradient and the area of a sample” (Vivar and Haddock, 2006):

$$Q = kiA \quad \text{Equation 5.6}$$

where:

Q = flow rate (cm^3/s);

k = coefficient of permeability (or simply permeability) (cm/s);

i = hydraulic gradient (cm/cm); and

A = total cross sectional area (cm^2).

“The equation assumes a homogeneous material, with steady state, laminar, one-dimensional flow conditions, and that the fluid is incompressible and the material completely saturated.” (Vivar and Haddock, 2006).

Florida Department of Transportation (FDOT) developed a permeability test device to evaluate the permeability of asphalt mixtures (Figure 4.1). According to the falling head method, the time required for a sample to lose a head of water is measured and used to determine the permeability (Vivar and Haddock, 2006). For this approach Darcy’s equation can be expressed as:

$$k = \frac{aL}{At} \ln\left(\frac{h_1}{h_2}\right) \quad \text{Equation 5.7}$$

where,

k = coefficient of permeability (cm/s);

a = area of the stand pipe (cm²);

h₁ and h₂ = water head at the beginning and end of the test (cm);

t = time over which head is allowed to fall (s);

L = length of the sample (cm); and

A = cross-sectional area of the sample (cm²).

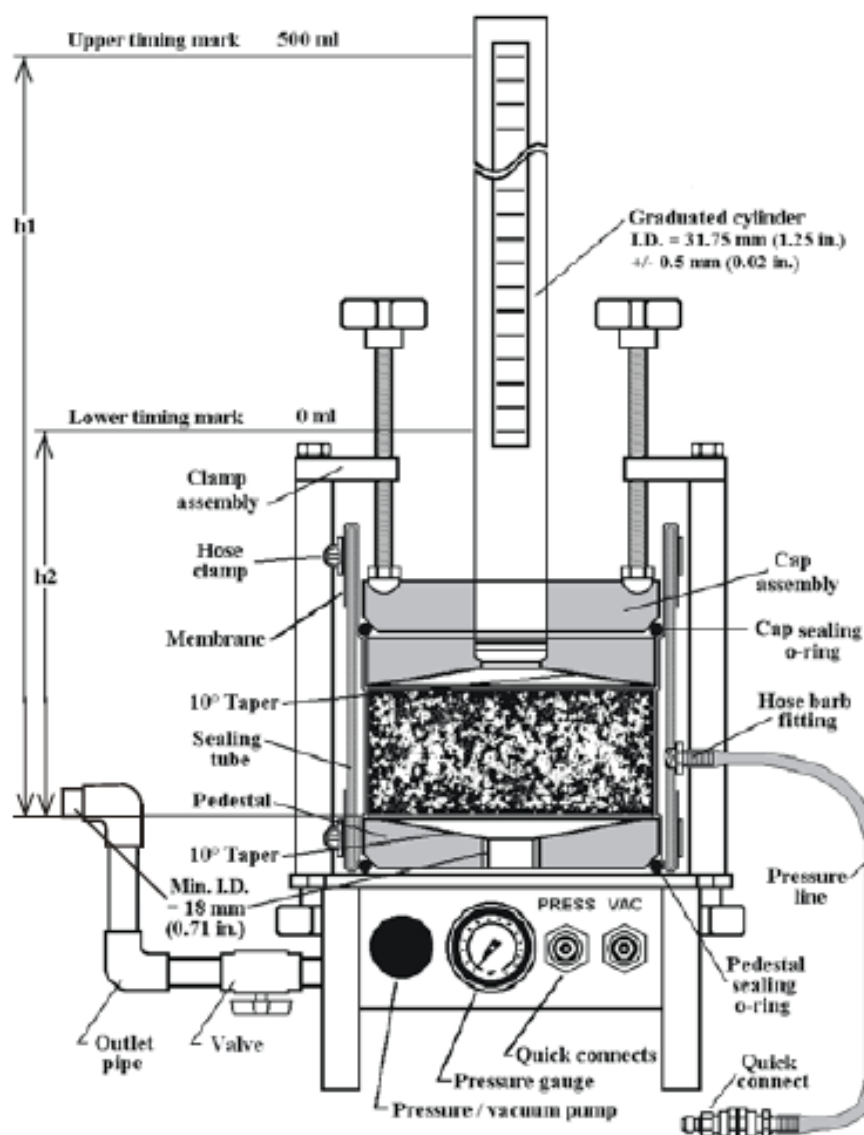


Figure 5.9 FDOT Hydraulic Conductivity (Falling Head Permeability) Permeameter (Vivar and Haddock, 2006).

Due to lack of material following dynamic modulus testing, the dynamic modulus specimens were cut to 38 ± 2 mm and tested based on FDOT FM 5-565 hydraulic conductivity test method. Table 5.21 shows the falling head permeability results for SR-13 project.

Table 5.21 Hydraulic Conductivity Results

Mixture	Sample 1	Sample 2	Sample 3	Sample 4	Avg. Hydraulic Conductivity	SD	Avg. Air Voids %
N100-Unaged	2.55E-05	7.75E-06	7.33E-05	1.53E-04	6.50E-05	6.51E-05	7.2
N100-Aged	3.55E-05	4.31E-05	1.93E-04	— ¹	9.06E-05	8.90E-05	7.4
N50-Unaged	1.18E-04	9.06E-05	5.92E-05	4.38E-04	1.76E-04	1.76E-04	4.4
N50-Aged	4.44E-04	8.97E-05	— ¹	— ¹	2.67E-04	2.51E-04	3.4

¹ No specimens were available for testing.

The hydraulic conductivity results are consistent with the porosity findings as the standard mixture has a lower permeability than the re-designed mixture for both aging conditions. This result is attributable to more pluggers for the re-designed mixture, which causes more water permeable channels to form in the mixture and increases the mixture permeability. Again, as reflected in the Table 5.21 data, as a mixture ages, the mixture permeability tends to increase.

5.1.3.6 Electrical Resistivity

Asphalt mixtures are an electrical insulator material with an electrical resistance of approximately $10^{13} \Omega$. However, it is possible to make an asphalt mixture specimen an electrical conductor by filling the void space (pores) with water to obtain its electrical resistivity (E_r). This electrical resistivity can then be related to the permeability and durability properties of the specimen (Forough et al, 2002). The relationship between electrical resistivity and tortuosity is shown in Equations 5.8 to 5.10. A higher value of E_r

indicates a more open air voids distribution and a higher value of tortuosity indicates more interconnected air voids. Since both the volume and the interconnectedness of the air voids in an asphalt mixture play a role in mixture durability, it is important to understand the differences in these two characteristics between the standard and re-designed mixtures. An understanding of these differences may help to increase industry knowledge of how asphalt mixture aggregate gradations affect air voids and thereby mixture durability.

$$\rho = \frac{RA}{L} \quad \text{Equation 5.8}$$

$$\frac{1}{\rho_0} = \sigma_0 \quad \frac{1}{\rho_t} = \sigma_t \quad \text{Equation 5.9}$$

$$\sigma_t = \sigma_0 \phi \beta \quad \text{Equation 5.10}$$

Where,

ρ = Resistivity of material (ohm.m)

R= Real impedance on minimum imaginary impedance (ohm)

A= Cross section of material (m²)

L= Length of material (m)

σ_0 = Conductivity of pore solution ((ohm.m)⁻¹)

σ_t = Conductivity of asphalt material ((ohm.m)⁻¹)

Φ = Porosity of asphalt Material

β = Tortuosity of Asphalt Material

For the SR-13 project, both the standard and re-designed mixtures, in both the aged and unaged conditions, were tested for resistivity according to AASHTO test method, “Electrical Resistivity of Concrete Cylinder Tested in a Uniaxial Resistance Test.” Due to lack of materials, after porosity testing was completed the same specimens were used for resistivity testing. The specimens were vacuum saturated in salt water (9.1% concentration, 100 g of sodium chloride in 1 L of water) for 24 hours before being tested. The resistivity test results can be used to calculate the tortuosity of asphalt mixtures, which may yield a better understanding of the interconnectedness of the air voids. The more interconnected the air voids, the more accessible they are to water and air. The tortuosity results are shown in Table 5.22.

Table 5.22 SR-13 Tortuosity Results

Mixture	Sample 1	Sample 2	Sample 3	Sample 4	Avg. Tortuosity	SD	Avg. Air Voids %
N100-Unaged	1.80E-08	1.36E-07	3.69E-08	3.74E-08	5.71E-08	5.36E-08	7.2
N100-Aged	3.99E-08	4.41E-08	3.22E-08	— ¹	3.87E-08	6.06E-09	7.4
N50-Unaged	9.21E-09	1.59E-08	2.51E-09	1.94E-08	1.18E-08	7.47E-09	4.4
N50-Aged	3.10E-09	2.60E-09	3.51E-09	— ¹	3.07E-09	4.58E-10	3.4

¹ No specimens were available for testing.

The data in Table 5.22 indicate that tortuosity decreases as a mixture ages, meaning the air and water channels become less interconnected with aging. As the binder ages, the asphalt binder thickness will decrease and creates more voids on the asphalt binder film but these voids are less interconnected. The re-designed mixture (N50) has lower tortuosity than does the standard mixture (N100) for both aging conditions, indicating the re-designed

mixture has less interconnected air voids and therefore should have better resistance to air and moisture damage than the standard mixture.

5.2 Georgetown Road

As mentioned before the second field trial was on Georgetown Road in Indianapolis. Similar to the SR-13 project two different mixture designs (standard and re-designed) were placed as a 3-inch thick intermediate layer, both designed as Category 3, 19.0-mm mixtures. The standard mixture was designed using 100 gyration of the SGC and choosing the optimum binder content at 4 percent air voids while, the re-designed mixture designed using 30 gyrations of the SGC and choosing the optimum binder content at 5 percent air voids.

In order to again test the hypothesis that re-designing mixtures to be more compactable will lead to more durable mixtures without making them more susceptible to permanent deformation, the testing plan shown in Table 5.23 was proposed and carried out for the Georgetown Road project.

Table 5.23 Georgetown Road Testing Plan.

Conditioning	Test	Plant Mixed-Laboratory Compacted ¹		Plant Mixed-Field Compacted (Cores) ¹	
		Control Mixture	Test Mixture	Control Mixture	Test Mixture
No Temperature Conditioning	Dynamic Modulus	4	4		
	Flow Number	4	4		
	Fatigue Properties	4	4		
	Porosity	4	4		
	Hydraulic Conductivity	4	4		
	Electrical Resistivity	4	4		
Long-term Oven Conditioning (AASHTO R30)	Dynamic Modulus	4	4		
	Flow Number	4	4		
	Fatigue Properties	4	4		
	Porosity	4	4		
	Hydraulic Conductivity	4	4		
	Electrical Resistivity	4	4		
No Temperature Conditioning	Pavement Density			20	20
	Dynamic Modulus			4	4
	Fatigue Properties			4	4
	Hamburg Testing			2	2
	Binder Recovery & Grading			3	3
Long-term Oven Conditioning (AASHTO R30)	Dynamic Modulus			4	4
	Fatigue Properties			4	4
	Binder Recovery & Grading			3	3

¹ The number indicates the number of replicates for the test. The shaded portion indicates the corresponding testing will not be completed.

5.2.1 Plant Mixed-Laboratory Compacted Testing

Material for the laboratory testing, approximately 300 kg (661 lbs) each for both the standard and re-designed mixtures, was collected from trucks before they left the hot-mix plant. The sampled mixture was placed into boxes and returned to the laboratory for testing.

As in the first trial project, test specimens for the original mixture design were laboratory compacted to produce 7 percent air voids according to current test method standards; the re-designed mixture specimens were produced at 5 percent air voids. In order to produce the test specimens, the field-sampled mixture had to be re-heated, split into appropriate sample sizes, and the specimens prepared. All re-heating was performed carefully and consistently at the lowest possible temperature.

5.2.1.1 Dynamic Modulus and Flow Number Testing

Dynamic modulus and FN were determined according to AASHTO TP 79 for both the original and re-designed mixtures in both post-construction (no oven conditioning) and long-term aged (AASHTO R30) conditions. In this case, separate sets of specimens were produced and tested to determine $|E^*|$ and FN. Figure 5.10 shows the $|E^*|$ master curve data for the two mixtures and two aging conditions. Figure 5.11 shows the same data in semi-log form, allowing a better view of the high frequency data.

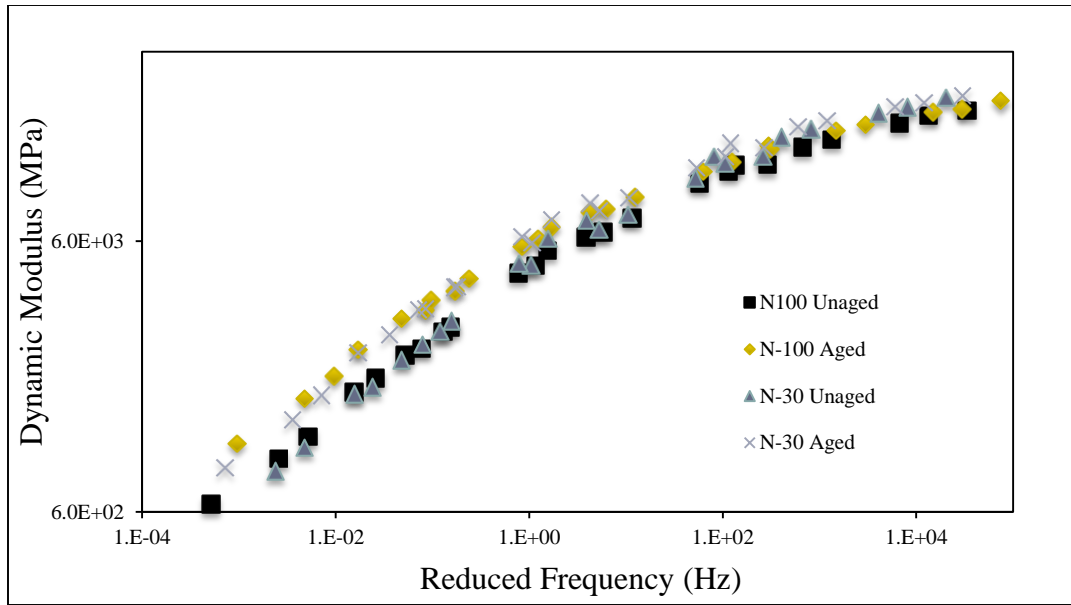


Figure 5.10 Laboratory compacted specimen master curves (log-log plot).

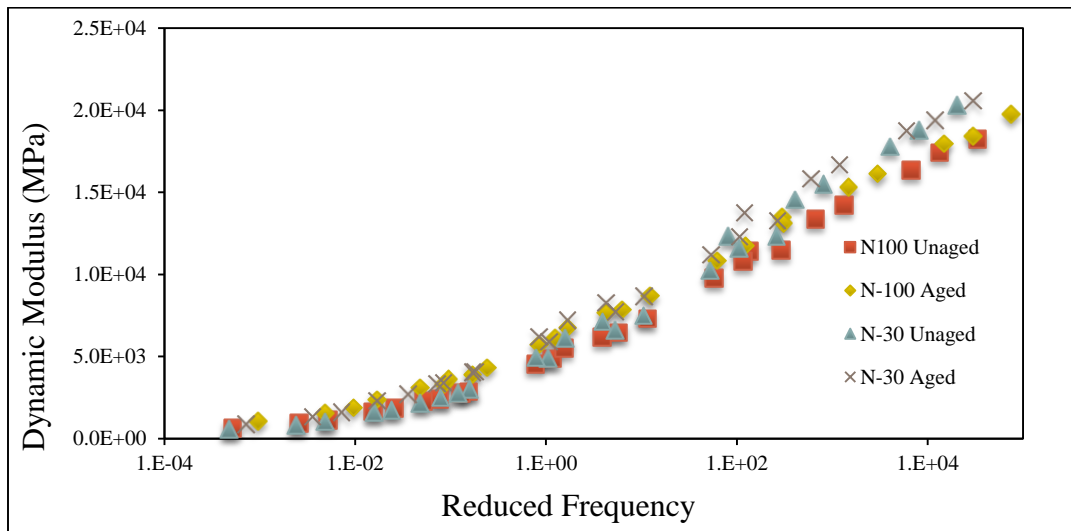


Figure 5.11 Laboratory compacted specimen master curves (semi-log plot).

Table 5.24 is a summary of the average $|E^*|$ data for the mixtures. To determine if significant differences exist between the $|E^*|$ values of the two mixtures a t-Test was used to compare the means. The Bonferroni method results are shown in Table 5.25. In this case the $|E^*|$ values are slightly higher for the re-designed mixture however, the statistical analysis indicates that with 95 percent confidence ($\alpha=0.05$), it can be concluded that the standard and re-designed mixture designs' $|E^*|$ values are not significantly different.

Table 5.24 Laboratory specimen dynamic modulus statistical summary.

25 Hz	N100 Unaged		N100 Aged		N30 Unaged		N30 Aged	
	Average $ E^* $, MPa	C.V., %	Average $ E^* $, MPa	C.V., %	Average $ E^* $, MPa	C.V., %	Average $ E^* $, MPa	C.V., %
4°C	18,236	9.1	19779	7.7	20326	4.3	20603	2.4
21°C	11,488	4.7	13129	6.4	12333	4.7	13280	5.7
37°C	6,205	3.2	7674	10.3	7130	11.3	8276	6.1
50°C	2,770	8.9	4355	5.2	2778	5.3	4071	8.9
10 Hz	N100 Unaged		N100 Aged		N30 Unaged		N30 Aged	
	Average $ E^* $, MPa	C.V., %	Average $ E^* $, MPa	C.V., %	Average $ E^* $, MPa	C.V., %	Average $ E^* $, MPa	C.V., %
4°C	17421	9.3	18422	6.4	18789	5.4	19396	3.6
21°C	10834	3.5	11774	5.1	11594	6.0	12297	3.9
37°C	5533	8.6	6778	9.7	6134	8.2	7209	6.1
50°C	2285	7.7	3630	2.8	2185	6.3	3355	9.4

Table 5.25 Laboratory specimen dynamic modulus Bonferroni groupings.

Test Frequency	25 Hz		10 Hz	
Test Temperature	p-value ($\alpha =$ 0.05)	Grouping	p-value ($\alpha =$ 0.05)	Grouping
4°C	0.0771 3	(N30A=N30U=N100A=N100U)	0.1678 9	(N30A=N30U=N100A=N100U)
21°C	0.0115 8	(N30A=N100A=N30U); (N100U)	0.0199 5	(N100A=N30U=N30A); (N100U)
37°C	0.0591	(N30A=N100A=N30U); (N100U)	0.0077 8	(N100A=N30U=N30A); (N100U)
50°C	0.0000 1	(N100A= N30A); (N100U=N30U)	0.0000 1	(N100A= N30A); (N100U=N30U)

Table 5.26 shows the FN results for the re-designed and standard mixtures for two aging conditions. The data indicate the standard mixture has a higher FN and less cumulative strain at FN than does the re-designed mixture for both aging conditions. This suggests the standard mixture may have better rutting performance than the re-designed mixture, opposite the FN results obtained during the mixture design phase of the field trial. As Table 5.27 shows, statistical analyses indicate there are significant differences between the standard and re-designed mixtures' flow numbers for both aging conditions. Only the aged original mixture has a strain at flow number that is statistically different from the other mixtures and aging conditions.

Table 5.26 Laboratory compacted FN summary (51°C).

	N100-Unaged					
	Sample 1	Sample 2	Sample 3	Sample 4	Average	C.V. %
Air voids, %	6.7	6.7	7.0	7.4	7.0	4.8
Flow Number (FN)	5629	4179	4315	3218	4335	22.9
Strain @ FN, $\mu\epsilon$	21,777	18,601	18,883	24,361	20906	13.0
	N30-Unaged					
	Sample 1	Sample 2	Sample 3	Sample 4	Average	C.V. %
Air voids, %	5.0	5.1	4.9	5.4	5.1	4.2
Flow number (FN)	2397	2608	3100	2293	2600	13.8
Strain @ FN, $\mu\epsilon$	24,419	22,170	20,421	24,294	22826	8.4
	N100-Aged					
	Sample 1	Sample 2	Sample 3	Sample 4	Average	C.V. %
Air voids, %	6.5	7.2	6.9	7.1	6.9	4.5
Flow Number (FN)	8124	8249	8507	10000	8720	10.0
Strain @ FN, $\mu\epsilon$	13,140	15,555	14,628	14,800	14531	7.0
	N30-Aged					
	Sample 1	Sample 2	Sample 3	Sample 4	Average	C.V. %
Air voids, %	5.0	5.3	5.1	5.1	5.1	2.5
Flow Number (FN)	6402	6180	6009	5412	6001	7.1
Strain @ FN, $\mu\epsilon$	20,278	19,078	18,475	17,514	18836	6.1

Table 5.27 Laboratory compacted FN Bonferroni groupings.

Flow Number (FN)		Strain @ FN, $\mu\epsilon$	
p-value ($\alpha = 0.05$)	Grouping	p-value ($\alpha = 0.05$)	Grouping
0.00001	(N100U); (N100A); (N30U); (N30A)	0.00896	(N100U=N30U=N30A); (N100A)

5.2.1.2 Semi-Circular Bend Testing

Due to the poor fatigue results obtained from the beam fatigue testing during the SR-13 first field trial, the research team chose to use the semi-circular bend (SCB) test to determine the fracture resistance of the asphalt mixtures for the Georgetown Road trial. This test is based on the elastic-plastic mechanism concept, which determines the critical strain energy release rate, or what is called the critical value of the J-integral (J_c). J_c is a function of the rate of strain energy change per notch depth as shown in equation 5.11 and represents the strain energy consumed to produce a unit area of fractured surface (crack) in a mixture. Higher J_c values indicate a material is more resistant to cracking and to crack propagation (Mohammad et al., 2012)

$$J_c = -\left(\frac{1}{b}\right) \frac{dU}{da} \quad \text{Equation 5.11}$$

where,

J_c = critical strain energy release rate (kJ/m²);

b = specimen thickness (m)

a = notch depth (m)

U = strain energy to failure (kN-m or kJ)

The SCB testing requires that each combination of mixture and aging be tested with three different notch depths. Since four replicates of each combination were tested, 12 specimens were needed. These were produced by compacting 150-mm diameter, 57-mm tall specimens in the SGC to meet the expected air void in the field (7% air void for standard and 5% air void for re-designed mixtures). The SGC specimens were sawn in half to produce semi-circular specimens and notches were cut perpendicular to the diameter at 0.025, 0.030 and 0.035 m in depth.

Figure 5.12 shows how fracture energy (area under load versus deformation curve) changes with notch depth for the combinations of mixture and aging condition. The J_c values for these combinations are given in Table 6.28. As previously stated, the higher the J_c value, the more resistant a mixture is to cracking and to crack propagation. In the post-construction condition the re-designed mixture appears to have better cracking performance than does the standard mixture. However, after oven conditioning to simulate eight years of in-service life, the two mixtures have almost the same cracking performance. While the former result seems plausible, the latter result is counterintuitive, if indeed the increased pavement density can improve mixture durability.

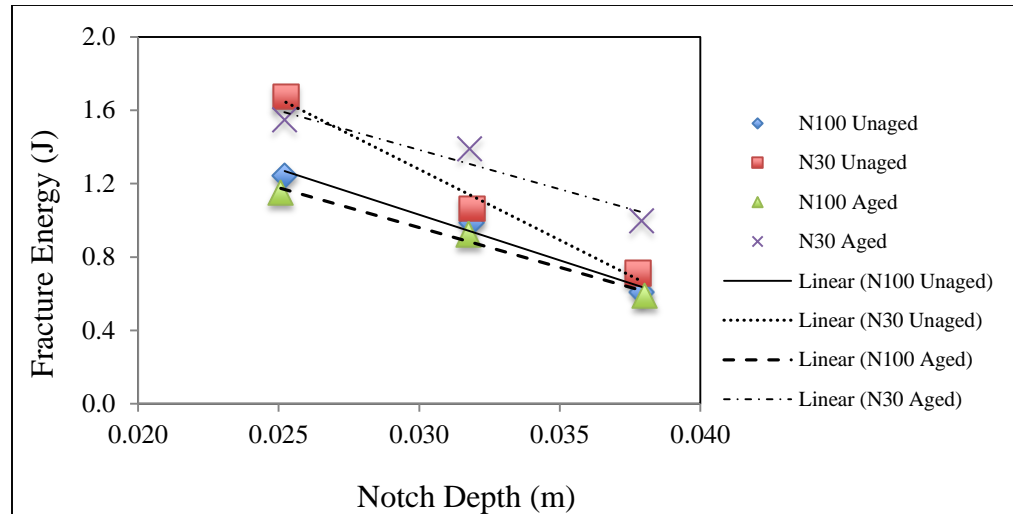


Figure 5.12 Laboratory specimen SCB test results.

Table 5.28 Laboratory specimen SCB critical strain energy release rate.

Mixture	Age, years	J_c (J/m ²)
N100	0 ¹	0.860
N30		1.402
N100	8	0.776
N30		0.747

¹ Denotes the post-construction condition

5.2.1.3 Porosity

As previously described, the porosity of standard and re-designed asphalt mixtures was determined. Due to lack of materials, asphalt specimens were retrieved after completion of the dynamic modulus test and the air voids calculated before completing the porosity testing. Porosity was determined for both the standard and re-designed mixtures in both aging conditions. Either four or five specimens were tested for each combination of mixture

and aging condition, depending on specimen availability. The results are shown in Table 5.29.

Table 5.29 Georgetown Rd, porosity test results

Mixture	Sample 1	Sample 2	Sample 3	Sample 4	Sample 5	Avg. Porosity	C.V. %	Avg. Air Voids %
N100-Unaged	4.79	6.89	6.62	7.20	7.67	6.63	16.6	7.2
N100-Aged	6.80	7.74	7.40	6.52	— ¹	7.12	7.8	7.4
N50-Unaged	4.34	4.52	5.08	6.27	— ¹	5.05	17.3	4.4
N50-Aged	5.22	5.23	5.71	5.42	— ¹	5.40	4.2	3.4

¹ No specimens were available for testing.

The data in Table 5.29 again show that an asphalt mixture ages its porosity increases. For both aging conditions, the re-designed mixture has lower porosity than the original mixture, indicating the re-designed mixture is less susceptible to oxidation and moisture damage than is the standard mixture.

5.2.1.4 Hydraulic Conductivity

The hydraulic conductivity of the two mixtures was determined according to FDOT FM 5-565. As before, due to lack of materials, the specimens used to determine mixture porosity were used for the testing. Table 5.30 shows the results. The data indicate that aging has not significantly changed the hydraulic conductivity of the mixtures. The re-designed mixture (N30) has a lower permeability than the standard mixture (N100) for both aging conditions,

again indicating the re-designed mixture is likely to be more resistant to oxidation and moisture damage.

Table 5.30 Hydraulic conductivity results vs. air void

Mixture	Sample 1	Sample 2	Sample 3	Sample 4	Sample 5	Avg. HD	SD	Avg. Air Voids %
N100-Unaged	4.62E-04	1.33E-04	2.46E-04	5.36E-04	5.12E-04	3.44E-04	1.87E-04	7.2
N100-Aged	1.66E-04	5.69E-04	2.85E-04	3.31E-04	— ¹	3.38E-04	1.69E-04	7.4
N30-Unaged	1.49E-05	0	2.19E-05	4.55E-05	0	2.06E-05	1.90E-05	4.4
N30-Aged	1.70E-05	6.30E-05	0	0	— ¹	2.00E-05	2.98E-05	3.4

¹ No specimens were available for testing.

5.2.1.5 Electrical Resistivity

Once porosity and hydraulic conductivity testing were complete, the compacted asphalt mixture specimens were used for electrical resistivity testing. Table 5.31 shows the results. As a mixture ages, tortuosity decreases, indicating the interconnectivity of the air voids in the asphalt mixture decreases. This finding is valid for both aging conditions. The re-designed mixture has lower tortuosity than the standard mixture for both aging conditions, again suggesting the re-designed mixture air void distribution has less interconnectivity than the standard mixture, making the re-designed mixture less prone to aging and more durable.

Table 5.31 Georgetown Road Tortuosity Results

Mixture	Sample 1	Sample 2	Sample 3	Sample 4	Sample 5	Avg. Tortuosity	SD	Avg. AV%
N100- Unaged	5.26E-08	2.84E-08	3.03E-08	2.72E-08	2.58E-08	3.46E-08	1.20E-08	7.2
N100- Aged	1.45E-08	3.51E-08	3.70E-08	3.24E-08	— ¹	2.98E-08	1.03E-08	7.4
N30- Unaged	3.12E-09	4.85E-09	2.37E-08	1.95E-08	3.09E-08	1.28E-08	1.03E-08	4.4
N30- Aged	3.59E-09	4.21E-09	3.98E-09	4.97E-09	— ¹	4.19E-09	5.81E-10	3.4

¹ No specimens were available for testing.

5.2.2 Plant-Mixed-Field-Compacted Testing

For both the standard and re-designed mixtures, 20 cores each were taken from the pavement immediately after construction. These 150-mm diameter cores were brought to the laboratory where the underlying layers were removed and the bulk specific gravity (G_{mb}) of each core was determined. Un-compacted mixture samples taken during mixture production were used to establish the maximum theoretical specific gravity (G_{mm}) for each mixture, allowing the in-place air voids to be determined. The results were shown before in Table 3.9.

5.2.2.1 Hamburg Testing

Four pavement cores (two cores per run) each from the control section and the experimental field section were tested in the Hamburg wheel-tracking machine to determine mixture susceptibility to permanent deformation (rutting). This testing was completed without performing oven conditioning on the cores since such conditioning would only serve to

increase a mixture's rutting resistance due to the stiffening effect. The test was completed according to AASHTO T324-14, "Hamburg Wheel-Track Testing of Compacted Hot Mix Asphalt (HMA)," at a test temperature of 50°C; the Illinois Department of Transportation (IDOT) maximum threshold of 12.5 mm rut depth at 20,000 passes was applied to determine if the mixtures might have rutting problems in the field. Figures 5.13 and 5.14 show the Hamburg results for the standard and re-designed mixtures. As the results indicate, the standard mixture (N100) had slightly lower rut depth than the re-designed mixture, although both mixtures have low rut depths and are well below the maximum allowable 12.5 mm of rutting.

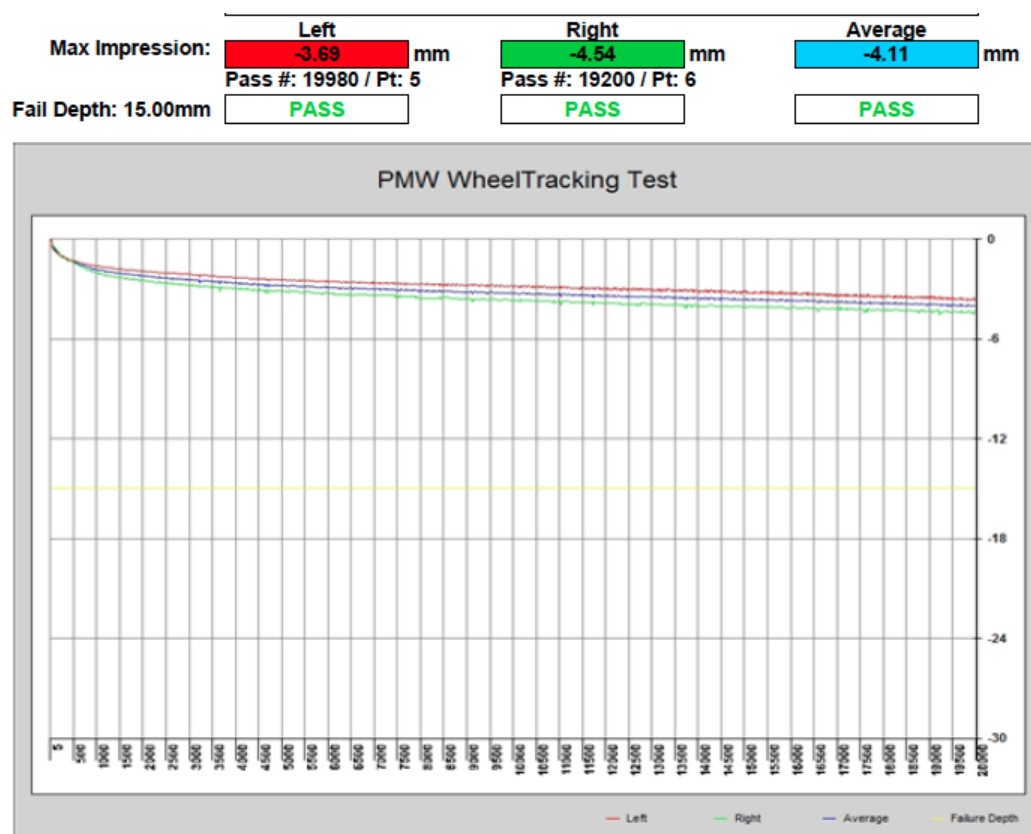


Figure 5.13 Hamburg test results, standard mixture cores.

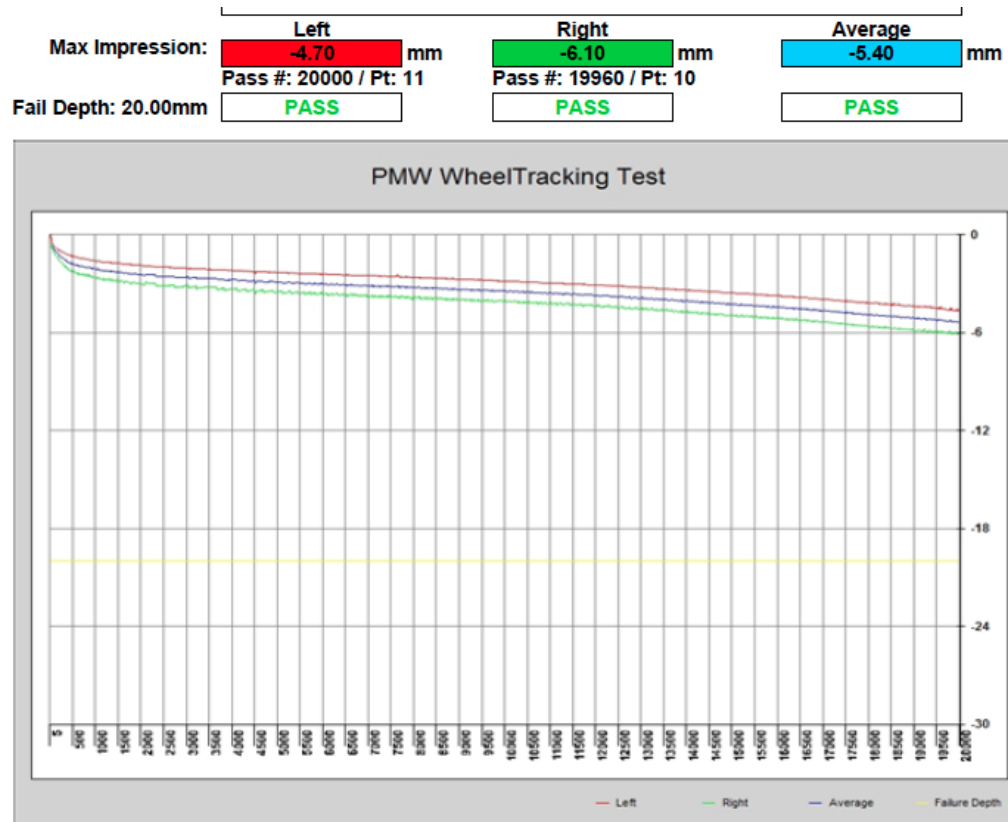


Figure 5.14 Hamburg test results, re-designed mixture cores.

5.2.2.2 Dynamic Modulus and Flow Number Testing

The pavement cores were not thick enough to use in dynamic modulus testing. Thus, the AMPT small specimen protocol was used instead to obtain the $|E^*|$ and FN results. Due to a limited number of cores, it was necessary to perform FN testing on specimens after the $|E^*|$ testing was complete. The air voids of the specimens were determined after $|E^*|$ testing and prior to FN testing, for informational purposes.

Specimens for small-scale $|E^*|$ and FN are testing are 38 mm in diameter and 110 mm tall and are cored horizontally from the road cores as shown in Figure 5.15. This allows two small specimens to be taken from each road core as shown in Figure 5.16. The testing protocol for small-scale samples is according to AASHTO TP 79, but only three test temperatures were used (4, 25, and 37C). At 50C the small specimens are unable to survive the testing.



Figure 5.15 Coring horizontally from road cores.



Figure 5.16 Two small specimens (38-mm x 110-mm) taken from road cores.

As with the conventional $|E^*|$ test, a master curve can be developed using the data from the small-scale test results (Figure 5.17). Figure 5.18 shows the data in semi-log form. The plots indicate the re-designed mixture (N30) has slightly higher $|E^*|$ values over the frequency range than the standard (N100) mixture design for both aging conditions. This result is consistent with the laboratory study results and those of the first field trial on SR-13.

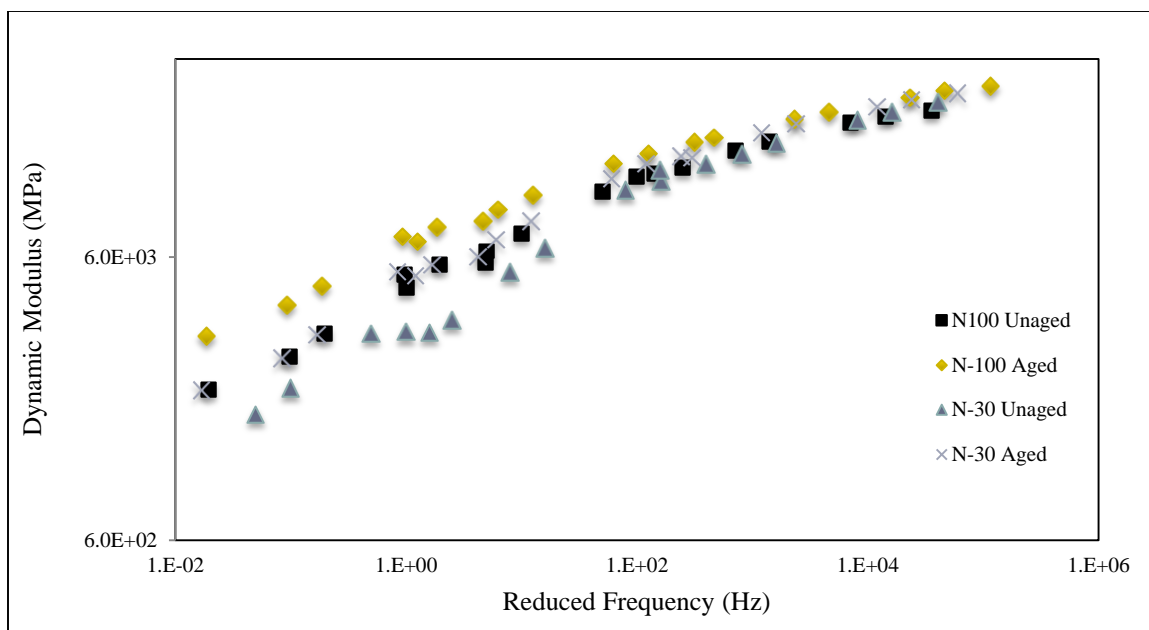


Figure 5.17 Master curves, field cores (log-log plot).

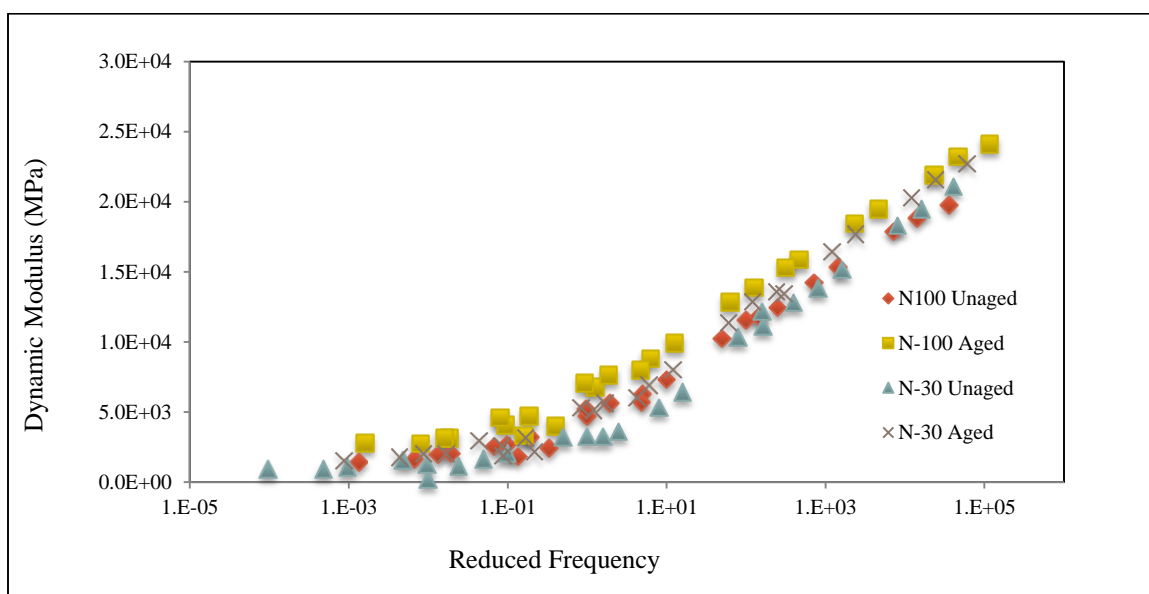


Figure 5.18 Master curves, field cores (semi-log plot).

To decide if any statistically significant differences exist between the $|E^*|$ values of the two mixtures, a t-Test was used to compare the means. Table 5.32 is a summary of the $|E^*|$ data. In this case the $|E^*|$ values are higher for the re-designed mixture, however the statistical analysis indicates that at a 95 percent confidence level ($\alpha=0.05$), the $|E^*|$ values of the standard and re-designed mixtures are not significantly different as shown in Table 5.33.

Table 5.32 Dynamic modulus summary, field cores.

25 Hz	N100 Unaged		N100 Aged		N30 Unaged		N30 Aged	
	Average $ E^* $, MPa	C.V., %	Average $ E^* $, MPa	C.V., %	Average $ E^* $, MPa	C.V., %	Average $ E^* $, MPa	C.V., %
4°C	18236	9.1	19779	7.7	20326	4.3	20603	2.4
21°C	11488	4.7	13129	6.4	12333	4.7	13280	5.7
37°C	6205	3.2	7674	10.3	7130	11.3	8276	6.1
10 Hz	N100 Unaged		N100 Aged		N30 Unaged		N30 Aged	
	Average $ E^* $, MPa	C.V., %	Average $ E^* $, MPa	C.V., %	Average $ E^* $, MPa	C.V., %	Average $ E^* $, MPa	C.V., %
4°C	17421	9.3	18422	6.4	18789	5.4	19396	3.6
21°C	10834	3.5	11774	5.1	11594	6.0	12297	3.9
37°C	5533	8.6	6778	9.7	6134	8.2	7209	6.1

Table 5.33 Dynamic modulus, field cores Bonferroni groupings.

Test Frequency	25 Hz		10 Hz	
Test Temperature	p-value ($\alpha = 0.05$)	Grouping	p-value ($\alpha = 0.05$)	Grouping
4°C	0.00097	(N30A=N30U=N100A); (N100U);	0.00577	(N30U=N100U); (N30A=N100A)
21°C	0.00113	(N30A=N100A=N30U); (N100U)	0.0237	(N30A=N100A=N30U); (N100U)
37°C	0.000001	(N30A); (N100A=N30U); (N100U)	0.000003	(N30A=N100A=N30U); (N100U)

5.2.2.3 Semi-Circular Bend Testing

The eighteen specimens for SCB testing were taken from field cores by cutting the cores in half. Before testing the air void content was determined for each specimen as shown in Table 5.34. Figure 5.19 shows the change in fracture energy with notch depth for the mixtures and aging conditions. Table 5.35 contains the calculated J_c for all mixtures. Again, the higher the J_c value, the more resistant mixtures are to cracking and to crack propagation. The results indicate that in the unaged condition (post construction) the re-designed mixture has a slightly lower J_c value than the standard mixture; after oven conditioning to simulate eight years of in-service life the re-designed mixture shows a significantly higher J_c value than the standard mixture.

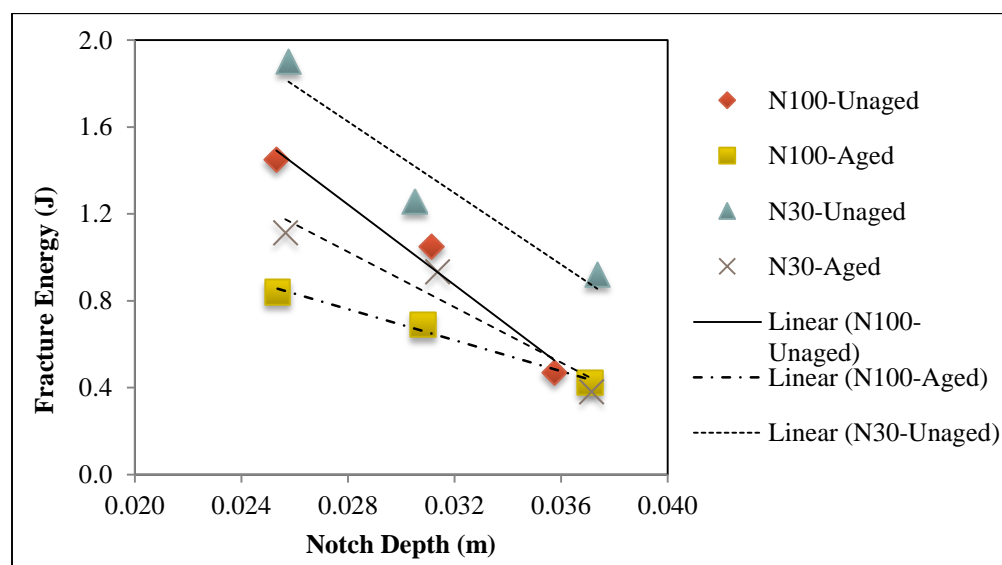


Figure 5.19 Georgetown Road field cores, SCB test results.

Table 5.34 Georgetown Road field semi-circular AV% data.

N100				N30					
Cores No.	G _{mb}	G _{mm}	AV%	Cores No.	G _{mb}	G _{mm}	AV%		
N100-11	2.391	2.509	4.7	N30-411	2.408	2.502	3.8		
N100-12	2.383		5.0	N30-412	2.401		4.0		
N100-41	2.379		5.2	N30-421	2.410		3.7		
N100-42	2.370		5.5	N30-422	2.406		3.8		
N100-51	2.378		5.2	N30-431	2.407		3.8		
N100-52	2.372		5.4	N30-432	2.411		3.6		
N100-61	2.363		5.8	N30-441	2.407		3.8		
N100-62	2.367		5.6	N30-442	2.402		4.0		
N100-71	2.362		5.9	N30-461	2.393		4.3		
N100-72	2.362		5.9	N30-462	2.386		4.6		
N100-81	2.363		5.8	N30-471	2.374		5.1		
N100-82	2.369		5.6	N30-472	2.376		5.1		
N100-91	2.352		6.2	N30-481	2.375		5.1		
N100-92	2.372		5.5	N30-482	2.367		5.4		
N100-181	2.334		7.0	N30-521	2.389		4.5		
N100-182	2.338		6.8	N30-522	2.386		4.6		
N100-191	2.325		7.3	N30-531	2.393		4.4		
N100-192	2.331		7.1	N30-532	2.397		4.2		
N100-201	2.360		5.9	N30-541	2.387		4.6		
N100-202	2.366		5.7	N30-542	2.391		4.4		
Average AV%	5.9			Average AV%	4.3				
SD AV%	0.71			SD AV%	0.53				

Table 5.35 Georgetown Road field cores, critical strain energy release rate.

Mixture	Aging Condition, years	J _c (J/m ²)
N100	0 ¹	1.627
N30		1.424
N100	8	0.624
N30		1.103

¹ Denotes the post-construction condition.

5.2.2.4 Binder Extraction, Recovery, and Grading

The asphalt binder from field cores was recovered and graded in both the unaged (post-construction) and long-term aged (eight-year in-service life) conditions. The binders were recovered using AASHTO T 319 and tested to determine its performance grading according to AASHTO M 320. The continuous high and low grades for the recovered binders are shown in Table 5.36.

Table 5.36 Georgetown Road field cores, recovered asphalt binder grades.

Mixture	Aging Condition, years	Original PG Grade	Recovered PG Grade
Standard	0 ¹	PG 58-28	PG 87-26
	8		PG 93-22
Re-designed	0 ¹		PG 80-28
	8		PG 85-24

¹ Denotes the post-construction condition.

The data in Table 5.33 indicate the original binder high temperature performance grades increased from 58 to 87 and 80 for the post-construction standard and re-designed mixtures, respectively. The low temperature performance grades increased from -28 to -26 for the post-construction standard mixture, while there was no change in the low temperature performance grade for the post-construction re-designed mixture.

After simulating eight years of in-service life with oven conditioning, the high temperature performance grade for the standard mixture increased from 58 to 93, while the re-designed

mixture increased to only 85. For the low temperature performance grade, the standard mixture increased from -28 to -22 and the re-designed mixture increased to -24. The results seem to indicate the standard mixture did in fact “age” more (binder became stiffer) when compared to the re-designed mixture, for both aging conditions. The re-designed mixture may therefore age less in the field, resulting in better mixture and pavement durability.

CHAPTER 6. SUMMARY AND CONCLUSIONS

The objective of the research was to enhance asphalt mixture laboratory design as it relates to field compaction in order to increase asphalt pavement durability without sacrificing the permanent deformation characteristics of the mixtures. Current asphalt mixture design methods specify a design air voids content of 4 percent. Asphalt mixtures thus designed are typically placed with 7 percent air voids or higher. This can result in lower than desired asphalt pavement service lives due to durability loss as the asphalt prematurely ages.

Compacting asphalt pavements to 5 percent in-place air voids (95 percent G_{mm} density), without the possibility of further densification from traffic would make them more durable thus extending asphalt pavement life. However, producing asphalt mixture laboratory designs by choosing optimum asphalt binder content at 4 percent and then attempting to compact such mixtures to 5 percent air voids in the field makes no more sense than the current method of designing at 4 percent air voids and compacting to 7 percent air voids in the field. Instead, the hypothesis of this research based on the precedent provided by the LCPC mix design approach, was that asphalt mixtures should be designed in the laboratory at 5 percent air voids and then compacted in the field to the same air voids.

Given this hypothesis, the research investigated the possibility of re-designing standard asphalt mixtures by varying the aggregate gradation, holding the effective binder content constant, and compacting mixture design test specimens to 5 percent air voids. Keeping the effective binder content constant for each mixture type ensures that mixture durability will not be compromised by removing asphalt binder from the mixtures. In doing so the major concern becomes possible changes to the permanent deformation characteristics of the mixtures. For this reason, the $|E^*|$ and FN values for the mixtures were examined to see if the re-designed mixtures could be expected to have $|E^*|$ and FN values as high as or higher than the standard mixtures. Results indicated that overall, the re-designed mixtures did have $|E^*|$ and FN values as high as or higher than the standard mixtures.

Finally, two field trials were placed to compare re-designed mixtures to conventionally designed mixtures. The re-designed mixtures were placed in the field at approximately 5 percent air voids without the necessity of changing roller types or patterns. No extra effort was required to achieve the target field density (air voids). Various type of testing were performed on both mixtures and aging conditions to evaluate different aspects of asphalt mixture performance such as rutting, fatigue, stiffness, and durability performance. Post-construction testing results for the standard and re-designed mixtures from the two field projects were varied, but overall it is expected that the re-designed mixtures should perform as well as, if not better than, the standard mixtures.

6.1 Conclusions

The findings from this study lead to the following conclusions:

- It is possible to design asphalt mixtures with 5 percent air voids without lowering the effective binder content; this can be accomplished by varying the aggregate gradation of the mixture.
- Asphalt mixtures designed using lower compaction levels than currently specified by the Superpave method can be designed to have $|E^*|$ and FN as high as or higher than, conventionally designed mixtures, without lowering the effective binder content.
- On average, the mixture data appeared to indicate that 53, 52, and 42 were the optimum numbers of gyrations for the three re-designed mixtures developed in the laboratory.
- Asphalt mixtures designed in the laboratory at 5 percent air voids can be compacted to 5 percent air voids in the field. The field tests indicate this can be done without additional compaction effort.
- Results of testing re-heated, plant-produced mixtures are somewhat variable, as indicated in the post-trial test results. Some test results seem to indicate the standard

mixtures may perform better, while other results favor the re-designed mixtures. The performance of the test sections will help confirm if the re-designed mixtures are, or are not better performers than the standard mixtures.

- For the first field trial, SR-13 project, results show that although the in-place density of the re-designed mixture was higher than the standard mixture, permeability of the re-designed mixture was higher than the standard mixture. Investigations were performed and it is believed that the aggregate structure is a dominant parameter affecting permeability. Based on the Bailey Method, mixtures with higher percentages of CA ratio or higher percentages of interceptors tend to have higher permeability.
- For the second field trial, the Georgetown Road project, results show that the re-designed mixture has lower permeability when compared to the standard mixture showing that the re-designed mixture tends to ages less and have higher durability than the standard mixture.
- Electrical resistivity results for both field trails show that the re-designed mixture has less interconnected air voids showing that this mixture tends to have better durability performance when compared to the standard mixture.

CHAPTER 7. RECOMMENDATIONS FOR SUPERPAVE MIXTURE DESIGN TO OBTAIN BETTER IN-FIELD COMPACTION AND DURABILITY

This study started as a JTRP (Joint Transportation Research Program) project between INDOT and Purdue University. Although the intent of this project was to overcome durability issues of asphalt mixtures in Indiana, it can be applicable to any state and agency. Based on the results of this study the following recommendations are offered as starting point:

- According to this study, states and agencies can now eliminate high gyration levels for the mixture designs and establish two different gyration levels; one for medium to high traffic, and another for low volume traffic.
- For medium to high traffic levels, 50 gyrations appear to be the correct number of gyrations to be used in designing asphalt mixtures with optimum binder content chosen at 5 percent air voids.
- For lower volume roads, 30 gyration mixture designs might be more appropriate. Further laboratory and field testing should be conducted to verify this number.

- Porosity testing should be completed for both standard and re-designed mixtures to help evaluate the permeability of asphalt mixtures. This testing has a good correlation with the falling head conductivity testing results.
- The CA ratio is a significant parameter that changes the permeability of asphalt mixtures. Mixtures with higher CA ratios tend to have higher permeability and lower durability performance.
- Further investigation should be performed on CA ratio value and set a threshold for each type of mixture and application.
- Low-temperature and moisture susceptibility testing should be completed for both standard and re-designed mixtures, to help quantify the enhanced durability of the re-designed mixtures.
- Additional laboratory work should be done so as to include the effects of more traffic levels; mixtures containing RAP, RAS, or both; and additional binder grades and aggregate types.
- The performance of the trial projects placed as part of this study should be monitored for performance.
- Additional trial projects should be placed and evaluated.

LIST OF REFERENCES

LIST OF REFERENCES

Advanced Asphalt Technologies, LLC, *A Manual for Design of Hot Mix Asphalt with Commentary*. Report No. 673, National Cooperative Highway Research Program, Transportation Research Board, Washington, DC, 2011.

Anderson, R. M., Turner, P. A. and Peterson, R. L., *Relationship of Superpave Gyrotory Compaction Properties to HMA Rutting Behavior*. Report No. 478, National Cooperative Highway Research Program, Transportation Research Board, pp 7-15, Washington, DC, 2002.

Asphalt Pavement Alliance, <http://driveasphalt.org/>, accessed 15 Nov 2014.

Asphalt Research Program, *Fatigue Response of Asphalt-Aggregate Mixes*, Report No. SHRP-A-404, University of California, Berkeley, 1994.

The Asphalt Institute, *Mix Design Methods for Asphalt Concrete and Other Mix Types, Manual Series No. 2*. The Asphalt Institute, 1993.

Brown, E. R., Kandhal, P. S., Roberts, F. L., Kim, Y. R., Lee, D. Y. and Kennedy, T. W., *Hot Mix Asphalt Materials, Mixture, Design, and Construction*. NAPA Research and Education Foundation, Lanham, 3ed., 2009.

Cominsky, R. J., *The Superpave Mix Design Manual for New Construction and Overlays*. Report No. A-407, Strategic Highway Research Program, National Research Council, Washington, DC, 2008.

Cominsky, R.J., Huber, G.A., Kennedy, T.W. and Anderson, R.M., *The Superpave Mix Design Manual for New Construction and Overlays*. Strategic Highway Research Program Report SHRP-A-407, National Research Council, Washington, DC, 1994.

Concrete Parking, <http://www.concreteparking.org/overlays/design.html>, accessed 14 Nov 2015.

Cooley, L. A., Prowell, B. D and Brown, E. R., *Issues Pertaining to the Permeability Characteristics of Coarse-Graded Superpave Mixes*. Report No. 02-06, National Center for Asphalt Technology, Auburn, 2002.

Forough, S. A., Nejad, F. M. and Hasan Ziari, H., “Investigating the Relationships between the Electrical Resistivity Characteristics and the Volumetric Properties of Asphalt Mixtures,” *Journal of Materials in Civil Engineering*, American Society of Civil Engineering (ASTM), 2013, Vol 25, pp 1692-1702.

Goetz, W.H., “The Evolution of Asphalt Concrete Mix Design,” *Asphalt Concrete Mix Design: Development of More Rational Approaches*, American Society for Testing and Materials STP 1041, Philadelphia, 1989.

Griffith, J. M., “Evaluation of the Method of Asphalt Pavement Design Developed by The Corps of Engineers,” *Proceedings of the Technical Sessions of the Association of Asphalt Paving Technologists*, pp 221 – 260, Detroit, 1949.

Huang, Y. H. *Pavement Analysis and Design*. Pearson Prentice Hall, Upper Saddle River, 2ed, 2004.

Hubbard, P. and Field, F.C., *Stability and Related Tests for Asphalt Paving Mixtures*, The Asphalt Institute, Research Series Number 1, October 1935.

Hubbard, P. and Field, F.C., “Adaptation of the Stability Test to Include Coarse Aggregate Asphalt Paving Mixtures,” *Proceedings of the Technical Sessions of the Association of Asphalt Paving Technologists*, January 1932, Detroit, Michigan, pp. 109 – 114.

Huber, G.A., Blankenship, P.B. and Mahboub, K.C., “Rational Method for Laboratory Compaction of Hot-Mix Asphalt,” *Journal of Transportation Research Record*, Transportation Research Board, Washington, DC, 1994.

Marasteanu, M., Falchetto and A. C., Moon, K. H., *Investigation of Low Temperature Cracking in Asphalt Pavements National Polled Fund Study – Phase II*. Report No. MN/RC 2012-23, Minnesota Department of Transportation, St. Paul, 2012.

McFadden, G. A., “Design and Field Control of Asphalt Paving Mixtures for Military Installations,” *Proceedings of the Technical Sessions of the Association of Asphalt Paving Technologists*, pp 93 – 113, Chicago, Illinois, 1984.

Mohammad, L. N., Kim, M., and Elseifi, M., "Characterization of asphalt mixture's fracture resistance using the semi-circular bending (SCB) test." *7th RILEM international conference on cracking in pavements*. Springer Netherlands, 2012.

Moutier, F., “La Presse à Cisaillement Giratoire; Modèle de Série,” *Bulletin Liaison Laboratoire Ponts et Chaussées*, 1974, pp 137 – 148.

Moutier, F., “Le Banc De Compactage,” *Bulletin Liaison Laboratoire Ponts et Chaussées*, 1977, pp. 132 – 136.

National Asphalt Pavement Association,

http://www.asphaltpavement.org/index.php?option=com_content&view=article&id=14&Itemid=33 , accessed 15 Nov 2014.

National Highway Institute, *Superpave for Senior Managers*, NHI Course Number 13151, Publication Number FHWA-HI 98-004, November 1998.

Oliver, J. W., “Asphalt Durability: from Laboratory Test to Field Implementation,” *Fuel Science and Technology International*, Taylor & Francis, 2007, Vol 10, pp 501-518.

Ortolani, L. A., “The Gyrotory-Shear Method of Molding Asphaltic Concrete Test Specimens; Its Development and Correlation with Field Compaction Methods. A Texas Highway Department Standard Procedure,” *Proceedings of the Technical Sessions of the Association of Asphalt Paving Technologists*, Vol 21, 1952.

Vavrik, W. R., Huber, G., Pine, W. J. and Bailey, R., “Bailey Method for Gradation Selection in HMA Mixture Design,” *Transportation Research Circular*, Transportation Research Board, Washington, DC, 2002.

Vivar, E. P. and Haddock, J. E., *HMA Pavement Performance and Durability*. Report No. FHWA/IN/JTRP-2005/14, Joint Transportation Research Program, Purdue University, pp 27-44, West Lafayette, 2006.

Vokac, R., “Studies in the Proportioning of Low Cost Bituminous Mixtures of Dense Graded Aggregate Type”, *Proceedings of the Technical Sessions of the Association of Asphalt Paving Technologists*. New Orleans, Louisiana, December 1932, pp. 84 – 102.

Whitaker, W., *William Whitaker's Words*, <http://archives.nd.edu/words.html>, accessed 15 Nov 2014.

BIBLIOGRAPHY

BIBLIOGRAPHY

Balay, J. M. and Kerzreho J. P., *Assessment of French design method for flexible pavement by mean of the LCPC's ALT facility*. Laboratoire Central des Ponts et Chaussées. Nantes, France, 2007.

Blackman, B.R.K, Cui, S., Kinloch, A.J., Taylor. L.C., "The Development of a Novel Test Method to Assess the Durability of Asphalt Road–Pavement Materials," *International Journal of Adhesion & Adhesives*, Elsevier Ltd, 2013, Vol 42, pp 1-10.

Bonaquist, R., *Ruggedness Testing of the Dynamic Modulus and Flow Number Tests with the Simple Performance Tester*. Report No. 629, National Cooperative Highway Research Program, Transportation Research Board, Washington, DC, 2008.

Brown, E. R. and Buchanan, M. S., *Verification of Gyration Levels in the Superpave N_{design} Table*. Literature Review on Report No. 573, National Cooperative Highway Research Program, Transportation Research Board, Washington, DC, 2001.

Brown, E. R. and Cross, S. A., *Comparison of Laboratory and Field Density Of Asphalt Mixtures*. Report No. 91-1, National Center for Asphalt Technology, Transportation Research Board, Washington, DC, 1991.

Christensen, D. W. Jr. and Bonaquist, R. F., *Volumetric Requirements for Superpave Mix Design*. Report No. 567, National Cooperative Highway Research Program, Transportation Research Board, Washington, DC, 2006.

Prowell, B.D. and Brown, E. R., *Superpave Mix Design: Verifying Gyration Levels in the N_{design} Table*. Appendices to Report No. 573, National Cooperative Highway Research Program, Transportation Research Board, Washington, DC, 2006.

Prowell, B.D. and Brown, E. R., *Superpave Mix Design: Verifying Gyration Levels in the N_{design} Table*. Report No. 573, National Cooperative Highway Research Program, Transportation Research Board, pp 24-28, Washington, DC, 2007.

Zeiadaab, W. A., Kalousha, K. E., Underwood, B. S. and Mamlouka, M. E., "Improved Method of Considering Air Void and Asphalt Content Changes on Long-Term Performance of Asphalt Concrete Pavements," *International Journal of Pavement Engineering*, Taylor & Francis, 2014, Vol 15, pp 718-730.

PUBLICATIONS

PUBLICATIONS

Hekmatfar, A., Shah, A., Huber, G., McDaniel, R.S. and Haddock, J. E., "Optimizing Laboratory Mixture Design to Improve Field Compaction," *Journal of Road Materials and Pavement Design*, pp 149-167, Taylor & Francis, 2015.

Huber, G., Haddock, J. E., Wielinski, J., Kriech, T., Hekmatfar, A., "Adjusting Design Air Voids Level in Superpave Mixtures to Enhance Durability," *Proceedings of the 6th Eurasphalt & Eurobitume (E&E) Congress*, Prague, Czech Republic, 2016. (accepted)

Hekmatfar, A., Shah, A., Huber, G., McDaniel, R.S. and Haddock, J. E., "Modifying Asphalt Mixture Design to Enhance Field Compaction: A Field Study," *Proceedings of the 15th International Society for Asphalt Pavements (ISAP)*, Jackson Hole, WY, 2016. (accepted)

Tian, Y., Hekmatfar, A., and Haddock, J. E., "Comparison of Rutting Performance Between the PURWheel and the NCAT Test Track," *Proceedings of the 14th International Society for Asphalt Pavements (ISAP)*, pp-1469-1480, Raleigh, NC, 2014.

VITA

VITA

Ali Hekmatfar earned his B.Sc. and M.Sc. from Sharif University of Technologies in Tehran, Iran. He joined Civil Engineering Materials Group at Purdue University in Spring 2012. He has been involved in research on asphalt materials since he was an undergraduate student. His research includes theoretical, analytical and experimental aspects of asphalt mixtures technology. Also he has more than 10 years experience in research, construction and consulting in the areas of constitutive modeling of asphalt pavement mixtures, rheological properties of asphalt binder, pavement structural and mixture design, pavement maintenance and management, roadway design, and project management. After obtaining his M.Sc. degree from Sharif University of Technologies, he joined Purdue University to pursue his PhD in asphalt materials.

Ali's doctoral dissertation was conducted under the direction of Professor John E. Haddock at Purdue University, and investigated new asphalt mixture design to enhance asphalt pavement durability. Throughout his research, he has been responsible for completing research on improving the Superpave mixture design method, improvements that should lead to asphalt pavements with increased durability and longer life cycles. This finding is extremely important for flexible pavement design and preservation. For the research that Ali performed at Purdue University, he received the William and Mary

Goetz graduate fellowship in civil engineering material science and the 2016 Emmons Award for best paper presented at the 2016 Annual Meeting of the Association of Asphalt Paving Technologists. The award was presented at the banquet during the 2016 meeting in Indianapolis on March 15th.

Ali's research interests include: (1) Pavement Materials and Engineering, (2) Infrastructure Maintenance and Management, (3) Materials Testing and Characterization, and (4) m Construction Engineering and Management. During his research, he has been able to publish several scientific and technical documents dealing with asphalt materials.